Regulation of the memory T cell development and islet β-cell survival by DAPK-related apoptosis-inducing protein kinase 2 (Drak2)

Jianning Mao

Département de Médecine

Faculté de Médecine

Université de Montréal

Thèse présentée à la Faculté des études supérieures
en vue de l'obtention du grade de
Philosophiae Doctor (Ph.D.)
en Sciences Biomédicales

June , 2009

Université de Montréal
Faculté des études supérieures

Cette thèse intitulée:

« Regulation of the memory T cell development and islet β-cell survival by DAPK-related apoptosis-inducing protein kinase 2 (Drak2) »

Présentée par:

Jianning Mao

A été évaluée par un jury composé des personnes suivantes:

Bertrand, Richard
……
Président du jury

Wu, Jiangping
……
Directeur de recherché

Luo, Hongyu
……
Codirectrice

Labrecque, Nathalie
……
Membre du jury

Di Battista, John
……
Examinateur externe

Lajeunesse, Daniel
……
Représentant du doyen de la FES

SUMMARY

Drak2 is a member of the death-associated protein family, and is a serine threonine kinase. In Drak2 null mutant mice, T cells have no apparent defect in activation-induced apoptosis after stimulation with anti-CD3 and anti-CD28, but have a lowered threshold to stimulation, compared with wild type (WT) T cells.

In our study, in situ hybridization analysis has revealed that Drak2 expression is ubiquitous at the mid-gestation stage in embryos, followed by more focal expression in various organs in the perinatal period and adulthood, notably in the thymus, spleen, lymph nodes, cerebellum, suprachiasmatic nuclei, pituitary, olfactory lobes, adrenal medulla, stomach, skin and testes. We generated Drak2 transgenic (Tg) mice using the human β-actin promoter. These Tg mice showed normal T cell *versus* B cell and CD4 *versus* CD8 populations in the spleen, but their spleen weight cellularity was lower in comparison with wild type mice. After TCR activation, the proliferation response in Drak2 Tg T cells was normal, although their interleukin (IL)-2 and IL-4 but not interferon-γ production was augmented. Activated Drak2 Tg T cells demonstrated significantly enhanced apoptosis in the presence of exogenous IL-2. At the molecular level, Drak2 Tg T cells manifested a lower increase of anti-apoptotic factors during activation; such a change probably rendered the cells vulnerable to subsequent IL-2 insults. The heightened apoptosis in Drak2 Tg T cells was associated with reduced numbers of T cells with the memory cell phenotype ($CD62L^{lo}$) and repressed secondary T cell responses in delayed type

hypersensitivity. These results demonstrate that Drak2 expresses in the T cell compartment but is not T cell-specific; and it plays critical roles in T cell apoptosis and memory T cell development.

Further, we investigated the role of Drak2 in β-cell survival and diabetes. Drak2 mRNA and protein were rapidly induced in islet β-cells after exogenous inflammatory cytokine or free fatty acid stimulation, which is present endogenously in either type 1 or type 2 diabetes. Drak2 upregulation was accompanied by increased β-cell apoptosis. The β-cells apoptosis caused by the said stimuli was inhibited by Drak2 knockdown using siRNA. Conversely, transgenic (Tg) Drak2 overexpression led to aggravated β-cell apoptosis triggered by the stimuli. Drak2 overexpression in islets compromised the increase of anti-apoptotic factors, such as Bcl-2, Bcl-xL and Flip, upon the cytokine and free fatty acid stimulation. Further in vivo experiments demonstrated that Drak2 Tg mice were prone to type 1 diabetes in a multiple-low-dose streptozotocin-induced diabetes model, and they were also prone to type 2 diabetes in a diet-induced obesity model. Our data show that Drak2 is detrimental to β-cell survival.

We also investigated the signalling pathway of Drak2. We found that purified Drak2 could phosphorylate p70S6 kinase in an in vitro kinase assay. Drak2 overexpression in NIT-1 cells led to enhanced p70S6 kinase phosphorylation, while Drak2 knockdown in these cells reduced the phosphorylation. These mechanistic studies proved that p70S6 kinase was a bona fide Drak2 substrate in vitro and in vivo.

This study has discovered the important functions of Drak2 in T cell homeostasis and diabetes. We proved that p70S6 kinase was a substrate of Drak2. Our findings have broadened our

knowledge of Drak2 in the immune and endocrine system. Some of our findings, such as the roles of Drak2 in memory T cell development and β cell survival could be explored for clinical application in the areas of transplantation and diabetes.

Key words: Drak2; transgenic; memory T cell; apoptosis; islet; diabetes.

Résumé

Drak2 est un membre de la famille des protéines associées à la mort et c'est une sérine/thréonine kinase. Chez les souris mutantes nulles Drak2, les cellules T ne présentent aucune défectuosité apparente en apoptose induite par activation, après stimulation avec anti-CD3 et anti-CD28, mais ont un seuil de stimulation réduit, comparées aux cellules T de type sauvage (TS).

Dans notre étude, l'analyse d'hybridation in situ a révélé que l'expression de Drak2 est ubiquiste au stade de la mi-gestation chez les embryons, suivie d'une expression plus focale dans les divers organes pendant la période périnatale et l'âge adulte, notamment dans le thymus, la rate, les ganglions lymphatiques, le cervelet, les noyaux suprachiasmatiques, la glande pituitaire, les lobes olfactifs, la médullaire surrénale, l'estomac, la peau et les testicules. Nous avons créé des souris transgéniques (Tg) Drak2 en utilisant le promoteur humain β-actine. Ces souris Tg montraient des ratios normaux entre cellules T *versus* B et entre cellules CD4 *versus* CD8, mais leur cellularité et leur poids spléniques étaient inférieurs comparé aux souris de type sauvage. Après activation TCR, la réponse proliférative des cellules T Tg Drak2 était normale, même si leur production d'interleukine (IL)-2 et IL-4 mais non d'interféron-γ était augmentée. Les cellules T Tg Drak2 activées ont démontré une apoptose significativement accrue en présence d'IL-2 exogène. Au niveau moléculaire, les cellules T Tg Drak2 ont manifesté une augmentation moins élevée des facteurs anti-apoptotiques durant l'activation; un tel changement a probablement rendu les cellules vulnérables aux attaques subséquentes d'IL-2. L'apoptose compromise dans les cellules T Tg Drak2 a été associée à un nombre réduit de cellules T ayant le phénotype des cellules mémoires ($CD62L^{lo}$) et avec des réactions secondaires réprimées des cellules T dans l'hypersensibilité de type différé. Ces résultats démontrent que Drak2 s'exprime

dans le compartiment des cellules T mais n'est pas spécifique aux cellules T; et aussi qu'il joue des rôles déterminants dans l'apoptose des cellules T et dans le développement des cellules mémoires T.

En outre, nous avons recherché le rôle de Drak2 dans la survie des cellules β et le diabète. L'ARNm et la protéine Drak2 ont été rapidement induits dans les cellules β de l'îlot après stimulation exogène par les cytokines inflammatoires ou les acides gras libres et qui est présente de façon endogène dans le diabète, qu'il soit de type 1 ou de type 2. La régulation positive de Drak2 a été accompagnée d'une apoptose accrue des cellules β. L'apoptose des cellules β provoquée par les stimuli en question a été inhibée par la chute de Drak2 en utilisant petit ARNi. Inversement, la surexpression de Drak2 Tg a mené à l'apoptose aggravée des cellules β déclenchée par les stimuli. La surexpression de Drak2 dans les îlots a compromis l'augmentation des facteurs anti-apoptotiques, tels que Bcl-2, Bcl-xL et Flip, sur stimulation par la cytokine et les acides gras libres. De plus, les expériences in vivo ont démontré que les souris Tg Drak2 étaient sujettes au diabète de type 1 dans un modèle de diabète provoqué par de petites doses multiples de streptozotocine et qu'elles étaient aussi sujettes au diabète de type 2 dans un modèle d'obésité induite par la diète. Nos données montrent que Drak2 est défavorable à la survie des cellules β.

Nous avons aussi étudié la voie de transmission de Drak2. Nous avons trouvé que Drak2 purifiée pouvait phosphoryler p70S6 kinase dans une analyse kinase in vitro. La surexpression de Drak2 dans les cellules NIT-1 a entraîné l'augmentation de la phosphorylasation p70S6 kinase tandis que l'abaissement de Drak2 dans ces cellules a réduit la phosphorylation. Ces recherches mécanistes ont prouvé que p70S6 kinase était véritablement un substrat de Drak2 in vitro et in vivo.

Cette étude a découvert les fonctions importantes de Drak2 dans l'homéostasie des cellules T et le diabète. Nous avons prouvé que p70S6 kinase était un substrat de Drak2. Nos résultats ont approfondi nos connaissances de Drak2 à l'intérieur des systèmes immunitaire et endocrinien. Certaines de nos conclusions, comme les rôles de Drak2 dans le développement des cellules mémoires T et la survie des cellules β, pourraient être explorées pour des applications cliniques dans les domaines de la transplantation et du diabète.

Mots clés : Drak2; transgénique; cellule mémoire T; apoptose; îlot; diabète.

TABLE OF CONTENTS

LIST OF FIGURES

Introduction;

Article 1:

LIST OF ABBREVIATIONS

ACAD	activated cell-autonomous death
AICD	activation-induced cell death
AMPK	5'-AMP-activated protein kinase
APAF	cytoplasmic apoptotic-protease-activating factor
APC	antigen presenting cell
ATF	activating transcription factor
BIM	BCL-2-interacting mediator of cell death
CARD	caspase-recruitment domain
CCR-7	CC-chemokine receptor-7
CHOP	(CCAAT/enhancer binding protein) homologous protein
CTL	cytotoxic T lymphocytes
DAG	diacylglycerols
DAPK	death-associated protein kinase
DD	death domain
DED	death-effector domain
DISC	death-inducing signalling complex
DR	death receptor
DRAK	DAPK-related apoptosis-inducing protein kinase
EAE	experimental autoimmune encephalomyelitis
ER	endoplasmic reticulum
ERK	extracellular signal-regulated kinase
FACS	fluorescence-activated cell sorting
FasL	Fas ligand
FFA	free fatty acid
GAD	glutamic acid decarboxylase
GIIS	glucose-induced insulin secretion

GLUT	glucose transporter type
GPAT	glycerol-3-phosphate acyltransferase
ICAD	inhibitor of the caspase-activated DNase
IFN-γ	Interferon-γ
IGF	insulin-like growth factor
IGT	impaired glucose tolerance
IL-12	Interleukin-12
IL-2	Interleukin-2
iNOS	inducible nitric oxide synthase
IRS	insulin receptor substrate
IκK-β	IκB kinase catalytic subunit-β
JAK/STAT	Janus Kinase-2/Signal Transducer and Activator of Transcription
JNK	c-Jun NH2-terminal kinase
LADA	latent autoimmune diabetes of the adult
LC-CoAs	long-chain acyl CoAs
MAPK	p38 mitogen-activated protein kinase
MCP1	monocyte chemotactic protein-1
MHC	major histocompatibility complex
mTOR	mammalian target of rapamycin
NEFAs	Non-esterified fatty acids
NF-κB	Transcription factor nuclear factor-κB
NO	nitric oxide
NOD	nonobese diabetic
PI3K	phosphatidylinositol 3-kinase
PKB	phosphatidylinositol-3'-kinase (PI3'K)/protein kinase-B
PKC	protein kinase C
PPAR	peroxisome proliferator activated receptor
PUMA	p53-upregulated modulator of apoptosis
RBP	Retinol-binding protein
ROS	reactive-oxygen species

S6K	ribosomal protein S6 kinase
SOCS	suppression of cytokine signalling
TAC	tricarboxylic acid
TCR	T-cell receptor
TG	triglyceride
TNF-α	tumor necrosis factor-α
TRAIL	TNF-related apoptosis-inducing ligand
XBP-1	x-box binding protein-1

ACKNOWLEDGEMENTS

I would like to express my sincere gratitude to my supervisor Dr. Jiangping Wu and Dr. Hongyu Luo for their scientific guidance and encouragement throughout this study and during the preparation of this thesis.

I also would like to thank all the colleagues in the lab for their splendid co-operation.

Thanks also extended to all my friends and those who always support me in different ways.

Finally, I would like to thank all of my family members for their understanding, patience, and their great support, which are critically important for me to complete this study.

I. INTRODUCTION

I. INTRODUCTION

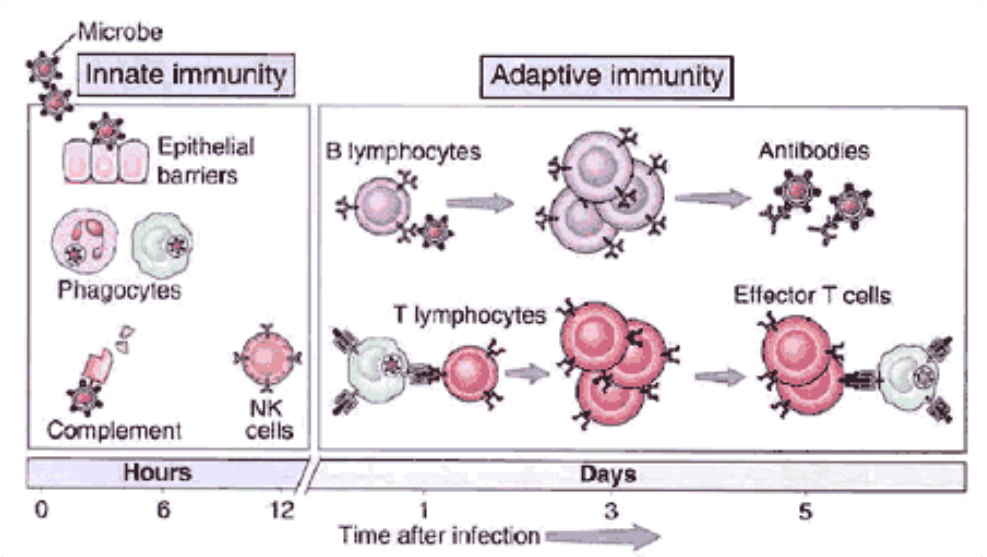

Act Against Allergy web-site, SHS International Ltd
Fig.1. Innate and adaptive immune system: The mechanisms of innate immunity provide the initial defense against infections. Adaptive immune responses develop later and consist of activation of lymphocytes.

An immune system is a collection of mechanisms that kill pathogens and tumor cells, as well as distinguish them from the organism's own healthy cells and tissues. It can be divided into innate and adaptive immune system (Fig.1). The innate immune system is usually triggered when microbes are identified by pattern recognition receptors, which recognize components that are conserved among broad groups of microorganisms. Innate immune defenses are non-specific, and do not confer long-lasting immunity against a pathogen. The adaptive immune system is stronger and also has immunological memory, where each pathogen is "remembered" by a signature antigen. The adaptive immune response is antigen-specific and requires the recognition of specific “non-self” antigens during a process called antigen presentation. The cells of the adaptive immune system are special types of leukocytes,

called lymphocytes. B cells and T cells are the major types of lymphocytes and are derived from hematopoietic stem cells in the bone marrow. B cells are involved in the humoral immune response; T cells are involved in cell-mediated immune response.

T lymphocytes consist of functionally distinct populations, the best defined of which are helper T cells and cytolytic, or cytotoxic, T lymphocytes (CTL). Most helper T cells are $CD4^+$, and most CTLs are $CD8^+$.

$CD4^+$ lymphocytes, or helper T cells, are immune response mediators, and play an important role in establishing and maximizing the capabilities of the adaptive immune response. Helper T cells express T cell receptors (TCR) that recognize antigen bound to major histocompatibility complex (MHC) Class II molecules. The activation of $CD4^+$ T cells requires engagement of the TCR and CD28 on the T cell by the MHC and B7 family members on the antigen presenting cell (APC). Both singals are required for production of an effective immune response. The activation of a naive helper T-cell causes it to release cytokines, which influences the activity of many cell types. Helper T cells can provide extra signals that "help" activate cytotoxic cells.

Cytotoxic T cells induce the death of cells that are infected with viruses (and other pathogens), or are otherwise damaged or dysfunctional. Naive cytotoxic T cells are activated when their T-cell receptor (TCR) strongly interacts with a peptide-bound MHC class I molecule. Once activated, the CTL undergoes a process called clonal expansion in which it gains functionality, and divides rapidly, to produce effector cells. Activated CTL will then travel throughout the body in search of cells bearing that unique MHC Class I peptide. To limit extensive tissue damage during an infection, CTL activation is tightly controlled and generally requires a very strong

MHC/antigen activation signal, or additional activation signals provided by helper T-cells. Upon resolution of the infection, most of the effector cells will die and be cleared away by phagocytes, but a few of these cells will be retained as memory cells.

T lymphocytes originate from hematopoietic stem cells in the bone marrow and seed the thymus. The thymus is the major site of maturation of T cells. The earliest thymocytes express neither CD4 nor CD8, and are therefore classed as *double-negative* ($CD4^-CD8^-$) cells. As they progress through their development they become *double-positive* thymocytes ($CD4^+CD8^+$), and finally mature to *single-positive* ($CD4^+CD8^-$ or $CD4^-CD8^+$) thymocytes that are then released from the thymus to peripheral tissues. About 98% of thymocytes die during the development processes in the thymus by failing either positive selection or negative selection, whereas the other 2% survive and leave the thymus to become mature immunocompetent T cells.

Positive selection "selects for" T-cells capable of interacting with MHC. Double-positive thymocytes ($CD4^+/CD8^+$) that bind the MHC/antigen complex with adequate affinity will receive a vital "survival signal." The thymocytes with low affinity die by apoptosis, and are engulfed by macrophages.

Negative selection removes thymocytes that are capable of strongly binding with "self" peptides presented by MHC. Thymocytes that survive positive selection migrate towards the boundary of the thymic cortex and thymic medulla. While in the medulla, they are again presented with self-antigen in complex with MHC molecules on APCs such as dendritic cells and macrophages. Thymocytes that interact too strongly with the antigen receive an apoptotic signal that leads to cell death. The vast majority of all thymocytes end up dying during this process. This process prevents the

formation of self-reactive T cells that are capable of generating autoimmune diseases in the host.

(Molecular Biology of the Cell; Fourth Edition)

1. T cell homeostasis and apoptosis

T cells are the most versatile cells in the body. The homeostasis of T cells plays an important role in the immune system (1).

T cells rest in peripheral lymphoid organs until they encounter activating signals, such as foreign antigen presented by antigen-presenting cells. They will undergo clonal expansion and differenciation and gain the ability to enter sites of inflammation. To maintain homeostasis after clonal expansion, activated T cells must be removed once the invading antigen has been eliminated (2). Only a few T cells that have been exposed to the antigen remain and develop into memory T cells. These memory cells will respond rapidly to subsequent exposure to the same antigen and are resistant to death by apoptosis (3;4).

1-1 T cell apoptosis

The peripheral T cells go to apoptosis by several mechanisms. Caspases have a central role in the regulation and execution of most types of apoptotic cell death. All caspases are catalytically inactive zymogens and will undergo proteolytic processing after activation (5). The initiator caspases (also known as apical caspases) are activated first, then they activate the effector caspases. It is generally accepted that activation of

initiator caspases takes place in large protein complexes that bring together several caspase zymogens (6). All initiator caspases are characterized by the presence of a stretch of 80–100 amino acids, which is called death domain (DD). The DD superfamily includes the DD subfamily, the death-effector domain (DED) subfamily and the caspase-recruitment domain (CARD) subfamily, which enables the recruitment of caspase into the initiation complex. Following dimerization in the initiation complex, initiator caspases are activated. They then cleave and activate the effector caspases, mainly caspase-3, caspase-6 and caspase-7.

Activation of the caspase cascade results in the cleavage of a number of important cellular proteins, known as the 'cell-death substrates'. Cleavage of nuclear lamins results in chromatin condensation and nuclear shrinkage; cleavage of the inhibitor of the caspase-activated DNase (ICAD) results in the release of the endonuclease, which travels to the nucleus to fragment DNA. Cleavage of cytoskeletal proteins, such as actin, plectin, and gelsolin, leads to cell fragmentation, blebbing, the formation of apoptotic bodies and the destruction of the cell. The dying cells express 'eat-me' signals, such as phosphatidyl serine and different surface sugars, and are removed by phagocytes (7).

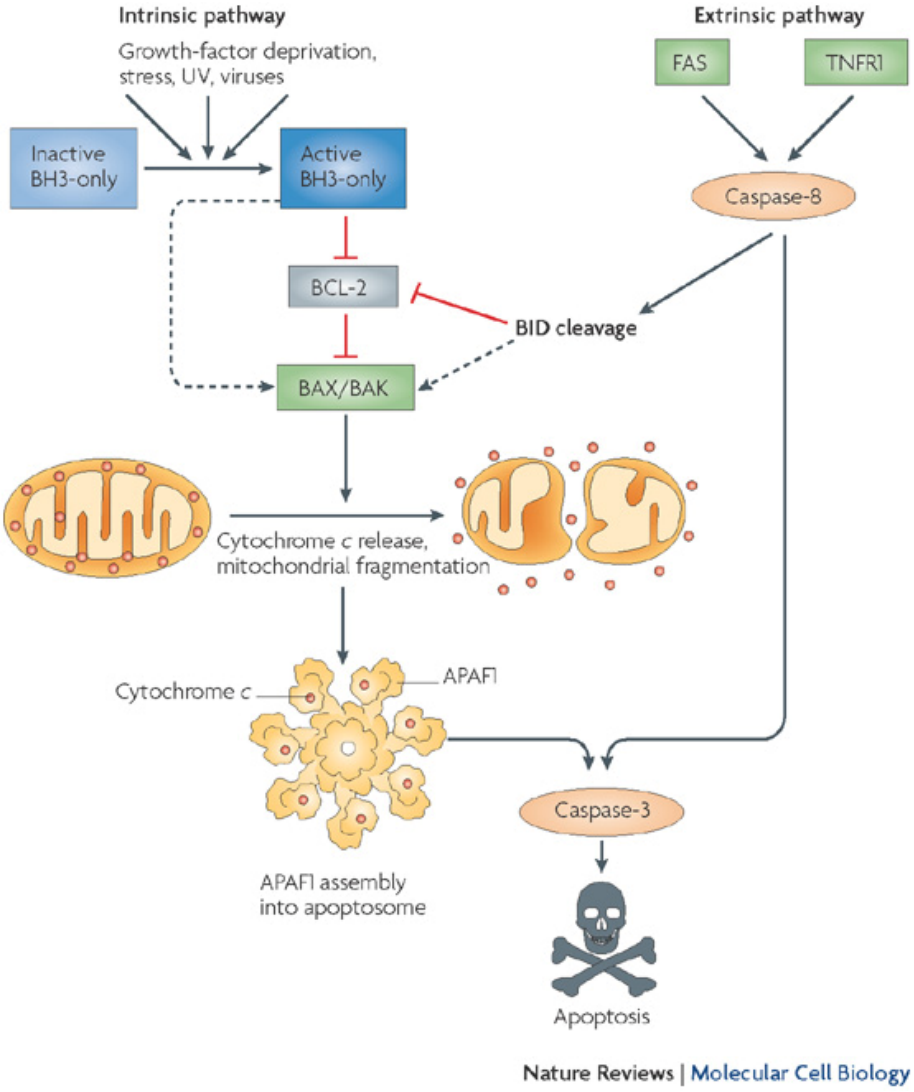

Youle, R. J. and Strasser, A. (2008) *Nat.Rev.Mol.Cell Biol.* **9,** 47-59

Fig 2. *Intrinsic and extrinsic pathway of apoptosis: The intrinsic pathway (left) starts with BH3-only protein induction or post-translational activation, which results in the inactivation of some BCL-2 family members. This relieves inhibition of BAX and BAK activation, which in turn promotes apoptosis. Some BH3-only proteins, such as BIM and PUMA, may also be able to activate BAX and/or BAK (as shown by the dotted line). Once activated, BAX and BAK promote cytochrome* c *release and mitochondrial fission, which leads to the activation of APAF1 into an apoptosome and activates caspase-9 to activate caspase-3. Caspases in turn cleave a series of substrates, activate DNases and orchestrate the demolition of the cell. The extrinsic pathway (right) can bypass the mitochondrial step and activate caspase-8 directly, which leads to caspase-3 activation and cell demolition. The BCL-2 family regulates the intrinsic pathway and can modulate the extrinsic pathway when cleavage of BID communicates between the two pathways.*

In lymphocytes, caspase activation and subsequent apoptosis may be induced by two distinct pathways. One is called the intrinsic, or mitochondrial, pathway of apoptosis,

which is associated with mitochondrial permeability changes. The other is called the extrinsic pathway of apoptosis, which is associated with signals from death receptors in the plasma membrane (Fig.2). Intrinsic apoptosis is passive cell death which results from loss of survival stimuli and extrinsic apoptosis is activation-induced cell death mediated by death receptors.

1-1-1 Extrinsic cell-death-receptor and caspase-dependent apoptosis

In the extrinsic apoptotic pathway, pro-apoptotic signals are delivered through cell-death-receptor-adaptor molecules to their ligands, such as tumour-necrosis factor (TNF), CD95 ligand (CD95L; also known as FASL) and TNF-related apoptosis-inducing ligand (TRAIL). The cell-death receptors, defined by the presence of a DD, include several members of the TNF receptor (TNFR) superfamily: TNFR1, CD95 (also known as FAS or APO-1), TRAIL receptor-1 (TRAILR1), TRAILR2, death receptor 3 (DR3) and DR6 (8-10). The transduction of the apoptotic signal from the cell-death receptors assembled a structure on the plasma membrane that is known as the DISC (death-inducing signalling complex). After the death domain is activated, further pro-apoptotic signals are delivered through caspase cascade. For example, CD95L bind to CD95, then leads to the formation of the CD95 DISC, which activate caspase-8 and caspase-10.

There are two types of CD95-mediated extrinsic apoptotic signalling pathways (11).

Type I: Cells are characterized by high levels of CD95 DISC formation and high amounts of active caspase-8. Activated caspase-8 and caspase-10 directly lead to the activation of downstream effector caspase-3, caspase-6 and caspase-7.

Type II: There are lower levels of CD95 DISC formation, therefore, lower levels of active caspase-8. In this case, signalling requires an additional amplification loop, which involving the molecules from mitochondria. In this loop, caspase-8 cleaved Bid into truncated Bid (tBid). Subsequently, tBid releases cytochrome c from the mitochondria. The release of cytochrome c from the mitochondria results in formation of a large protein complex, called apoptosome. Apoptosome activates pro-caspase-9, which in turn allows caspase-9 to cleave the downstream effectors pro-caspase-3, pro-caspase-6 and pro-caspase-7. CD95 signalling in Type II cells can be blocked by Bcl-2 family members, such as Bcl-2 and Bcl-xL.

1-1-2 Intrinsic mitochondria and caspase-dependent apoptosis

In the intrinsic pathway of apoptosis, the caspase cascade can be triggered by several stimuli, including TCR stimulation, UV-irradiation, DNA damage, endoplasmic reticulum (ER) stress, hormones (such as glucocorticoids) and cytokine deprivation. This pathway crucially depends on permeabilization of the outer mitochondrial membrane (12;13). Mitochondrial membrane permeabilization results in the release of mitochondrial content, such as cytochrome c. Cytochrome c and cytoplasmic apoptotic-protease-activating factor 1 (APAF1) form the protein complex apoptosome. At apoptosome, the initiator pro-caspase-9 is recruited by the interaction of CARD with APAF1. Then caspase-9 is activated and leads to the activation of the effectors caspase-3, caspase-6 and caspase-7. Therefore, the extrinsic and intrinsic apoptotic pathways converge at the level of the effector caspases.

The release of apoptogenic factors from mitochondria is regulated by the interaction of a group of pro- and anti-apoptotic members from Bcl-2 family (14)(Fig.3). Structurally, members of the Bcl-2 family contain up to four conserved homology domains (BH-domains), and optionally a transmembrane segment. Bcl-2, Bcl-xL, Bcl-w, Mcl-1, A1, and CED-9, the homolog in C. elegans, share the BH domains 1–4 and promote cell survival, while mammalian Bax, Bak, Bok, and D. melanogaster DEBCL/DROB are related to Bcl-2 at BH1–3, and promote cell death. There is another sub-class of pro-apoptotic Bcl-2 family members, the BH3-only proteins: mammalian Bad, Bik, Blk, Hrk/DP5, Bid, Bim, Noxa, and C. elegans EGL-1. They share with their relatives only the short BH3 interaction domain (13). Apoptosis is initiated by the BH3-only Bcl-2 family members. And pro-apoptotic Bax and Bak act downstream in this pathway. Notably, Bid works as a conection between death-receptor pathway and the mitochondrial route of apoptosis. As mentioned before, upon CD95-ligation, Bid is cleaved by caspase-8 and migrates to the mitochondria to promote the release of cytochrome c. There is also evidence showing that Bid directly interactes with Bax and Bak.

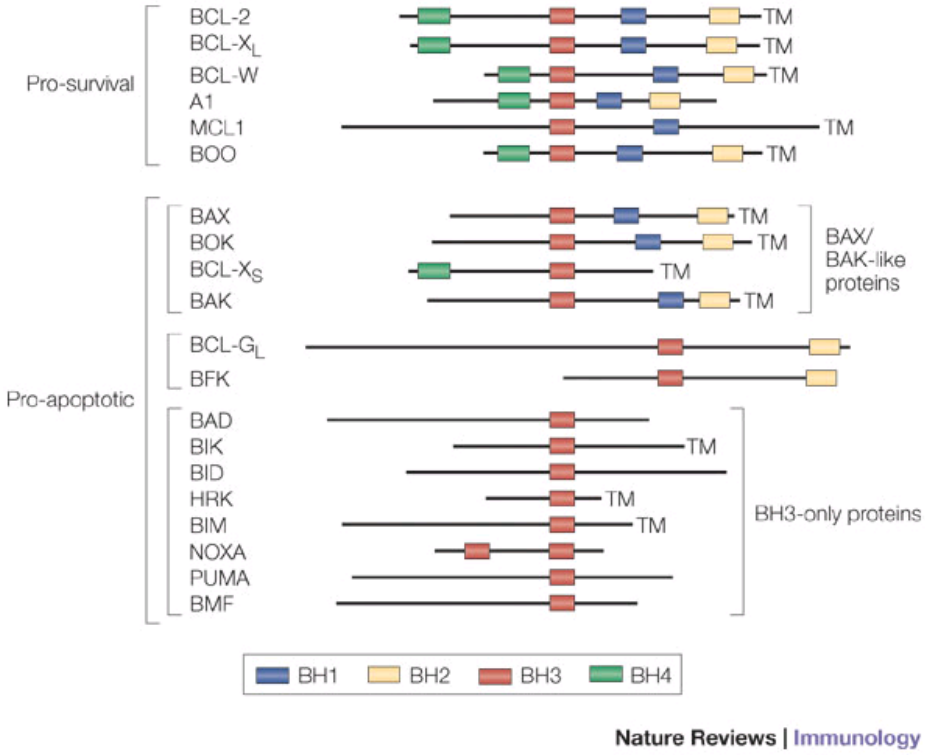

Strasser, A. (2005) *Nature Rev.Immunol.* 5, 189-200

Fig 3. *Mammalian BCL-2 family member: The pro-survival family members — BCL-2, BCL-XL, BCL-W, A1, MCL1 (myeloid-cell leukaemia sequence 1) and BOO (BCL-2 homologue of ovary) — each have two or four distinct BCL-2-homology (BH) domains. The pro-apoptotic members of the BCL-2 family can be subdivided into at least two groups: the BAX /BAK-like proteins — BAX, BOK (BCL-2-related ovarian killer), BCL-X_S and BAK; and the BH3-only proteins — BAD, BIK, BID, HRK (harakiri), BIM, NOXA, PUMA and BMF (BCL-2-modifying factor) — which share with each other and other members of the BCL-2 family only the short (9–16 amino acid) BH3 domain.*

After an infection is cleared, most T cells generated during the clonal expansion phase are removed through either of two apoptotic pathways, termed activation-induced cell death (AICD) and activated cell autonomous death (ACAD). AICD is thought to depend mainly on an extrinsic form of apoptosis induced by the ligation of death receptors such as Fas on the surface of the T cell. ACAD is thought to depend on an intrinsic form of cell death which is regulated by Bcl family (15).

1-1-3 Activation-induced cell death (AICD)

TCR restimulation of already expanded T cells in the absence of appropriate co-stimulation may also lead to the efficient induction of cell death. This is called activation-induced cell death (AICD) (16;17).

AICD involves stimulation through CD95 (18;19) TNFR1 (20) TRAILR (21-23) and other mechanisms independent of cell-death receptor (24). Some findings suggest that TNF is involved in the late phase of AICD (25). AICD can be mimicked by an in vitro model system using TCR-activated T cells cultured with IL-2 and restimulated through the TCR or by PMA and ionomycin (26).

After approximately 4 to 7 days of TCR restimulation in vitro culture results in the expression of CD95L (27-29). This induces CD95-mediated cell death either of the same cell (suicide) or of neighbouring cells (fratricide). The induction of CD95L expression requires calcium mobilization and production of reactive oxygen species (ROS) which is mediated by protein kinase Cθ (PKCθ) (30). Therefore, the CD95 system has been considered to be an important regulator of T-cell homeostasis. Mice with decreased levels of CD95 or mutations in the gene encoding CD95L (lpr or gld mice, respectively) produce autoantibodies and develop lymphoproliferative disease (31;32). However, specific deletion of the gene encoding CD95 in all T cells leads to lymphocyte depletion and pulmonary fibrosis-like disease (33). Therefore, CD95 inactivation in T cells alone is not sufficient for the pathogenesis of lymphoproliferation. These results indicate that in addition to the CD95 system, there are other CD95-independent AICD pathways that regulate T-cell homeostasis.

After TCR triggering, the expression of Bim is also increased, which suggests Bim is a mediator of AICD as well. Upregulation of Bim expression by TCR triggering

depends on the activities of p38 and JNK, and may also involve PKC and calcium signaling (24).

Non-caspase proteases have also been implicated in T-cell death. A serine protease called granzyme B plays a role in AICD of TH2 cells but not of TH1 cells (24). Granzyme B is an effector molecule of cytotoxic T cells which is located in intracellular lytic granules (34). Subsequently, granzyme B was found to be upregulated in response to TCR stimulation in TH2 cells and led to AICD which was independent of CD95–CD95L engagement. In granzyme-B-deficient mice, AICD was abrogated in TH2 cells. And the accumulation of TH2-cell-associated cytokines increased their susceptibility to allergen-induced asthma.

It has further been shown that in epithelial cells, lysosomes are also involved in the execution of cell death (35). Lysosomal proteases, such as cathepsin B, are activated by proteolytic processing as a result of lysosomal stress and are released into the cytosol. Cell death by cathepsins might involve the mitochondria (36;37), or cell-death-receptor stimulation (38).

1-1-4 Activated cell-autonomous death (ACAD)

Autonomous cell death occurs in the absence of appropriate survival signals such as cytokine deprivation or by neglect. This is called activated cell-autonomous death (ACAD) (39).

Bim is essential for ACAD. The expression of Bim or PUMA increased after cytokine deprivation (40). On the mitochondrial membrane, Bim or PUMA can bind Bcl-2 or Bcl-xL, which abrogates the inhibition of Bax or Bak and results in cytochrome c

release and the induction of T-cell death (41;42). During the expansion phase T cells can switch from a Bcl-xL high to a Bcl-xL low state, which allow the activation of the intrinsic apoptotic pathway (43). Bad also plays a role in activating or enhancing apoptosis in cells removed from required cytokines. In the presence of cytokines, Bad is phosphorylated by kinases such as Akt, PKA, and Rsk and is sequestered by 14-3-3 proteins in the cytosol. Upon removal of cytokine, Bad is dephosphorylated and translocates to the mitochondria, where it binds Bcl-2 and Bcl-xL and inhibits their antiapoptotic function (15).

1-2 T cell memory

Prior to contact with antigen, naive T cells congregate in the secondary lymphoid tissues (spleen, lymph nodes, and Peyer's patches) and migrate continuously from one lymphoid organ to another via blood and lymph (44). After encountering pathogens, naive T cells go through clonal expansion and differentiation into effector cells. In a typical viral infection, this will last 7–10 days until the pathogen is eliminated. After that, these activated T cells will undergo clonal shrinkage to keep T cell homeostasis.

The disappearance of activated T cells at the end of the primary response involves two distinct mechanisms, death and homing to nonlymphoid tissues. First, many of the activated T cells leave the spleen and localize in nonlymphoid tissues, notably the lungs, liver, and gut (44). Second, in both lymphoid and nonlymphoid tissues, the majority of the T cells (90–95%) die within 5 days, those cells that survived become memory cells (45) (Fig.4).

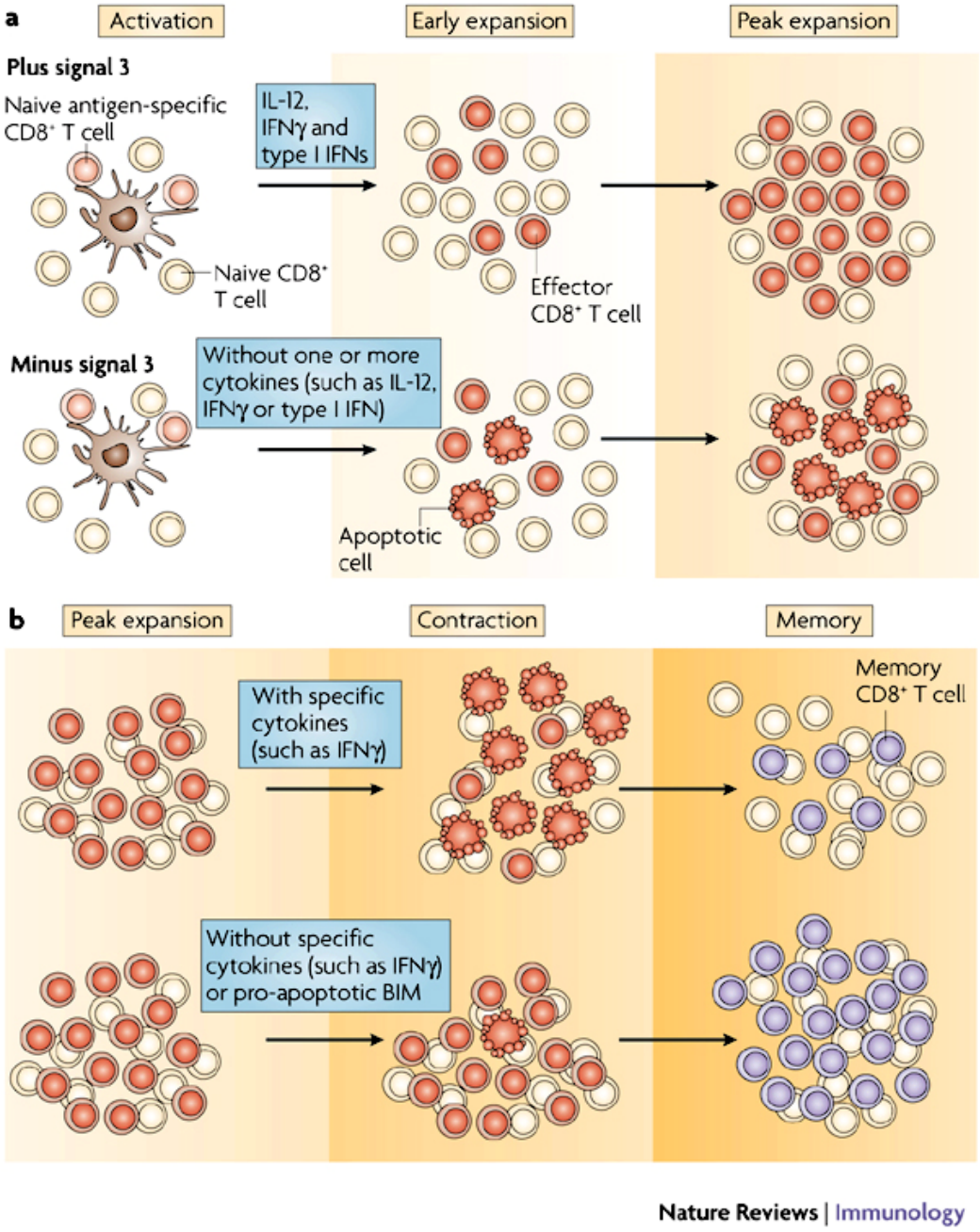

Harty, J. T. and Badovinac, V. P. (2008) *Nat.Rev.Immunol.* **8,** 107-119

Fig 4*. Inflammatory cytokines and CD8+ T-cell homeostasis after infection: Antigenic peptides presented naive CD8+ T cells trigger their proliferative expansion and differentiation into effector CD8+ T cells.5–10% of CD8+ T cells detected at the peak of the expansion survive the contraction phase and initiate the memory CD8+ T-cell pool. The contraction phase is diminished in the absence of inflammation (for example the absence of IFNγ) or when the balance and activation state of pro- and anti-apoptotic BCL-2 family members expressed by CD8+ T cells is altered. Diminished contraction results in increased numbers of memory CD8+ T cells.*

Based on the expression of homing molecules on their surface, memory T cells can be divided into two subsets. $CD62L^{low}$ CCR7(CC-chemokine receptor 7)^{low} are defined as effector memory T cells, while $CD62L^{hi}$ $CCR7^{hi}$ are defined as central memory T cells (46-48).

Current evidence suggests that the survival of memory T cells is not dependent on persistent antigen. In fact, memory T cells are less dependent on antigen receptor engagement for survival than naive T cells. Instead, cytokines are important in maintaining memory T cell viability. After pathogen and antigen are cleared in acute infection, memory $CD8^+$ T cells are maintained by signals through receptors that contain the common cytokine receptor γ-chain such as receptors for IL-7 and IL-15. IL-7 and IL-15 appear to deliver survival and proliferative signals to memory $CD8^+$ T cells, respectively (49;50).

1-2-1 Clonal expansion

Naive T cell activation needs both peptide–MHC complexes (signal 1), and co-stimulatory signals (signal 2) (51;52). Moreover, activation of innate immune cells induces the production of pro-inflammatory cytokines, such as type I IFNs, IL-12 and IFNγ (53). Recent studies demonstrated that pro-inflammatory cytokines act directly on responding $CD8^+$ T cells to affect crucial aspects of memory generation (signal 3). Early *in vitro* studies showed that the addition of IL-12 or type I IFNs to T-cell cultures enhanced the proliferation and survival of the activated T cells. These studies led to the concept that signal 3 was important for optimal $CD8^+$ T-cell responses (54;55). T cells deficient in various cytokine receptors (for example, for type I IFNs,

IL-12 or IFNγ) have reduced expansion (56-58). Importantly, the absence of these pro-inflammatory cytokine receptors does not compromise proliferation of these gene-deficient TCR-transgenic T cells; instead it decreases their survival rates (56-58). How these cytokines act on the survival of activated T cells is not clear yet, but it's possible that they might increase the expression of pro-survival molecules such as Bcl-3 or potentially alter the balance of pro-apoptotic and anti-apoptotic Bcl-2-family members to promote T-cell survival during proliferation (54;59).

1-2-2 Clonal contraction

Following acute or persistent infection, activated T-cells go to clonal contraction through two apoptotic pathways, AICD and ACAD (60).

Early *in vitro* studies showed that effector, but not memory $CD8^+$ T cells exhibited heightened sensitivity to AICD through CD95 and TNF-mediated cell-death pathways (61;62), whereas *in vivo* studies showed normal contraction of $CD8^+$ T cells that lack both of these molecules (63;64). Current studies show that the balance and activation state of pro- and anti-apoptotic Bcl-2 family members modulate the death of activated T cells (39;65-68). Deletion of Bim severely compromises the death of superantigen-activated T cells *in vivo* (39) and results in reduced contraction of antigen-specific $CD8^+$ T cells after herpesvirus infection (66). However, in Bim-deficient mice infected with LCMV, some antigen-specific $CD8^+$ T-cells eventually contract. This suggests that additional pathways might contribute to the death of activated $CD8^+$ T cells (14;69;70).

Inflammatory cytokines such as IFNγ and IL-12 can influence the contraction phase as well. $CD8^+$ T cells failed to contract in BALB/c IFNγ-deficient mice after infection with an attenuated (*actA*-deficient) strain of *L. monocytogenes* that was otherwise cleared in wild-type and immunocompromised hosts (71). Also, BALB/c IFNγ-deficient mice and B6 IFNγ-deficient mice have reduced contraction after LCMV infection (71;72). After infection with *L. monocytogenes*, both $CD8^+$ and $CD4^+$ T cells exhibit abnormal contraction in IFNγ-deficient or IFNγR-deficient mice that were treated with antibiotics to eliminate the infection at day 4. So, persistent infection does not explain how IFNγ regulates $CD8^+$ and $CD4^+$ T-cell contraction after infection with *L. monocytogenes* (73;74). IFNγ might act indirectly through cells other than T cells to influence $CD8^+$ T-cell contraction (72;75). Finally, the absence of the IL-12 receptor on antigen-specific T cells not only reduced expansion but also reduced contraction after infection (76). So, pro-inflammatory cytokines contribute important signals to regulate the contraction phase, perhaps by regulating Bcl-2-family members.

Recent studies also suggested that pro-inflammatory signals, specifically IL-12, control the amount of T-bet expression in the responding $CD8^+$ T cells (77). In this model, relative T-bet expression is thought to differentiate short-lived effector $CD8^+$ T cells ($T\text{-}bet^{hi}$) from memory precursor effector $CD8^+$ T cells ($T\text{-}bet^{low}$) and thus determines the cell's fate. However, T-bet-deficient TCR-transgenic $CD8^+$ T cells from P14 mice still contract by more than 80% from the peak of the response following LCMV infection (77) and the LCMV-specific $CD8^+$ T-cell response

appears to undergo normal contraction in T-bet-deficient mice (78). So the link between T-bet and the contraction of the $CD8^+$ T-cell response is still not clear.

How a precise fraction (5–10%) of the responding $CD8^+$ T cells survives to initiate the memory pool is still not clear. Recent data demonstrate that naive $CD8^+$ T cells undergo an initial asymmetric division after interaction with APCs (79). This raised the possibility that the segregation between long-term memory T cells versus short-lived effector-T-cell may be a very early event in the $CD8^+$ T-cell response.

Many molecules are involved in T cell activation and apoptosis program. Through DNA microarray analysis of the mRNA expression profile of activation versus resting mouse T cells, we identified a group of differentially expressed genes, which are likely important in T-cell activation and apoptosis. Drak2 is a gene in this group.

2. DAPK and Drak2

2-1 Death-associated protein kinase (DAPK)

Death-associated protein kinase (DAPK) is a Ca^{2+}/calmodulin (CaM)-regulated Ser/Thr kinase that mediates cell death (80-84). Increased DAPK activity, due to overexpression of the kinase, leads to pronounced death-associated cellular changes, which include membrane blebbing, cell rounding, detachment from extracellular matrix, and the formation of autophagic vesicles. Furthermore, DAPK activity is necessary for the induction of cell death by multiple death signals, including those

generated by death receptors, cytokines, matrix detachment, and oncogene-induced hyperproliferation (80).

DAPK belongs to a family of related death kinases, all of which share significant sequence and functional homology (85). This family consists of DAP (86) , DRP-1(DAPk-related protein 1, also known as DAPk2) (87), ZIP kinase [also known as Dlk (DAP-like kinase) or DAPk3] (88), DAPK2 (89), Drak1 and Drak2 (DAPK-related apoptosis-inducing protein kinase-1 and -2) (90)(Fig.5). Each DAPk family member contains at its N terminus a catalytic domain composed of the typical 11 subdomains found in all Ser/Thr kinases (80). Phylogenetically, the DAPK family is most closely related to the family of CaM-regulated kinases, in particular to myosin light chain kinase, which shares 44% identity within the corresponding catalytic domain (83). Beyond the common kinase domain, the family members differ in structure. DAP, DRP-1 and DAPK2 have a calmodulin regulatory domain following the kinase domains, ZIP, Drak1 and Drak2 do not (85). This domain serves to suppress catalytic activity by binding to the catalytic cleft, and functions as a pseudosubstrate. In addition, this domain undergoes autophosphorylation at Ser308, an inhibitory event that reduces its affinity to CaM and may further stabilize its docking within the substrate-binding site (80). The C terminus of DAPk contains a death domain, followed by a 17-aa tail rich in Ser residues, a feature common to other death domain-containing proteins (87). The 52-kDa ZIPk possesses a C-terminal leucine zipper motif, which mediates homodimerization and interactions between ZIPk and additional leucine zipper-containing proteins, such as activating transcription factor (ATF)4 (88).

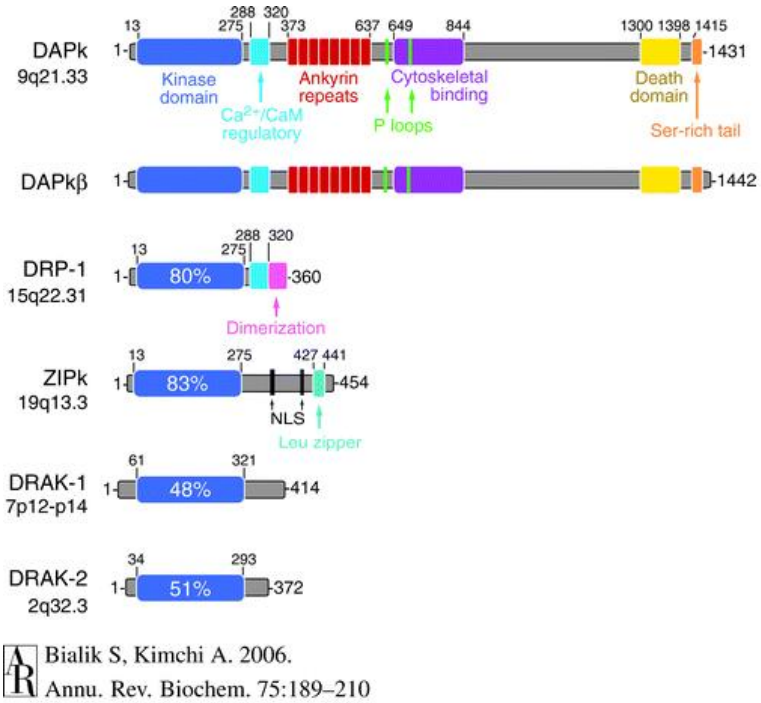

Bialik, S. and Kimchi, A. (2006) *Annu.Rev.Biochem.* **75,** 189-210

Fig 5. *Death-associated protein kinase (DAPK) family member: The numbers above the proteins demarcate the amino acid position of each domain. The quantities within the kinase domains indicate the degree of amino acid identity to the kinase domain of DAPk.*

2-2 DRAK2

Drak2 shares about 50% identity in the kinase domain with other members of the DAPK family (86). DAP, DAPK2, and DRP-1 are localized in the cytosol, ZIP kinase and Drak1 reside mainly in the nuclei, whereas Drak2 is found in both the cytosol and nuclei (90;91), suggesting different mechanisms of action. An *in vitro* kinase assay revealed that both DRAKs are autophosphorylated and phosphorylate myosin light chain as an exogenous substrate (91). Furthermore, overexpression of both DRAKs induces the morphological changes of apoptosis in NIH 3T3 cells, suggesting the role of DRAKs in apoptotic signaling (90). CHP interacts with the carboxyl-terminal

region of the kinase domain of DRAK2 and specifically inactivates DRAK2 kinase activity (92).

In *Drak2*$^{-/-}$ mice, *Drak2*$^{-/-}$ T cells did not demonstrate any defects in apoptosis or negative selection. However, T cells from *Drak2*$^{-/-}$ mice exhibited enhanced sensitivity to T cell receptor-mediated stimulation with a reduced requirement for costimulation. *Drak2*$^{-/-}$ mice were remarkably resistant to experimental autoimmune encephalomyelitis (EAE) (93). This study suggests that DRAK2 raises the threshold for T cell activation by negatively regulating signals through the TCR.

However, our study (to be elaborated later) demonstrated that the conclusion based on Drak2$^{-/-}$ mouse study was flawed, due to the superficial investigation by McGargill et al. As a matter of fact, Drak2 is actively involved in T-cell apoptosis and memory T cell development (94).

At the molecular level, apoptosis of T cells and other type of cells shares many common mechanisms. The important role of Drak2 in T-cell apoptosis led us to believe it is also essential in the survival of other type of cells, such as β-cells in the pancreatic islets, which are vital in maintaining normal blood glucose levels. Pathological changes in islets lead to diabetes.

3. Diabetes

Diabetes mellitus is one of the most common endocrine disorders in the world (Fig.6). Now, almost 6% of the world's population is affected by this disease. And the number will reach 300 million in 2025, within them, 97% will be type 2 diabetes (95).

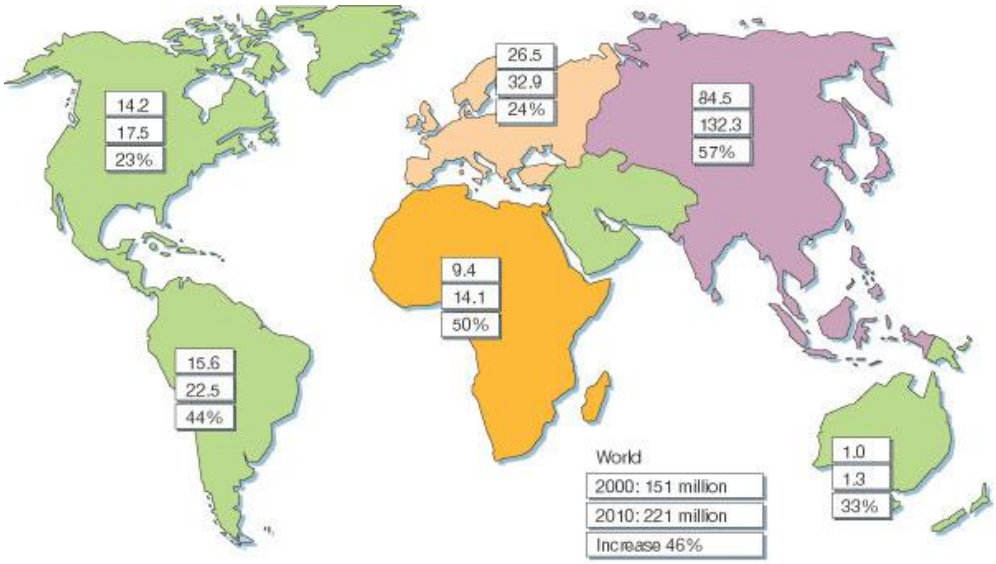

Zimmet, P., Alberti, K. G., and Shaw, J. (2001) *Nature* **414,** 782-787
Fig 6*. Numbers of people with diabetes (in millions) for 2000 and 2010 (top and middle values, respectively), and the percentage increase.*

There are two main forms of diabetes, type 1 and type 2. Both types are characterized by progressive ß-cell failure (Fig.7). Type 1 diabetes is caused by an autoimmune assault against the ß-cells (96), while the cause of type 2 diabetes is more variable, including environmental factors such as physical inactivity, obesity and genetic factors. Environmental factors can modify the expression of susceptible diabetes genes, and cause ß-cell failure and insulin resistance (96).

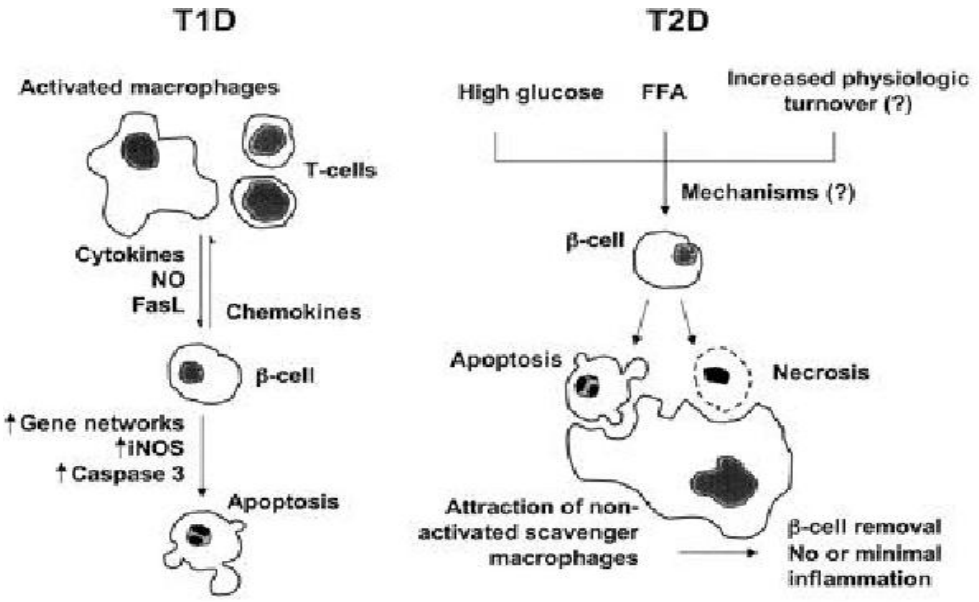

Cnop, M., Welsh, N., Jonas, J. C., Jorns, A., Lenzen, S., and Eizirik, D. L. (2005) *Diabetes* 54 Suppl 2**,** S97-107

Fig 7. *β-cell death in T1D and T2D: Overview of the putative sequence of events leading to β-cell death in animal models of type 1 and type 2 diabetes.*

3-1 Type 1 diabetes

In type 1 diabetes, β-cell mass is reduced by 70–80% at the time of diagnosis (97). Because of the variable degrees of insulitis and absence of detectable β-cell necrosis, it was suggested that β-cell loss occurs slowly over years. In antibody-positive individuals, progressive decline in first-phase insulin secretion, impaired fasting or glucose tolerance are usually found long before the development of overt diabetes (97). For patients with long-term type 1 diabetes, some β-cell function remains (C-peptide secretion), although β-cell mass is usually decreased to less than 1% of normal (98).

The β-cell loss is due to autoimmune attack. Typically in type 1 diabetes, autoantibodies reacting with glutamic acid decarboxylase (GAD65), insulin, and

insulinoma antigen-2 can be found (99). Some adults with type 2 diabetes also express anti-islet autoantibodies (most often GAD65 autoantibodies). These patients are called LADA (latent autoimmune diabetes of the adult). They have both insulin resistance as well as anti-islet autoimmunity. So type 1 and type 2 diabetes can coexist (100).

β-cell death in the course of insulitis is caused by direct contact with activated macrophages and T-cells, and/or exposure to soluble mediators secreted by these cells, including cytokines, nitric oxide (NO), and oxygen free radicals (101). The execution of β-cell death occurs through activation of mitogen-activated protein kinases, ER stress and by the release of mitochondrial death signals (96). In vitro exposure of β-cells to IL-1β, or to IL-1β + IFN-γ, causes functional changes similar to those observed in pre-diabetic patients, such as elevated proinsulin/insulin levels (102), and a preferential loss of first-phase insulin secretion in response to glucose.

Apoptosis is the main cause of β-cell death at the onset of type 1 diabetes. It is a highly regulated process, which is activated and/or modified by extracellular signals, intracellular ATP levels, phosphorylation cascades, and expression of pro- and anti-apoptotic genes (101). Cytokines induce stress response genes that are either protective or deleterious for β-cell survival. There are around 700 genes identified to be up- or downregulated in purified rat β-cells or insulin-producing cells after 1–24 hour of exposure to IL-1β and/or IFN-γ by microarray experiments (Fig.8). IL-1β activates the transcription factor nuclear factor (NF)-κB in rodent and human islet cells (101), and IκB protects pancreatic β-cells against cytokine-induced apoptosis (103;104). NF-κB was also found to downregulate the expression of other transcription factors responsible for β-cell differentiation and function. NF-κB

regulates expression of inducible nitric oxide synthase (iNOS) in β-cells, and ~50% of the ß-cell genes modified after 12 h of cytokine exposure are secondary to iNOS-mediated NO formation. So IL-1β induced NF-κB activation plays a crucial role in controlling multiple and distinct gene regulatory networks in β cell. It affects the β-cell differentiation and ER Ca^{2+} homeostasis, attracts and activates immune cells, and directly contributes to β-cell apoptosis.

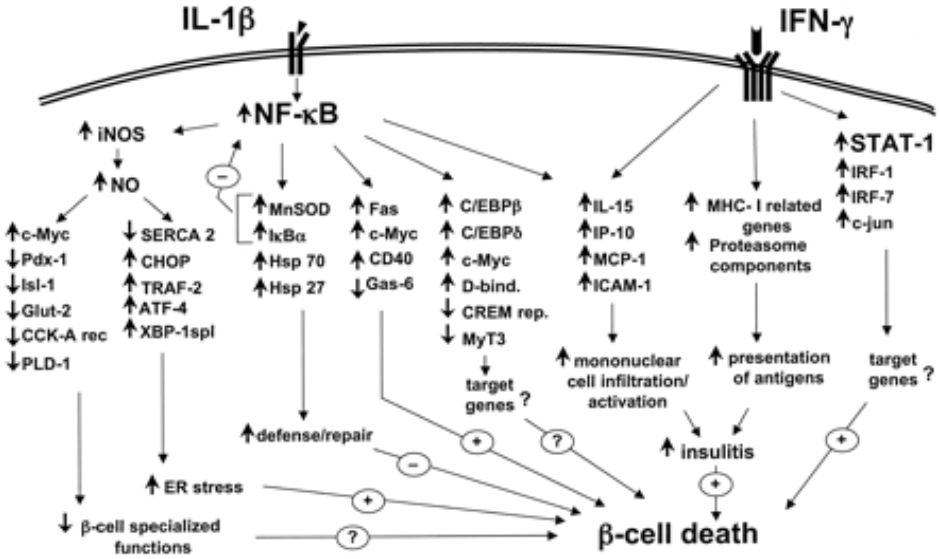

Cnop, M., Welsh, N., Jonas, J. C., Jorns, A., Lenzen, S., and Eizirik, D. L. (2005) *Diabetes* 54 Suppl 2**,** S97-107

Fig 8. *The transcription factor and gene networks putatively involved in the cytokine-promoted ß-cell "decision" to undergo apoptosis: The transcription factors NF-κB and STAT-1 are the main regulators of the pathways triggered by IL-1β and IFN-γ, respectively.*

However, exposure of purified human or rodent β-cells to IL-1β alone is not sufficient to induce apoptosis, but when IL-1β is combined with IFN-γ, ~50% of these cells undergo apoptosis after 6–9 days (101). This suggests that IFN-γ signal transduction must synergize with IL-1β signaling to trigger β-cell apoptosis (Fig.9). IFN-γ binds to cell surface receptors and activates the tyrosine kinases JAK1 and JAK2. These

kinases phosphorylate the transcription factor STAT-1, which dimerizes and translocates to the nucleus to bind to γ-activated sites of diverse genes (101). STAT-1 mediates the potentiating effect of IFN-γ on IL-1β–induced iNOS expression. Fluorescence-activated cell sorting (FACS)-purified β-cells from STAT-1–deficient mice (STAT-$1^{-/-}$) are protected against IL-1β + IFN-γ–induced apoptosis. Because excessive activation of JAK/STAT signaling may lead to cell death, STAT transcriptional activity is regulated by multiple negative feedback mechanisms. These include dephosphorylation of JAK and cytokine receptors by SHP, and inhibition of JAK enzymatic activities by the suppressor of cytokine signaling (SOCS) family. Upregulation of SOCS-1 or SOCS-3 protects β-cells in vitro and in vivo against cytokine-induced death. SOCS-3 also protects insulin-producing cells against IL-1β–mediated apoptosis via NF-κB inhibition. The results indicate that β-cell fate after cytokine exposure depends on the duration and severity of perturbation of key β-cell gene networks. NF-κB and STAT-1 play important roles in this network.

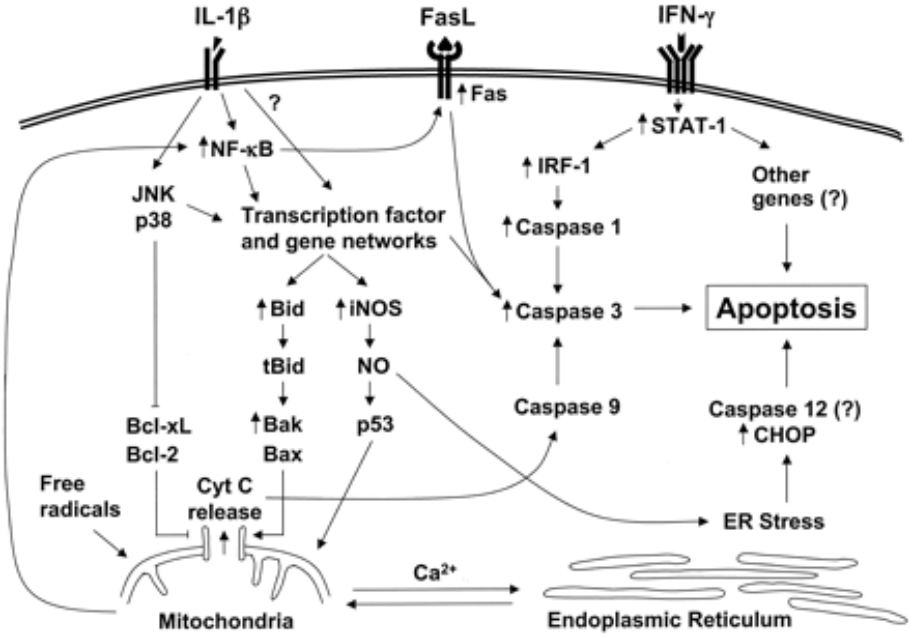

Cnop, M., Welsh, N., Jonas, J. C., Jorns, A., Lenzen, S., and Eizirik, D. L. (2005) *Diabetes* 54 Suppl 2**,** S97-107

Fig 9. *Cytokine-induced ß-cell apoptosis: Arrows indicate genes for which expression was modified by cytokines in a time course microarray analysis. β-Cell apoptosis is probably mediated by three main pathways—namely JNK, ER stress, and liberation of pro-apoptotic proteins from the mitochondria.*

Another question is to understand how the cytokine-activated gene expression results in β-cell death. The probable mechanisms include the following: *1*) Fas/FasL pathway (105), 2) activation of the stress-activated protein kinases c-Jun NH_2-terminal kinase (JNK), p38 mitogen-activated protein kinase (MAPK), and extracellular signal-regulated kinase (ERK); 3) triggering of ER stress; and 4) the release of death signals from the mitochondria.

Effector T cells induce apoptosis of β-cells. This then leads to absolute insulin deficiency and clinically manifest as diabetes, at least in the murine model of the autoimmune diabetes-NOD (nonobese diabetic) mice. T cell effector pathways involving Fas/Fas-ligand (Fas-FasL) interaction or the perforin/granzyme system are primarily responsible for the beta cell destruction. Perforin production from $CD8^+$ T cells initiates the immune response, and then Fas/FasL interaction causes $CD4^+$ T cell-induced beta cell death (100; 104).

JNK is a member of the MAPK family. Pancreatic β-cells exposed to IL-1β have an early and sustained increase in JNK activity, which can be potentiated by IFN-γ or TNF-α (101;106). Cell-permeable peptide inhibitors of JNK prevent cytokine-induced apoptosis in insulin-producing cells (107), but this remains to be confirmed in primary β-cells. p38 MAPK and ERK are also activated by cytokines, and pharmacological inhibition of these MAPKs diminish cytokine-induced rat islet cell death (108;109),

probably by attenuating transcriptional activation of iNOS. In addition, the tumor suppressor p53 is activated in response to cytokine-induced NO production (110). It is conceivable that stabilization of the pro-apoptotic protein p53 lies downstream of the NO-induced activation of MAPKs.

Disruption of ER homeostasis, as induced by changes in ER Ca^{2+} concentrations, triggers accumulation of unfolded proteins and activation of a specific stress response, which is called the ER stress response. This cellular response is a coordinated attempt to restore ER homeostasis and function, and it includes translational attenuation, upregulation of ER chaperones, and degradation of misfolded proteins. In prolonged and severe ER stress, the apoptosis program will be activated and executed by the transcription factor CHOP (C/EBP(CCAAT/enhancer binding protein) homologous protein), MAPK JNK, and caspase-12. Because of their high rate of protein synthesis, β-cells are particularly susceptible to ER stress (111). And NO induced ER stress response in β-cells leads to CHOP expression and apoptosis (112).

Mitochondria play an important role in β-cell function and survival (113), as well as in triggering apoptosis. Members of the Bcl-2 protein family regulate the mitochondrial response to pro-apoptotic signals (114), preventing release of mitochondrial proteins such as cytochrome c. When cytochrome c is liberated to the cytosol, it will sequentially activate caspase-9 and -3 and execute cell death (115). Overexpression of Bcl-2 partially protects mouse (116) and human (117) islets against cytokine-induced cell death, but does not prevent adenovirus-induced islet cell death (118) or spontaneous diabetes in NOD mice (119). Caspase-1 is induced in β-cells exposed to IL-1ß + IFN-γ (120) , and blocking caspase-1 decreases β-cell apoptosis after 4 days

exposure to cytokine, but can not prevent their subsequent death by necrosis after 9 days. These results suggest the possibility that during the early stage of cytokine exposure, nucleus, mitochondria, and ER could work togther to decide the fate of β-cell to undergo apoptosis or not. Other pro-apoptotic genes that are induced by cytokines, as detected by microarray analysis (121), includes Bid, Bak, and caspase-3.

3-2 Type 2 diabetes

Modern lifestyle, with abundant nutrient supply and reduced physical activity, resulted in dramatic increases of type 2 diabetes (95). It occurs when the endocrine pancreas fails to secrete sufficient insulin to cope with the metabolic demand (122). Initially, reduced insulin sensitivity is the major problem, but at later stage, islet apoptosis also occurs (Fig.10). Three mechanisms are involved in type 2 diabetes: 1. Insulin risistance, 2. β-cell secretory dysfunction, 3. decreased β-cell mass. In type 2 diabetic subjects, initial pathological studies suggested a β-cell loss of 25–50%. However, recent studies showed a significant reduction in β-cell mass and a threefold increase in β-cell apoptosis (122).

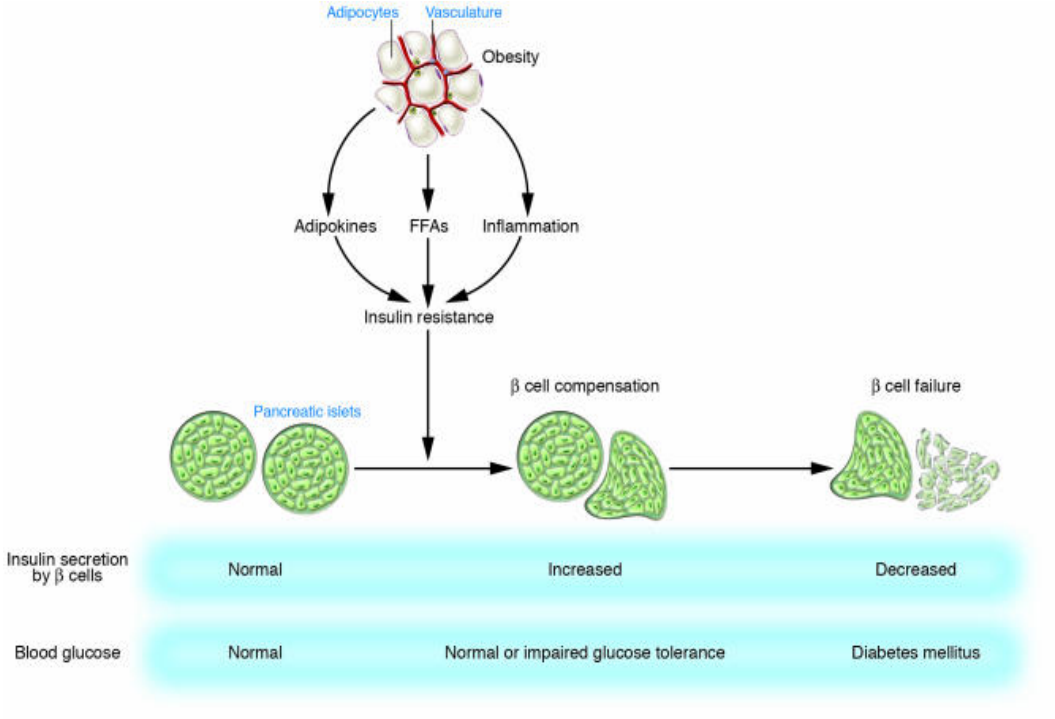

Kasuga, M. (2006) *J.Clin.Invest* **116,** 1756-1760
Fig 10. *Development of type 2 diabetes: Insulin resistance associated with obesity is induced by adipokines, FFAs, and chronic inflammation in adipose tissue. Pancreatic β cells compensate for insulin resistance by hypersecretion of insulin. However, at some point, β cell compensation is followed by β cell failure, and diabetes ensues.*

3-2-1 Insulin resistance

Changes in lifestyle, such as consumption of a high-calorie diet and lack of exercise, have increased the global prevalence not only of diabetes but also of obesity. Between 60% and 90% of cases of type 2 diabetes now appear to be related to obesity. Insulin resistance, which is an impairment of insulin action that precedes the development of hyperglycemia is usually associated with obesity. It is therefore important to characterize the mechanisms of insulin resistance associated with obesity in order to develop approaches to prevent type 2 diabetes.

3-2-1-1 Adipokines

Adipokines are a group of hormones and cytokines that are produced by adipocytes. Adipocytes can store excess lipids and this fuction becomes saturated in obesity, resulting in abnormal redistribution of lipids to other organs and tissues. In the ob/ob mouse, which exhibits hyperphagia, hyperlipidaemia and insulin resistance, the mutated gene is the cytokine-related molecule leptin (123). Leptin and adiponectin have been categorized as 'anti-diabetogenic'; their common function is to decrease triglyceride (TG) synthesis, stimulate β-oxidation and enhance insulin action in both skeletal muscle and liver. These effects can be explained in part by their common ability to activate 5'-AMP-activated protein kinase (AMPK) (124). This enzyme responds to a fall in ATP and a rise in AMP levels by activating both glucose and fatty acid oxidation. Interestingly, leptin levels are increased and adiponectin levels are decreased in insulin-resistant obese humans and animals, which suggests that obesity leads to a state of leptin resistance and adiponectin deficiency.

Animals lacking white adipose tissue have severe hepatic and muscle insulin resistance, and exhibit large increases in TG stores in both tissues (125). This further proves the importance of adipose tissue in the normal regulation of insulin action. Transplantation of normal fat tissue into such mice restores insulin sensitivity (126). Leptin infusion ameliorates insulin resistance in these mice (127;128), while transplantation of fat from leptin-deficient mice into such animals fails to improve insulin sensitivity (129). These data suggest that leptin seems to be the major player in this model. Furthermore, leptin administration to humans with severe lipodystrophy partially reverses their insulin resistance and hyperlipidaemia (130).

Adipose cells also produce other peptide hormones, including adiponectin, retinol-binding protein-4 (RBP4) and resistin, and proinflammatory cytokines such as IL-6 and TNFα (124;131).

Mice with an adipose-specific knockout of the Glucose transporter type 4 (GLUT4) have impaired insulin sensitivity in muscle and liver (132). Circulating RBP4 levels are increased in these mice, and infusion or transgenic expression of RBP4 in normal mice causes insulin resistance (133). Interestingly, food deprivation (fasting) also causes a form of insulin resistance and is associated with a decrease in adipose GLUT4 expression (134). So the original purpose of adipocyte-derived insulin-desensitizing molecules, such as RBP4, TNFα and resistin, may have been to prevent hypoglycaemia in the fasted state, while in modern life style, with abundant nutrient supply, the function of these molecules has been subverted to pathophysiology (135).

3-2-1-2 Inflammatory mediators

Insulin resistance may also caused by inflammatory component (136). High-fat diets or obesity result in activation of the transcription factor NF-κB and its targets in the liver. Overexpression of a constitutively active version of the NF-κB-activating kinase, IκB kinase catalytic subunit-β (IκKβ), in the liver of normal rodents results in liver and muscle insulin resistance and diabetes. In addition, both high-fat feeding and IκKβ overexpression increase hepatic production of IL-6, IL-1β and TNFα; antibody-mediated neutralization of IL-6 in animals fed on a high-fat diet partially restores insulin sensitivity (137). Deletion of IκKβ in the liver can protect mice from diet-induced hepatic insulin resistance, while muscle and adipose insulin resistance still develop. However, myeloid cells specific IκKβ knockout mice remain globally

insulin sensitive (138). In rodents, after one week on high-fat feeding, adipocyte increases the expression of monocyte chemotactic protein-1 (MCP1), which recruits macrophage to adipocytes (139;140). This may be a mechanism by which inflammatory signalling is enhanced during the development of diabetes. Overall, evidence is accumulating that insulin resistance is at least partly caused by changes in hormone and cytokine production by the liver, adipose tissue and infiltrating immune cells in response to chronic exposure to lipids and other metabolic fuels.

3-2-1-3 Metabolic overload in the liver

Lipid species accumulation in the liver results in the redirection of long-chain acyl CoAs (LC-CoAs) into ER-localized and cytosolic lipid species, such as diacylglycerols (DAGs), ceramides and TGs. This is thought to be regulated mostly by glucose-induced increases of malonyl CoA. Malonyl CoA serves both as the immediate precursor of de novo lipogenesis and as an inhibitor of carnitine palmitoyltransferase-1 (CPT1), which is the rate-limiting enzyme for import of LC-CoAs into the mitochondria for β-oxidation (141). Indeed, infusion of lipids or ingestion of high-fat diets in rodents leads to the accumulation of TGs, LC-CoAs, DAGs and ceramides (142-144). Suppression of mitochondrial glycerol-3-phosphate acyltransferase-1 (GPAT1, the first enzyme in TG synthesis) or acetyl CoA carboxylase-2 (ACC2) activity results in increased fatty acid oxidation, lowered DAG levels and reversal of hepatic insulin resistance (145-147). Pharmacological inhibition of Ser palmitoyltransferase-1 (SPT1) or genetic knockout of dihydroceramide desaturase-1 (Degs1) — both of which are involved in the synthesis of ceramides from the saturated precursor palmitoyl CoA — prevented hepatic insulin resistance

induced by glucocorticoid administration or infusion of saturated (but not unsaturated) fats in rodents (148). Finally, when obese patients with type 2 diabetes were fed on a hypocaloric low-fat diet, a modest weight loss (8 kg on average) was observed, but a reversal of hepatic insulin resistance was also seen in concert with a large decrease in intrahepatic, but not intramuscular, lipid deposits (149).

3-2-1-4 Metabolic overload in muscle

In muscle, intramuscular levels of lipid signalling molecules, such as LC-CoAs, DAG and ceramides, positively correlate with TG content and negatively correlate with insulin sensitivity (150;151). Pharmacological or genetic inhibition of ceramide biosynthesis in rodents attenuated muscle insulin resistance caused by infusion of high concentrations of palmitate (151), but not linoleic acid. This suggests discrete mechanisms for different fatty acids. Another study showed that transgenic overexpression of diacylglycerol acyltransferase-1 (DGAT1) in skeletal muscle increased TG content and prevented diet-induced insulin resistance, as well as reduce 20–30% DAG and ceramide levels in muscle (152). However, muscle β-oxidation was not evaluated, and could have been reduced as a consequence of repartitioning lipids into esterification pathways.

Recent work has suggested that mitochondrially derived by-products of lipid oxidation may have a key role in the development of insulin resistance in skeletal muscle (153). Chronic exposure of muscle to elevated lipids induces an increase in expression of genes of the fatty acid β-oxidative pathway (153;154). And the upregulation of the enzymatic machinery for β-oxidation in muscle is not coordinated with upregulation of downstream metabolic pathways, such as the tricarboxylic acid

(TCA) cycle and electron transport chain. This leads to incomplete metabolism of fatty acids and accumulation of lipid-derived metabolites in the mitochondria (153;154). Isolated mitochondria from insulin-resistant rat's skeletal muscles have higher rates of incomplete fat oxidation compared with those from insulin-sensitive muscles (155). These abnormalities were reversed by exercise intervention in mice that were fed on a high-fat diet, in association with increased TCA cycle activity and restoration of insulin sensitivity and glucose tolerance.

Other work has shown that obesity results in impaired switching from fatty acid to carbohydrate substrates during the fasting-to-fed transition and in a coincident reduction in levels of several TCA cycle intermediates (156). This phenomenon, known as metabolic inflexibility (157), was apparent at both the whole-body level and in isolated muscle mitochondria.

3-2-1-5 Relating metabolic overload to insulin signalling

Lipid-derived by-products such as DAG can regulate members of the protein kinase C (PKC) family. These kinases phosphorylate Ser on the insulin receptor and/or its immediate targets, insulin receptor substrate-1 (IRS1) and -2 (IRS2). In this way, they impair insulin-receptor-mediated Tyr phosphorylation of IRS1 and interfere with insulin signalling (158-161). Moreover, overexpression of GPAT1 in rat liver induces hepatic steatosis as well as increased hepatic DAG levels and activation of PKCε (162). While Gpat1-I knockout mice exhibit decreased PKCε activity and enhanced hepatic insulin sensitivity (163). Furthermore, silencing of hepatic PKCε in liver is sufficient to prevent hepatic insulin resistance caused by short-term high-fat feeding (164).

In skeletal muscle, PKCε is activated by lipid infusion in both humans and rodents, and PKCθ-knockout mice are protected from insulin resistance that is caused by acute lipid infusion (144). However, PKCθ is also required for the maintenance of normal skeletal muscle insulin sensitivity (165;166).

Besides lipids, the concentrations of several amino acids are also elevated in obese patients with type 2 diabetes (167). And infusion of amino acids in rodent models or humans impairs skeletal muscle glucose uptake, increases hepatic gluconeogenesis and impairs insulin action (168-170). The machanism of amino acids on insulin signalling involves the activation of mTOR (mammalian target of rapamycin) and ribosomal protein S6 kinase-1 (S6K1). S6k1-knockout mice have increased insulin sensitivity and are protected against diet-induced insulin resistance. In modern lifestyle, the consumption of protein is also increased, so amino-acid-induced pathways might synergize with lipid-induced mechanisms to cause the full syndrome of obesity-associated impairment of insulin action.

Excess lipids and other metabolic changes associated with overnutrition may trigger stress responses in the ER (171). ER stress activates JNKs, which phosphorylate IRS1, thereby interfering with insulin action.

3-2-2 β-cell secretory dysfunction

The two major mechanisms causing β-cell secretory dysfunction are glucotoxicity and lipotoxicity.

3-2-2-1 Glucotoxicity

Hyperglycemia reduces glucose-induced insulin secretion (GIIS) in β-cell, thereby contributing to the progression from glucose intolerance to overt type 2 diabetes (172).

Rodent β-cells chronically exposed to high glucose display several alterations of their phenotype, including changes in glucose stimulus-secretion coupling, gene expression, cell survival, and cell growth (173). These alterations could result from cytokine, oxidative stress, or ER stress–induced changes in gene expression and cell survival (174;175) or from functional changes such as accumulation of glycogen (176).

The genes involved in GIIS in in vivo and in vitro models of prolonged exposure to high glucose include insulin, GLUT2, glucokinase and voltage-dependent Ca2+ channels, and the transcription factors that regulate their expression (177). These changes have some similarities with those happening under exposure of cytokines (178). On the other hand, several genes expressed at low levels in normal β-cells are induced by hyperglycemia, including hexokinase 1, lactate dehydrogenase and glucose-6 phosphatase. In addition, pro- and anti-apoptotic factors, antioxidant enzymes, and some transcription factors are upregulated. Some of these genes, such as c-Myc, A20, and heme-oxygenase 1, are induced by hyperglycemia as well as cytokines. Hyperglycemia might increase β-cell production of IL-1ß in human islets (106). Howerever, iNOS and IκBα, two NF-κB–dependent genes markedly induced by IL-1β, are not induced in rodent β-cells exposed to high glucose. Other genes, such as lactate dehydrogenase A, the mitochondrial uncoupling protein UCP-2, and the transcription factor CREM, are induced by hyperglycemia and downregulated by cytokines.

3-2-2-2 Lipotoxicity

Circulating adipose tissue–derived products, such as free fatty acid (FFA)s and adipokines, play a direct role in pancreatic ß-cell dysfunction and death. It is proved

that a high plasma concentration of FFAs is indeed a risk factor for the development of type 2 diabetes, independently of its effects on insulin sensitivity (179).

Circulating FFAs are solubilized and transported in millimolar concentrations, because of their tight binding to albumin. Unbound FFA levels measure in the nanomolar range (5–20 nmol/l); at this concentration they are rapidly taken up via a protein-mediated transport. FFAs acutely stimulate insulin secretion, but prolonged β-cell exposure to high FFA levels reduces GIIS in vitro (180) and in vivo, especially in individuals genetically predisposed to type 2 diabetes (181). Studies in the Zucker diabetic fatty (ZDF) rat, which is a type 2 diabetes model and has both insulin resistance and inadequate beta-cell compensation, indicate that high circulating FFAs and triglyceride levels induce triglyceride accumulation in pancreatic islets (182). The associated rise in cytoplasmic FFA levels would increase ceramide formation and induce iNOS, resulting in NO-mediated β-cell apoptosis (183).

For in vitro experiments, physiological concentrations of palmitate and oleate are used to mimic the effect of FFA (96;184). FFAs are toxic to FACS-purified rat β-cells and insulin-producing INS-1E cells. Cytotoxicity depends on the unbound FFA concentration and palmitate has more effect than oleate. The toxic effects of FFAs are potentiated when β-cells are concomitantly exposed to high glucose levels (185;186). FFA-induced cell death occurred in the absence of iNOS expression or NO production, and it was not counteracted by antioxidant or free radical scavenging compounds, suggesting that oxidative stress is not its main mediator. Moreover, oleate or palmitate did not activate NF-κB in INS-1E or β-cells. FFA-induced cytoplasmic triglyceride accumulation was inversely correlated to β-cell death. A mixture of oleate and

palmitate caused the lowest cell death and the highest triglyceride accumulation, whereas bromopalmitate, which did not increase cellular triglycerides, exerted the highest toxicity (187). These findings suggest that storage of excess FFAs as triglycerides protects the cell against accumulation of potentially deleterious fatty acyl-CoA.

FFA-induced β-cell toxicity might occur at the ER level, where FFA esterification takes place. Both oleate and palmitate caused alternative splicing of x-box binding protein-1 (XBP-1), activation of ATF6, and induction of the ER chaperone BiP in INS-1E cells. Besides these specific ER stress markers, ATF4 and CHOP are also activated. It is thus conceivable that a high FFA load, which exceeds the β-cell's esterification capacity, impairs ER functions and triggers an ER stress response, thus contributing to β-cell toxicity. ER stress has been proposed as the cellular/molecular mechanism linking obesity with insulin resistance. So FFAs might be responsible for the ER stress response and impaired β-cell function observed in the hepatocytes and adipocytes of obese mice (188;189).

3-2-3 Decreased β-cell mass

Obese individuals who do not develop diabetes exhibit an increase in β-cell mass that appears to compensate for the increased metabolic load and obesity-associated insulin resistance. However, finaly this β-cell adaptation fails and the subset of obese individuals start to develop type 2 diabetes (122;190).

Pancreatic ß-cell mass is regulated by at least four independent mechanisms: 1. β-cell replication, 2. β-cell size, 3. β-cell neogenesis, 4. β-cell apoptosis.

3-2-3-1 Adaptation of β-cell mass to metabolic load

During adulthood, the β-cell mass is highly adaptive to changes in metabolic homeostasis. When obesity and the inherent insulin resistance occur in humans, β-cell mass first increase through an increase in β-cell replication and neogenesis, as well as β–cell hypertrophy (191). A small increase in β-cell apoptosis has also been observed in nondiabetic obesity; however, this is outweighed by increases in β-cell replication, neogenesis, and cell size, resulting in a net increase in β-cell mass.

3-2-3-2 Failure of β-cell mass to compensate for metabolic load

Although there is an initial compensatory increase in β-cell mass, the onset of type 2 diabetes in both humans and rodent models is accompanied by a progressive decrease in β-cell mass. This β-cell loss arises from a marked increase in β-cell apoptosis, which far outweighs modest increases in β-cell replication and neogenesis (192). As the type 2 diabetic state progresses, the situation gets worse; the incidence of β-cell replication decreases and the β-cell population declines. In humans, the increased β-cell apoptosis in type 2 diabetes is further exacerbated by the formation of amyloid plaque deposits in islets (193). Eventually, type 2 diabetes occurs and the patient must be treated with insulin replacement therapy.

3-2-4 The role of IRS-2 signaling in β-cell survival and apoptosis

Many mechanisms could trigger the increase in β-cell apoptosis that occurs during the pathogenesis of type 2 diabetes such as ER stress, chronic hyperglycemia, chronic hyperlipidemia, oxidative stress, and certain cytokines (122;190).

IRS-2 is an especially potent pathway in promoting β-cell survival and dampening of IRS-2 signaling leads to insulin resistance as well as β-cell apoptosis (194) (Fig.11).

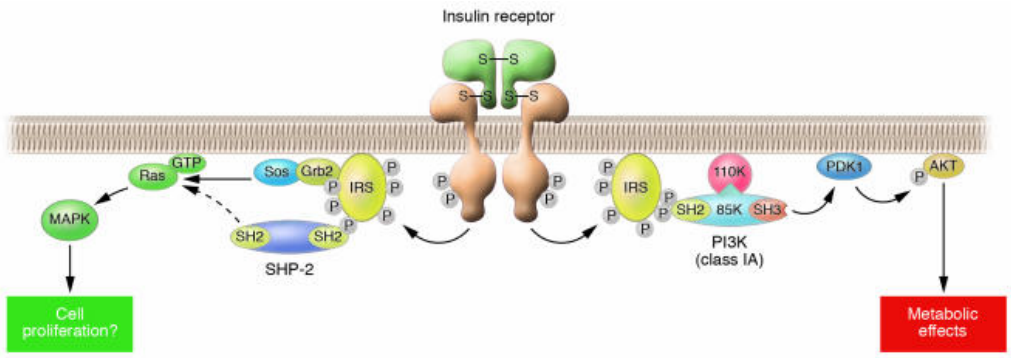

Kasuga, M. (2006) *J.Clin.Invest* **116,** 1756-1760

Fig 11. *Insulin signaling in cells: Insulin elicits its effects by binding to its specific receptor and activating its tyrosine kinase. The activated insulin receptor kinase phosphorylates the intracellular substrate IRS, which then binds various signaling molecules containing the SH2 domain. Among them, the Grb2-Sos complex and SHP-2 transmit mitogenic signals through the activation of Ras. In contrast, PI3K (class IA) transmits the major metabolic actions of insulin via downstream effectors such as phosphoinositide-dependent kinase 1 (PDK1) and Akt.*

IRS protein family are intracellular tyrosine kinase substrates that act as signaling interfaces immediately downstream of cell surface receptors, such as the insulin and insulin-like growth factor-1 (IGF-1) receptors (173). Deletion of IRS-1 and IRS-2 leads to marked insulin resistance, indicating that these genes play a key role in insulin action (195;196). Once an IRS molecule is tyrosine phosphorylated, certain signaling proteins dock to this specific IRS phosphotyrosine site by means of their SH2-domains, resulting in activation of downstream signaling pathways. For examples, phosphatidylinositol-3'-kinase (PI3'K)/protein kinase-B (PKB, also known as Akt) pathway and the Ras pathway that leads to activation of the MAP kinases Erk-1 and Erk-2 (197). Both IRS-1 and IRS-2 are expressed in pancreatic β-cells. IRS-1 is not involved in the control of β-cell mass, but appears to function in cellular Ca2+ homeostasis (198). IRS-2 plays a critical role in regulation of β-cell growth (199). Increased IRS-2 expression can promote ß-cell replication, neogenesis, and survival

(194), whereas decreased IRS-2 expression causes spontaneous β-cell apoptosis (200). Thus, IRS-2 is critically important for maintaining β-cell mass, especially by promoting β-cell survival (194). So, mechanisms leading to suppression of IRS-2 expression in β-cells may be linked to the increased incidence of β-cell apoptosis and the onset of type 2 diabetes.

Tyrosine phosphorylation of IRS-2 leads to increased β-cell growth and survival (192). However, IRS-2 also contains multiple sites for serine/threonine phosphorylation, which, for the most part, have a negative effect on IRS signal transduction by promoting IRS degradation (201). Several mechanisms relevant to the pathogenesis of type-2 diabetes could potentially increase IRS-2 serine/threonine phosphorylation, subsequently resulting in IRS-2 ubiquitination, proteosomal degradation, and ultimately β-cell apoptosis.

Chronic hyperglycemia can lead to chronic activation of mTOR in β cells. Activated mTOR triggers serine/threonine phosphorylation of IRS-2 and its subsequent proteosomal degradation, leading to increased β-cell apoptosis (202). Chronic hyperglycemia can also trigger β-cell apoptosis by additional mechanisms, such as "glucotoxicity."

Hyperlipidemia also causes ß-cell apoptosis by lipotoxicity (203). Other lipotoxic mechanisms include the mitochondrial apoptotic pathway; inhibition of PKB (204); and fatty acid/ceramide–induced activation of the c-Jun N-terminal kinase (Jnk)/p38 stress kinase pathway (205). Interestingly, Jnk/p38-mediated phosphorylation of IRS-2 may also be induced by hyperglycemia, underscoring a likely interplay between glucotoxicity and lipotoxicity mechanisms in β-cell apoptosis (206).

IL-1β also plays a role in inducing β-cell apoptosis in type 2 diabetes (207). In obesity-linked diabetes, leptin, TNFα, and IL-6 are increased. Leptin has recently been shown to modulate IL-1β induced apoptosis in human β cells (208). Some of these cytokines can induce β-cell apoptosis through induction of signaling pathways that activate the transcription factor NF-κB (209). However, they may also activate signaling pathways that trigger increased degradation of IRS-2. Certain cytokines, such as leptin, IL-6, and IFN-γ, activate JAK/STAT. This leads to increased expression of SOCS-1 and SOCS-3 proteins, which normally bind to the leptin, IL-6, and IFN-γ receptors and inhibit JAK-2/STAT signaling. SOCS-1 and SOCS-3 have also been shown to bind to the C terminus of IRS molecules, leading to their ubiquitination and subsequent degradation (210). Thus leptin and IL-6 may cause β-cell apoptosis by decreasing β-cell IRS-2 levels through a similar mechanism. IL-1β and TNFα promote activation of the protein kinase IκK (106). IκK phosphorylates the cytosolic inhibitory protein IκB, resulting in release and activation of NF-κB (106). However, IκK has also been shown to phosphorylate IRS molecules on serine/threonine sites, promoting their degradation (211). In β cells, this could trigger apoptosis. In addition, IL-1β and TNFα are known to activate Jnk/p38 "stress protein kinases" as well PKCδ. Jnk/p38 and PKCδ may also increase the serine/threonine phosphorylation state of IRS-2, leading to IRS-2 degradation and ultimately β-cell apoptosis.

4. Objectives of my work

Our DNA microarray data indicated that Drak2 was significantly modulated during T cell activation. We thus decided to investigate the role of this molecule in the immune system and then extended our study to its role in islet survival and diabetes. The objectives of our studies were as follows.

1) To study the Drak2 expression pattern during ontogeny using in situ hybridization analysis;

   Previous publication on Drak2 failed to detect Drak2 expression outside the T-cell compartment (93). We will employ in situ hybridization to identify localized Drak2 expression in organs and during embryonic development.

2) To investigate the role of Drak2 in T-cell immune response, T-cell survival, and memory T-cell development;

   Drak2 belongs to DAP kinase family which is involved in apoptosis. So we will investigate the role of Drak2 in T cell apoptosis and immune response.

3) To explore the role of Drak2 in islet β-cell survival and its role in type 1 and type 2 diabetes pathogenesis;

   Drak2 gene located close to type 1 and type 2 diabetes loci. This leads us to investigate the role of Drak2 in diabetes.

4) To identify the substrate of Drak2 kinase.

   It's known that Drak2 autophosphorylates itself, and phosphorylates myosin light chain as an exogenous substrate (90). Its endogenous substrates, other than itself, have not been identified. We decide to identify the substrate of Drak2 for the investigation of its signalling pathway.

Reference List

(1) Zhang N, Hartig H, Dzhagalov I, Draper D, He YW. The role of apoptosis in the development and function of T lymphocytes. Cell Res 2005 Oct;15(10):749-69.

(2) Strasser A, Pellegrini M. T-lymphocyte death during shutdown of an immune response. Trends Immunol 2004;25:610-5.

(3) Krueger A, Fas SC, Baumann S, Krammer PH. The role of CD95 in the regulation of peripheral T-cell apoptosis. Immunol Rev 2003;193:58-69.

(4) Krammer PH, Arnold R, Lavrik IN. Life and death in peripheral T cells. Nat Rev Immunol 2007 Jul;7(7):532-42.

(5) Thornberry NA, Lazebnik Y. Caspases: enemies within. Science 1998;281:1312-6.

(6) Lavrik I, Golks A, Krammer PH. Death receptor signaling. J Cell Sci 2005;118:265-7.

(7) Igney FH, Krammer PH. Immune escape of tumors: apoptosis resistance and tumor counterattack. J Leukoc Biol 2002;71:907-20.

(8) Krammer PH. CD95's deadly mission in the immune system. Nature 2000;407:789-95.

(9) Ashkenazi A, Dixit VM. Death receptors: signaling and modulation. Science 1998;281:1305-8.

(10) Tartaglia LA, Ayres TM, Wong GHW, Goeddel DV. A novel domain within the 55 kd TNF receptor signals cell death. Cell 1993;74:845-53.

(11) Scaffidi C. Two CD95 (APO-1/Fas) signaling pathways. EMBO J 1998;17:1675-87.

(12) Kroemer G, Galluzzi L, Brenner C. Mitochondrial membrane permeabilization in cell death. Physiol Rev 2007;87:99-163.

(13) Erlacher M. BH3-only proteins Puma and Bim are rate-limiting for [gamma]-radiation- and glucocorticoid-induced apoptosis of lymphoid cells in vivo. Blood 2005;106:4131-8.

(14) Wojciechowski S. Bim/Bcl-2 balance is critical for maintaining naive and memory T cell homeostasis. J Exp Med 2007;204:1665-75.

(15) Rathmell JC, Thompson CB. Pathways of apoptosis in lymphocyte development, homeostasis, and disease. Cell 2002 Apr;109 Suppl:S97-107.

(16) Mercep M, Weissmann A, Frank S, Klausner R, Ashwell J. Activation-driven programmed cell death and T cell receptor [zeta][eta] expression. Science 1989;246:1162-5.

(17) Shi Y, Sahai BM, Green DR. Cyclosporin A inhibits activation-induced cell death in T-cell hybridomas and thymocytes. Nature 1989;339:625-6.

(18) Dhein J, Walczak H, Baumler C, Debatin KM, Krammer PH. Autocrine T-cell suicide mediated by APO-1/(Fas/CD95). Nature 1995;373:438-41.

(19) Trauth B. Monoclonal antibody-mediated tumor regression by induction of apoptosis. Science 1989;245:301-5.

(20) Sytwu HK, Liblau RS, McDevitt HO. The roles of Fas/APO-1 (CD95) and TNF in antigen-induced programmed cell death in T cell receptor transgenic mice. Immunity 1996;5:17-30.

(21) Martinez-Lorenzo MJ. Involvement of APO2 ligand TRAIL in activation-induced death of Jurkat and human peripheral blood T cells. Eur J Immunol 1998;28:2714-25.

(22) Lamhamedi-Cherradi SE, Zheng SJ, Maguschak KA, Peschon J, Chen YH. Defective thymocyte apoptosis and accelerated autoimmune diseases in TRAIL-/- mice. Nature Immunol 2003;4:255-60.

(23) Janssen EM. CD4+ T-cell help controls CD8+ T-cell memory via TRAIL-mediated activation-induced cell death. Nature 2005;434:88-93.

(24) Devadas S. Granzyme B is critical for T cell receptor-induced cell death of type 2 helper T cells. Immunity 2006;25:237-47.

(25) Green DR, Droin N, Pinkoski M. Activation-induced cell death in T cells. Immunol Rev 2003;193:70-81.

(26) Lenardo MJ. Interleukin-2 programs mouse alpha beta T lymphocytes for apoptosis. Nature 1991 Oct 31;353(6347):858-61.

(27) Baumann S. Glucocorticoids inhibit activation-induced cell death (AICD) via direct DNA-dependent repression of the CD95 ligand gene by a glucocorticoid receptor dimer. Blood 2005;106:617-25.

(28) Li-Weber M, Krammer PH. Function and regulation of the CD95 (APO-1/Fas) ligand in the immune system. Sem Immunol 2003;15:145-57.

(29) Gulow K. HIV-1 Trans-activator of transcription substitutes for oxidative signaling in activation-induced T cell death. J Immunol 2005;174:5249-60.

(30) Kaminski M, Kiessling M, Suess D, Krammer PH, Gulow K. Novel role for mitochondria: protein kinase C[thgr]-dependent oxidative signalling organelles in activation induced T cell death. Mol Cell Biol 2007;27:3625-39.

(31) Takahashi T. Generalized lymphoproliferative disease in mice, caused by a point mutation in the fas ligand. Cell 1994;76:969-76.

(32) Watanabe-Fukunaga R, Brannan CI, Copeland NG, Jenkins NA, Nagata S. Lymphoproliferation disorder in mice explained by defects in Fas antigen that mediates apoptosis. Nature 1992;356:314-7.

(33) Hao Z, Hampel B, Yagita H, Rajewsky K. T cell-specific ablation of Fas leads to Fas ligand-mediated lymphocyte depletion and inflammatory pulmonary fibrosis. J Exp Med 2004;199:1355-65.

(34) Lord SJ, Rajotte RV, Korbutt GS, Bleackley RC. Granzyme B: a natural born killer. Immunol Rev 2003;193:31-8.

(35) Turk V, Turk B, Turk D. Lysosomal cysteine proteases: facts and opportunities. EMBO J 2001;20:4629-33.

(36) Bidere N. Cathepsin D triggers Bax activation, resulting in selective apoptosis-inducing factor (AIF) relocation in T lymphocytes entering the early commitment phase to apoptosis. J Biol Chem 2003;278:31401-11.

(37) Boya P. Lysosomal membrane permeabilization induces cell death in a mitochondrion-dependent fashion. J Exp Med 2003;197:1323-34.

(38) Deiss LP, Galinka H, Berissi H, Cohen O, Kimchi A. Cathepsin D protease mediates programmed cell death induced by interferon-[gamma], Fas/APO-1 and TNF-[alpha]. EMBO J 1996;15:3861-70.

(39) Hildeman DA. Activated T cell death in vivo mediated by proapoptotic bcl-2 family member bim. Immunity 2002;16:759-67.

(40) You H. FOXO3a-dependent regulation of Puma in response to cytokine/growth factor withdrawal. J Exp Med 2006;203:1657-63.

(41) Sandalova E, Wei CH, Masucci MG, Levitsky V. Regulation of expression of Bcl-2 protein family member Bim by T cell receptor triggering. Proc Natl Acad Sci USA 2004;101:3011-6.

(42) Willis SN. Apoptosis initiated when BH3 ligands engage multiple Bcl-2 homologs, not Bax or Bak. Science 2007;315:856-9.

(43) Schmitz I. An IL-2-dependent switch between CD95 signaling pathways sensitizes primary human T cells toward CD95-mediated activation-induced cell death. J Immunol 2003;171:2930-6.

(44) Surh CD, Boyman O, Purton JF, Sprent J. Homeostasis of memory T cells. Immunol Rev 2006 Jun;211:154-63.

(45) Harty JT, Badovinac VP. Shaping and reshaping CD8+ T-cell memory. Nat Rev Immunol 2008 Feb;8(2):107-19.

(46) Weninger W, Manjunath N, von Andrian UH. Migration and differentiation of CD8+ T cells. Immunol Rev 2002;186:221-33.

(47) Wherry EJ. Lineage relationship and protective immunity of memory CD8 T cell subsets. Nature Immunol 2003;4:225-34.

(48) Sallusto F, Geginat J, Lanzavecchia A. Central memory and effector memory T cell subsets: function, generation, and maintenance. Annu Rev Immunol 2004;22:745-63.

(49) Becker TC. Interleukin 15 is required for proliferative renewal of virus-specific memory CD8 T cells. J Exp Med 2002;195:1541-8.

(50) Goldrath AW. Cytokine requirements for acute and Basal homeostatic proliferation of naive and memory CD8+ T cells. J Exp Med 2002;195:1515-22.

(51) Watts TH. TNF/TNFR family members in costimulation of T cell responses. Annu Rev Immunol 2005;23:23-68.

(52) Greenwald RJ, Freeman GJ, Sharpe AH. The B7 family revisited. Annu Rev Immunol 2005;23:515-48.

(53) Haring JS, Badovinac VP, Harty JT. Inflaming the CD8+ T cell response. Immunity 2006;25:19-29.

(54) Mescher MF. Signals required for programming effector and memory development by CD8+ T cells. Immunol Rev 2006;211:81-92.

(55) Curtsinger JM. Inflammatory cytokines provide a third signal for activation of naive CD4+ and CD8+ T cells. J Immunol 1999;162:3256-562.

(56) Aichele P. CD8 T cells specific for lymphocytic choriomeningitis virus require type I IFN receptor for clonal expansion. J Immunol 2006;176:4525-9.

(57) Curtsinger JM, Johnson CM, Mescher MF. CD8 T cell clonal expansion and development of effector function require prolonged exposure to antigen, costimulation, and signal 3 cytokine. J Immunol 2003;171:5165-71.

(58) Kolumam GA, Thomas S, Thompson LJ, Sprent J, Murali-Krishna K. Type I interferons act directly on CD8 T cells to allow clonal expansion and memory formation in response to viral infection. J Exp Med 2005;202:637-50.

(59) Mitchell TC. Immunological adjuvants promote activated T cell survival via induction of Bcl-3. Nature Immunol 2001;2:397-402.

(60) Badovinac VP, Porter BB, Harty JT. Programmed contraction of CD8+ T cells after infection. Nature Immunol 2002;3:619-26.

(61) Badovinac VP, Harty JT. Programming, demarcating, and manipulating CD8+ T-cell memory. Immunol Rev 2006;211:67-80.

(62) Kaech SM, Hemby S, Kersh E, Ahmed R. Molecular and functional profiling of memory CD8 T cell differentiation. Cell 2002;111:837-51.

(63) Reich A, Korner H, Sedgwick JD, Pircher H. Immune down-regulation and peripheral deletion of CD8 T cells does not require TNF receptor-ligand interactions nor CD95 (Fas, APO-1). Eur J Immunol 2000;30:678-82.

(64) Nguyen LT. TNF receptor 1 (TNFR1) and CD95 are not required for T cell deletion after virus infection but contribute to peptide-induced deletion under limited conditions. Eur J Immunol 2000;30:683-8.

(65) Grayson JM, Zajac AJ, Altman JD, Ahmed R. Cutting edge: increased expression of Bcl-2 in antigen-specific memory CD8+ T cells. J Immunol 2000;164:3950-4.

(66) Pellegrini M, Belz G, Bouillet P, Strasser A. Shutdown of an acute T cell immune response to viral infection is mediated by the proapoptotic Bcl-2 homology 3-only protein Bim. Proc Natl Acad Sci USA 2003;100:14175-80.

(67) Plas DR, Rathmell JC, Thompson CB. Homeostatic control of lymphocyte survival: potential origins and implications. Nature Immunol 2002;3:515-21.

(68) Hildeman D, Jorgensen T, Kappler J, Marrack P. Apoptosis and the homeostatic control of immune responses. Curr Opin Immunol 2007;19:516-21.

(69) Wojciechowski S. Bim mediates apoptosis of CD127lo effector T cells and limits T cell memory. Eur J Immunol 2006;36:1694-706.

(70) Grayson JM, Weant AE, Holbrook BC, Hildeman D. Role of Bim in regulating CD8+ T-cell responses during chronic viral infection. J Virol 2006;80:8627-38.

(71) Badovinac VP, Tvinnereim AR, Harty JT. Regulation of antigen-specific CD8+ T cell homeostasis by perforin and interferon-[gamma]. Science 2000;290:1354-8.

(72) Tewari K, Nakayama Y, Suresh M. Role of direct effects of IFN-[gamma] on T cells in the regulation of CD8 T cell homeostasis. J Immunol 2007;179:2115-25.

(73) Haring JS, Harty JT. Aberrant contraction of antigen-specific CD4 T cells after infection in the absence of [gamma] interferon or its receptor. Infect Immun 2006;74:6252-63.

(74) Badovinac VP, Porter BB, Harty JT. CD8+ T cell contraction is controlled by early inflammation. Nature Immunol 2004;5:809-17.

(75) Sercan O, Hammerling GJ, Arnold B, Schuler T. Innate immune cells contribute to the IFN-[gamma]-dependent regulation of antigen-specific CD8+ T cell homeostasis. J Immunol 2006;176:735-9.

(76) Pearce EL, Shen H. Generation of CD8 T cell memory is regulated by IL-12. J Immunol 2007;179:2074-81.

(77) Joshi NS. Inflammation directs memory precursor and short-lived effector CD8+ T cell fates via the graded expression of T-bet transcription factor. Immunity 2007;27:281-95.

(78) Intlekofer AM. Requirement for T-bet in the aberrant differentiation of unhelped memory CD8+ T cells. J Exp Med 2007;204:2015-21.

(79) Chang JT. Asymmetric T lymphocyte division in the initiation of adaptive immune responses. Science 2007;315:1687-91.

(80) Bialik S, Kimchi A. The death-associated protein kinases: structure, function, and beyond. Annu Rev Biochem 2006;75:189-210.

(81) Raveh T, Kimchi A. DAP kinase-a proapoptotic gene that functions as a tumor suppressor. Exp Cell Res 2001 Mar 10;264(1):185-92.

(82) Cohen O, Kimchi A. DAP-kinase: from functional gene cloning to establishment of its role in apoptosis and cancer. Cell Death Differ 2001 Jan;8(1):6-15.

(83) Shohat G, Shani G, Eisenstein M, Kimchi A. The DAP-kinase family of proteins: study of a novel group of calcium-regulated death-promoting kinases. Biochim Biophys Acta 2002 Nov 4;1600(1-2):45-50.

(84) Schneider-Stock R, Roessner A, Ullrich O. DAP-kinase--protector or enemy in apoptotic cell death. Int J Biochem Cell Biol 2005 Sep;37(9):1763-7.

(85) Gozuacik D, Kimchi A. DAPk protein family and cancer. Autophagy 2006 Apr;2(2):74-9.

(86) Deiss LP, Feinstein E, Berissi H, Cohen O, Kimchi A. Identification of a novel serine/threonine kinase and a novel 15-kD protein as potential mediators of the gamma interferon-induced cell death. Genes Dev 1995 Jan 1;9(1):15-30.

(87) Inbal B, Shani G, Cohen O, Kissil JL, Kimchi A. Death-associated protein kinase-related protein 1, a novel serine/threonine kinase involved in apoptosis. Mol Cell Biol 2000 Feb;20(3):1044-54.

(88) Kawai T, Matsumoto M, Takeda K, Sanjo H, Akira S. ZIP kinase, a novel serine/threonine kinase which mediates apoptosis. Mol Cell Biol 1998 Mar;18(3):1642-51.

(89) Kawai T, Nomura F, Hoshino K, Copeland NG, Gilbert DJ, Jenkins NA, et al. Death-associated protein kinase 2 is a new calcium/calmodulin-dependent protein kinase that signals apoptosis through its catalytic activity. Oncogene 1999 Jun 10;18(23):3471-80.

(90) Sanjo H, Kawai T, Akira S. DRAKs, novel serine/threonine kinases related to death-associated protein kinase that trigger apoptosis. J Biol Chem 1998 Oct 30;273(44):29066-71.

(91) Matsumoto M, Miyake Y, Nagita M, Inoue H, Shitakubo D, Takemoto K, et al. A serine/threonine kinase which causes apoptosis-like cell death interacts with a calcineurin B-like protein capable of binding Na(+)/H(+) exchanger. J Biochem (Tokyo) 2001 Aug;130(2):217-25.

(92) Kuwahara H, Kamei J, Nakamura N, Matsumoto M, Inoue H, Kanazawa H. The apoptosis-inducing protein kinase DRAK2 is inhibited in a calcium-dependent manner by the calcium-binding protein CHP. J Biochem (Tokyo) 2003 Aug;134(2):245-50.

(93) McGargill MA, Wen BG, Walsh CM, Hedrick SM. A deficiency in Drak2 results in a T cell hypersensitivity and an unexpected resistance to autoimmunity. Immunity 2004 Dec;21(6):781-91.

(94) Mao J, Qiao X, Luo H, Wu J. Transgenic drak2 overexpression in mice leads to increased T cell apoptosis and compromised memory T cell development. J Biol Chem 2006 May 5;281(18):12587-95.

(95) Zimmet P, Alberti KG, Shaw J. Global and societal implications of the diabetes epidemic. Nature 2001 Dec 13;414(6865):782-7.

(96) Cnop M, Welsh N, Jonas JC, Jorns A, Lenzen S, Eizirik DL. Mechanisms of pancreatic beta-cell death in type 1 and type 2 diabetes: many differences, few similarities. Diabetes 2005 Dec;54 Suppl 2:S97-107.

(97) Achenbach P, Bonifacio E, Koczwara K, Ziegler AG. Natural history of type 1 diabetes. Diabetes 2005 Dec;54 Suppl 2:S25-S31.

(98) Meier JJ, Bhushan A, Butler AE, Rizza RA, Butler PC. Sustained beta cell apoptosis in patients with long-standing type 1 diabetes: indirect evidence for islet regeneration? Diabetologia 2005 Nov;48(11):2221-8.

(99) Wang J, Miao D, Babu S, Yu J, Barker J, Klingensmith G, et al. Prevalence of autoantibody-negative diabetes is not rare at all ages and increases with older age and obesity. J Clin Endocrinol Metab 2007 Jan;92(1):88-92.

(100) Eisenbarth GS. Update in type 1 diabetes. J Clin Endocrinol Metab 2007 Jul;92(7):2403-7.

(101) Eizirik DL, Mandrup-Poulsen T. A choice of death--the signal-transduction of immune-mediated beta-cell apoptosis. Diabetologia 2001 Dec;44(12):2115-33.

(102) Hostens K, Pavlovic D, Zambre Y, Ling Z, Van SC, Eizirik DL, et al. Exposure of human islets to cytokines can result in disproportionately elevated proinsulin release. J Clin Invest 1999 Jul;104(1):67-72.

(103) Giannoukakis N, Rudert WA, Trucco M, Robbins PD. Protection of human islets from the effects of interleukin-1beta by adenoviral gene transfer of an Ikappa B repressor. J Biol Chem 2000 Nov 24;275(47):36509-13.

(104) Heimberg H, Heremans Y, Jobin C, Leemans R, Cardozo AK, Darville M, et al. Inhibition of cytokine-induced NF-kappaB activation by adenovirus-mediated expression of a NF-kappaB super-repressor prevents beta-cell apoptosis. Diabetes 2001 Oct;50(10):2219-24.

(105) Wu Y, Han B, Luo H, Roduit R, Salcedo TW, Moore PA, et al. DcR3/TR6 effectively prevents islet primary nonfunction after transplantation. Diabetes 2003 Sep;52(9):2279-86.

(106) Donath MY, Storling J, Maedler K, Mandrup-Poulsen T. Inflammatory mediators and islet beta-cell failure: a link between type 1 and type 2 diabetes. J Mol Med 2003 Aug;81(8):455-70.

(107) Bonny C, Oberson A, Negri S, Sauser C, Schorderet DF. Cell-permeable peptide inhibitors of JNK: novel blockers of beta-cell death. Diabetes 2001 Jan;50(1):77-82.

(108) Larsen CM, Wadt KA, Juhl LF, Andersen HU, Karlsen AE, Su MS, et al. Interleukin-1beta-induced rat pancreatic islet nitric oxide synthesis requires both the p38 and extracellular signal-regulated kinase 1/2 mitogen-activated protein kinases. J Biol Chem 1998 Jun 12;273(24):15294-300.

(109) Saldeen J, Lee JC, Welsh N. Role of p38 mitogen-activated protein kinase (p38 MAPK) in cytokine-induced rat islet cell apoptosis. Biochem Pharmacol 2001 Jun 15;61(12):1561-9.

(110) Saldeen J, Tillmar L, Karlsson E, Welsh N. Nicotinamide- and caspase-mediated inhibition of poly(ADP-ribose) polymerase are associated with p53-independent cell cycle (G2) arrest and apoptosis. Mol Cell Biochem 2003 Jan;243(1-2):113-22.

(111) Harding HP, Zeng H, Zhang Y, Jungries R, Chung P, Plesken H, et al. Diabetes mellitus and exocrine pancreatic dysfunction in perk-/- mice reveals a role for translational control in secretory cell survival. Mol Cell 2001 Jun;7(6):1153-63.

(112) Oyadomari S, Takeda K, Takiguchi M, Gotoh T, Matsumoto M, Wada I, et al. Nitric oxide-induced apoptosis in pancreatic beta cells is mediated by the endoplasmic reticulum stress pathway. Proc Natl Acad Sci U S A 2001 Sep 11;98(19):10845-50.

(113) Maechler P, Wollheim CB. Mitochondrial function in normal and diabetic beta-cells. Nature 2001 Dec 13;414(6865):807-12.

(114) Newmeyer DD, Ferguson-Miller S. Mitochondria: releasing power for life and unleashing the machineries of death. Cell 2003 Feb 21;112(4):481-90.

(115) Friedlander RM. Apoptosis and caspases in neurodegenerative diseases. N Engl J Med 2003 Apr 3;348(14):1365-75.

(116) Iwahashi H, Hanafusa T, Eguchi Y, Nakajima H, Miyagawa J, Itoh N, et al. Cytokine-induced apoptotic cell death in a mouse pancreatic beta-cell line: inhibition by Bcl-2. Diabetologia 1996 May;39(5):530-6.

(117) Rabinovitch A, Suarez-Pinzon W, Strynadka K, Ju Q, Edelstein D, Brownlee M, et al. Transfection of human pancreatic islets with an anti-

apoptotic gene (bcl-2) protects beta-cells from cytokine-induced destruction. Diabetes 1999 Jun;48(6):1223-9.

(118) Barbu AR, Akusjarvi G, Welsh N. Adenoviral-induced islet cell cytotoxicity is not counteracted by Bcl-2 overexpression. Mol Med 2002 Nov;8(11):733-41.

(119) Allison J, Thomas H, Beck D, Brady JL, Lew AM, Elefanty A, et al. Transgenic overexpression of human Bcl-2 in islet beta cells inhibits apoptosis but does not prevent autoimmune destruction. Int Immunol 2000 Jan;12(1):9-17.

(120) Karlsen AE, Pavlovic D, Nielsen K, Jensen J, Andersen HU, Pociot F, et al. Interferon-gamma induces interleukin-1 converting enzyme expression in pancreatic islets by an interferon regulatory factor-1-dependent mechanism. J Clin Endocrinol Metab 2000 Feb;85(2):830-6.

(121) Kutlu B, Cardozo AK, Darville MI, Kruhoffer M, Magnusson N, Orntoft T, et al. Discovery of gene networks regulating cytokine-induced dysfunction and apoptosis in insulin-producing INS-1 cells. Diabetes 2003 Nov;52(11):2701-19.

(122) Donath MY, Halban PA. Decreased beta-cell mass in diabetes: significance, mechanisms and therapeutic implications. Diabetologia 2004 Mar;47(3):581-9.

(123) Pelleymounter MA. Effects of the obese gene product on body weight regulation in ob/ob mice. Science 1995;269:540-3.

(124) Sethi JK, Vidal-Puig AJ. Thematic review series: adipocyte biology. Adipose tissue function and plasticity orchestrate nutritional adaptation. J Lipid Res 2007;48:1253-62.

(125) Reitman ML, Gavrilova O. A-ZIP/F-1 mice lacking white fat: a model for understanding lipoatrophic diabetes. Int J Obes Relat Metab Disord 2000;24(Suppl. 4):S11-S14.

(126) Gavrilova O. Surgical implantation of adipose tissue reverses diabetes in lipoatrophic mice. J Clin Invest 2000;105:271-8.

(127) Shimomura I, Hammer RE, Ikemoto S, Brown MS, Goldstein JL. Leptin reverses insulin resistance and diabetes mellitus in mice with congenital lipodystrophy. Nature 1999;401:73-6.

(128) Ebihara K. Transgenic overexpression of leptin rescues insulin resistance and diabetes in a mouse model of lipoatrophic diabetes. Diabetes 2001;50:1440-8.

(129) Colombo C. Transplantation of adipose tissue lacking leptin is unable to reverse the metabolic abnormalities associated with lipoatrophy. Diabetes 2002;51:2727-33.

(130) Oral EA. Leptin-replacement therapy for lipodystrophy. N Engl J Med 2002;346:570-8.

(131) Trujillo ME, Scherer PE. Adipose tissue-derived factors: impact on health and disease. Endocr Rev 2006;27:762-78.

(132) Abel ED. Adipose-selective targeting of the GLUT4 gene impairs insulin action in muscle and liver. Nature 2001;409:729-33.

(133) Yang Q. Serum retinol binding protein 4 contributes to insulin resistance in obesity and type 2 diabetes. Nature 2005;436:356-62.

(134) Sivitz WI, Desautel SL, Kayano T, Bell GI, Pessin JE. Regulation of glucose transporter messenger-RNA in insulin-deficient states. Nature 1989;340:72-4.

(135) Muoio DM, Newgard CB. Metabolism: A is for adipokine. Nature 2005;436:337-8.

(136) Wellen KE, Hotamisligil GS. Inflammation, stress, and diabetes. J Clin Invest 2005;115:1111-9.

(137) Cai D. Local and systemic insulin resistance resulting from hepatic activation of IKK-[beta] and NF-[kappa]B. Nature Med 2005;11:183-90.

(138) Arkan MC. IKK-[beta] links inflammation to obesity-induced insulin resistance. Nature Med 2005;11:191-8.

(139) Chen A. Diet induction of monocyte chemoattractant protein-1 and its impact on obesity. Obes Res 2005;13:1311-20.

(140) Xu H. Chronic inflammation in fat plays a crucial role in the development of obesity-related insulin resistance. J Clin Invest 2003;112:1821-30.

(141) McGarry JD. Banting Lecture 2001: dysregulation of fatty acid metabolism in the etiology of type 2 diabetes. Diabetes 2002;51:7-18.

(142) Chavez JA, Holland WL, Bar J, Sandhoff K, Summers SA. Acid ceramidase overexpression prevents the inhibitory effects of saturated fatty acids on insulin signaling. J Biol Chem 2005;280:20148-53.

(143) Chavez JA, Summers SA. Characterizing the effects of saturated fatty acids on insulin signaling and ceramide and diacylglycerol accumulation in 3T3-

L1 adipocytes and C2C12 myotubes. Arch Biochem Biophys 2003;419:101-9.

(144) Griffin ME. Free fatty acid induced insulin resistance is associated with activation of protein kinase C[thgr] and alterations in the insulin signaling cascade. Diabetes 1999;48:1270-4.

(145) Neschen S. Prevention of hepatic steatosis and hepatic insulin resistance in mitochondrial acyl-CoA:glycerol-sn-3-phosphate acyltransferase 1 knockout mice. Cell Metab 2005;2:55-65.

(146) Savage DB. Reversal of diet-induced hepatic steatosis and hepatic insulin resistance by antisense oligonucleotide inhibitors of acetyl-CoA carboxylases 1 and 2. J Clin Invest 2006;116:817-24.

(147) bu-Elheiga L, Oh W, Kordari P, Wakil SJ. Acetyl-CoA carboxylase 2 mutant mice are protected against obesity and diabetes induced by high-fat/high-carbohydrate diets. Proc Natl Acad Sci USA 2003;100:10207-12.

(148) Holland WL. Inhibition of ceramide synthesis ameliorates glucocorticoid-, saturated-fat-, and obesity-induced insulin resistance. Cell Metab 2007;5:167-79.

(149) Petersen KF. Reversal of nonalcoholic hepatic steatosis, hepatic insulin resistance, and hyperglycemia by moderate weight reduction in patients with type 2 diabetes. Diabetes 2005;54:603-8.

(150) Shulman GI. Cellular mechanisms of insulin resistance. J Clin Invest 2000;106:171-6.

(151) Hulver MW. Skeletal muscle lipid metabolism with obesity. Am J Physiol Endocrinol Metab 2003;284:E741-E747.

(152) Liu L. Upregulation of myocellular DGAT1 augments triglyceride synthesis in skeletal muscle and protects against fat-induced insulin resistance. J Clin Invest 2007;117:1679-89.

(153) Muoio DM, Newgard CB. Obesity-related derangements in metabolic regulation. Annu Rev Biochem 2006;75:367-401.

(154) Koves TR. Peroxisome proliferator-activated receptor-[gamma] co-activator 1[alpha]-mediated metabolic remodeling of skeletal myocytes mimics exercise training and reverses lipid-induced mitochondrial inefficiency. J Biol Chem 2005;280:33588-98.

(155) An J. Hepatic expression of malonyl-CoA decarboxylase reverses muscle, liver and whole-animal insulin resistance. Nature Med 2004;10:268-74.

(156) Koves TR. Mitochondrial overload and incomplete fatty acid oxidation contribute to skeletal muscle insulin resistance. Cell Metab 2008;7:45-56.

(157) Kelley DE, Goodpaster B, Wing RR, Simoneau JA. Skeletal muscle fatty acid metabolism in association with insulin resistance, obesity, and weight loss. Am J Physiol 1999;277:E1130-E1141.

(158) Hirosumi J. A central role for JNK in obesity and insulin resistance. Nature 2002;420:333-6.

(159) Saltiel AR, Pessin JE. Insulin signaling pathways in time and space. Trends Cell Biol 2002;12:65-71.

(160) Perseghin G, Petersen K, Shulman GI. Cellular mechanism of insulin resistance: potential links with inflammation. Int J Obes Relat Metab Disord 2003;27:S6-S11.

(161) Shoelson SE, Lee J, Yuan M. Inflammation and the IKK[beta]/I-[kappa]B/NF-[kappa]B axis in obesity- and diet-induced insulin resistance. Int J Obes Relat Metab Disord 2003;27(Suppl. 3):S49.

(162) Nagle CA. Hepatic overexpression of glycerol-sn-3-phosphate acyltransferase 1 in rats causes insulin resistance. J Biol Chem 2007;282:14807-15.

(163) Hammond LE. Mitochondrial glycerol-3-phosphate acyltransferase-1 is essential in liver for the metabolism of excess acyl-CoAs. J Biol Chem 2005;280:25629-36.

(164) Samuel VT. Inhibition of protein kinase C[epsiv] prevents hepatic insulin resistance in nonalcoholic fatty liver disease. J Clin Invest 2007;117:739-45.

(165) Serra C. Transgenic mice with dominant negative PKC-[thgr] in skeletal muscle: a new model of insulin resistance and obesity. J Cell Physiol 2003;196:89-97.

(166) Gao Z. Inactivation of PKC[thgr] leads to increased susceptibility to obesity and dietary insulin resistance in mice. Am J Physiol Endocrinol Metab 2007;292:E84-E91.

(167) Felig P, Wahren J, Hendler R, Brundin T. Splanchnic glucose and amino acid metabolism in obesity. J Clin Invest 1974;53:582-90.

(168) Tremblay F. Overactivation of S6 kinase 1 as a cause of human insulin resistance during increased amino acid availability. Diabetes 2005;54:2674-84.

(169) Um SH, D'Alessio D, Thomas G. Nutrient overload, insulin resistance, and ribosomal protein S6 kinase 1, S6K1. Cell Metab 2006;3:393-402.

(170) Krebs M. Mechanism of amino acid-induced skeletal muscle insulin resistance in humans. Diabetes 2002;51:599-605.

(171) Ozcan U. Endoplasmic reticulum stress links obesity, insulin action, and type 2 diabetes. Science 2004;306:457-61.

(172) U.K. prospective diabetes study 16. Overview of 6 years' therapy of type II diabetes: a progressive disease. U.K. Prospective Diabetes Study Group. Diabetes 1995 Nov;44(11):1249-58.

(173) Rhodes CJ. Type 2 diabetes [mdash] a matter of [beta]-cell life and death? Science 2005;307:380-4.

(174) Kosaka K, Kuzuya T, Akanuma Y, Hagura R. Increase in insulin response after treatment of overt maturity-onset diabetes is independent of the mode of treatment. Diabetologia 1980 Jan;18(1):23-8.

(175) Schroder M, Kaufman RJ. ER stress and the unfolded protein response. Mutat Res 2005 Jan 6;569(1-2):29-63.

(176) Malaisse WJ, Maggetto C, Leclercq-Meyer V, Sener A. Interference of glycogenolysis with glycolysis in pancreatic islets from glucose-infused rats. J Clin Invest 1993 Feb;91(2):432-6.

(177) Weir GC, Laybutt DR, Kaneto H, Bonner-Weir S, Sharma A. Beta-cell adaptation and decompensation during the progression of diabetes. Diabetes 2001 Feb;50 Suppl 1:S154-S159.

(178) Eizirik DL, Kutlu B, Rasschaert J, Darville M, Cardozo AK. Use of microarray analysis to unveil transcription factor and gene networks contributing to Beta cell dysfunction and apoptosis. Ann N Y Acad Sci 2003 Nov;1005:55-74.

(179) Paolisso G, Tataranni PA, Foley JE, Bogardus C, Howard BV, Ravussin E. A high concentration of fasting plasma non-esterified fatty acids is a risk factor for the development of NIDDM. Diabetologia 1995 Oct;38(10):1213-7.

(180) Zhou YP, Grill VE. Long-term exposure of rat pancreatic islets to fatty acids inhibits glucose-induced insulin secretion and biosynthesis through a glucose fatty acid cycle. J Clin Invest 1994 Feb;93(2):870-6.

(181) Kashyap S, Belfort R, Gastaldelli A, Pratipanawatr T, Berria R, Pratipanawatr W, et al. A sustained increase in plasma free fatty acids

impairs insulin secretion in nondiabetic subjects genetically predisposed to develop type 2 diabetes. Diabetes 2003 Oct;52(10):2461-74.

(182) Lee Y, Hirose H, Ohneda M, Johnson JH, McGarry JD, Unger RH. Beta-cell lipotoxicity in the pathogenesis of non-insulin-dependent diabetes mellitus of obese rats: impairment in adipocyte-beta-cell relationships. Proc Natl Acad Sci U S A 1994 Nov 8;91(23):10878-82.

(183) Shimabukuro M, Ohneda M, Lee Y, Unger RH. Role of nitric oxide in obesity-induced beta cell disease. J Clin Invest 1997 Jul 15;100(2):290-5.

(184) Cnop M. The concurrent accumulation of intra-abdominal and subcutaneous fat explains the association between insulin resistance and plasma leptin concentrations: distinct metabolic effects of two fat compartments. Diabetes 2002;51:1005-15.

(185) Briaud I, Kelpe CL, Johnson LM, Tran PO, Poitout V. Differential effects of hyperlipidemia on insulin secretion in islets of langerhans from hyperglycemic versus normoglycemic rats. Diabetes 2002 Mar;51(3):662-8.

(186) Maestre I, Jordan J, Calvo S, Reig JA, Cena V, Soria B, et al. Mitochondrial dysfunction is involved in apoptosis induced by serum withdrawal and fatty acids in the beta-cell line INS-1. Endocrinology 2003 Jan;144(1):335-45.

(187) Cnop M, Hannaert JC, Hoorens A, Eizirik DL, Pipeleers DG. Inverse relationship between cytotoxicity of free fatty acids in pancreatic islet cells and cellular triglyceride accumulation. Diabetes 2001 Aug;50(8):1771-7.

(188) Nakatani Y, Kaneto H, Kawamori D, Yoshiuchi K, Hatazaki M, Matsuoka TA, et al. Involvement of endoplasmic reticulum stress in insulin resistance and diabetes. J Biol Chem 2005 Jan 7;280(1):847-51.

(189) Kharroubi I, Ladriere L, Cardozo AK, Dogusan Z, Cnop M, Eizirik DL. Free fatty acids and cytokines induce pancreatic beta-cell apoptosis by different mechanisms: role of nuclear factor-kappaB and endoplasmic reticulum stress. Endocrinology 2004 Nov;145(11):5087-96.

(190) Kloppel G, Lohr M, Habich K, Oberholzer M, Heitz PU. Islet pathology and the pathogenesis of type 1 and type 2 diabetes mellitus revisited. Surv Synth Pathol Res 1985;4:110-25.

(191) Butler AE, Janson J, Bonner-Weir S, Ritzel R, Rizza RA, Butler PC. Beta-cell deficit and increased beta-cell apoptosis in humans with type 2 diabetes. Diabetes 2003 Jan;52(1):102-10.

(192) Lingohr MK, Buettner R, Rhodes CJ. Pancreatic beta-cell growth and survival--a role in obesity-linked type 2 diabetes? Trends Mol Med 2002 Aug;8(8):375-84.

(193) Jaikaran ET, Clark A. Islet amyloid and type 2 diabetes: from molecular misfolding to islet pathophysiology. Biochim Biophys Acta 2001 Nov 29;1537(3):179-203.

(194) Hennige AM. Upregulation of insulin receptor substrate-2 in pancreatic [beta] cells prevents diabetes. J Clin Invest 2003;112:1521-32.

(195) Tamemoto H, Kadowaki T, Tobe K, Yagi T, Sakura H, Hayakawa T, et al. Insulin resistance and growth retardation in mice lacking insulin receptor substrate-1. Nature 1994 Nov 10;372(6502):182-6.

(196) Araki E, Lipes MA, Patti ME, Bruning JC, Haag B, III, Johnson RS, et al. Alternative pathway of insulin signalling in mice with targeted disruption of the IRS-1 gene. Nature 1994 Nov 10;372(6502):186-90.

(197) Rhodes CJ, White MF. Molecular insights into insulin action and secretion. Eur J Clin Invest 2002 Jun;32 Suppl 3:3-13.

(198) Borge PD, Jr., Wolf BA. Insulin receptor substrate 1 regulation of sarco-endoplasmic reticulum calcium ATPase 3 in insulin-secreting beta-cells. J Biol Chem 2003 Mar 28;278(13):11359-68.

(199) Withers DJ, Burks DJ, Towery HH, Altamuro SL, Flint CL, White MF. Irs-2 coordinates Igf-1 receptor-mediated beta-cell development and peripheral insulin signalling. Nat Genet 1999 Sep;23(1):32-40.

(200) Withers DJ, Gutierrez JS, Towery H, Burks DJ, Ren JM, Previs S, et al. Disruption of IRS-2 causes type 2 diabetes in mice. Nature 1998 Feb 26;391(6670):900-4.

(201) Zick Y. Insulin resistance: a phosphorylation-based uncoupling of insulin signaling. Trends Cell Biol 2001;11:437-41.

(202) Briaud I, Dickson LM, Lingohr MK, McCuaig JF, Lawrence JC, Rhodes CJ. Insulin receptor substrate-2 proteasomal degradation mediated by a mammalian target of rapamycin (mTOR)-induced negative feedback down-regulates protein kinase B-mediated signaling pathway in beta-cells. J Biol Chem 2005 Jan 21;280(3):2282-93.

(203) Unger RH, Orci L. Diseases of liporegulation: new perspective on obesity and related disorders. FASEB J 2001 Feb;15(2):312-21.

(204) Wrede CE, Dickson LM, Lingohr MK, Briaud I, Rhodes CJ. Protein kinase B/Akt prevents fatty acid-induced apoptosis in pancreatic beta-cells (INS-1). J Biol Chem 2002 Dec 20;277(51):49676-84.

(205) Willaime-Morawek S, Brami-Cherrier K, Mariani J, Caboche J, Brugg B. C-Jun N-terminal kinases/c-Jun and p38 pathways cooperate in ceramide-induced neuronal apoptosis. Neuroscience 2003;119(2):387-97.

(206) Poitout V, Robertson RP. Minireview: Secondary beta-cell failure in type 2 diabetes--a convergence of glucotoxicity and lipotoxicity. Endocrinology 2002 Feb;143(2):339-42.

(207) Maedler K, Sergeev P, Ris F, Oberholzer J, Joller-Jemelka HI, Spinas GA, et al. Glucose-induced beta cell production of IL-1beta contributes to glucotoxicity in human pancreatic islets. J Clin Invest 2002 Sep;110(6):851-60.

(208) Maedler K, Sergeev P, Ehses JA, Mathe Z, Bosco D, Berney T, et al. Leptin modulates beta cell expression of IL-1 receptor antagonist and release of IL-1beta in human islets. Proc Natl Acad Sci U S A 2004 May 25;101(21):8138-43.

(209) Dickson LM, Rhodes CJ. Pancreatic beta-cell growth and survival in the onset of type 2 diabetes: a role for protein kinase B in the Akt? Am J Physiol Endocrinol Metab 2004 Aug;287(2):E192-E198.

(210) Rui L, Yuan M, Frantz D, Shoelson S, White MF. SOCS-1 and SOCS-3 block insulin signaling by ubiquitin-mediated degradation of IRS1 and IRS2. J Biol Chem 2002 Nov 1;277(44):42394-8.

(211) Gao Z. Inactivation of PKC[thgr] leads to increased susceptibility to obesity and dietary insulin resistance in mice. Am J Physiol Endocrinol Metab 2007;292:E84-E91.

II. ARTICLES

Article 1.

TRANSGENIC DRAK2 OVEREXPRESSION IN MICE LEADS TO INCREASED T-CELL APOPTOSIS AND COMPROMISED MEMORY T-CELL DEVELOPMENT

Jianning Mao, Xiaoying Qiao, Hongyu Luo, and Jiangping Wu

J.Biol.Chem. 281 (18):12587-12595, 2006.

Note: In this paper, as co-author, Xiaoying Qiao prepared the constructs to generate transgenic mouse and for in vitro transfection. In addition, she also performed northern blot analysis as shown in Figure 2O. The remaining works were performed by Jianning Mao.

TRANSGENIC DRAK2 OVEREXPRESSION IN MICE LEADS TO INCREASED T-CELL APOPTOSIS AND COMPROMISED MEMORY T-CELL DEVELOPMENT

Jianning Mao*, Xiaoying Qiao*, Hongyu Luo*, and Jiangping Wu*+

Running title: Compromised memory T-cell development in Drak2 transgenic mice

From *the Laboratory of Immunology and +Nephrology Service, Centre hospitalier de l'Université de Montréal (CHUM), Notre Dame Hospital, Montreal, Quebec, Canada

Correspondence may be addressed to: Dr. Jiangping Wu, Laboratory of Immunology, Research Centre, CHUM, Notre Dame Hospital, Pavilion DeSève, Room Y-5616, 1560 Sherbrooke Street East, Montreal, Quebec H2L 4M1, Canada. Telephone: (514) 890-8000 ext. 25164; Fax: (514) 412-7596. Correspondence may also be addressed to Dr. Hongyu Luo at the same address. Telephone: (514) 890-8000 ext. 27421; Fax: (514) 412-7590.

ABSTRACT

Drak2 is a death-associated protein (DAP) family serine threonine kinase. Its expression and roles in the immune system were investigated in this study. According to in situ hybridization, Drak2 expression was ubiquitous at the mid-gestation stage in embryos, followed by more focal expression in various organs in the perinatal period and adulthood, notably in the thymus, spleen, lymph nodes, cerebellum, suprachiasmatic nuclei, pituitary, olfactory lobes, adrenal medulla, stomach, skin and testes. Its expression was high in resting T cells, but was downregulated after T cell activation. Drak2 transgenic (Tg) mice were generated using the human β-actin promoter. These Tg mice showed normal T- versus B-cell and CD4 versus CD8 populations in the spleen, but their spleen weight cellularity was lower in comparison to wild type mice. After TCR activation, the proliferation response in Drak2 Tg T cells was normal, although their IL-2 and IL-4 but not IFN-γ production was augmented. Activated Drak2 Tg T cells demonstrated significantly enhanced apoptosis in the presence of exogenous IL-2. At the molecular level, Drak2 Tg T cells manifested a lower increase of anti-apoptotic factors during activation; such a change probably rendered the cells vulnerable to subsequent IL-2 insults. The compromised apoptosis in Drak2 Tg T cells was associated with reduced numbers of T cells with the memory cell phenotype ($CD62L^{lo}$), and repressed secondary T-cell responses in delayed-type hypersensitivity. Our study demonstrates that Drak2 expresses in the T-cell compartment, but is not T-cell-specific; it plays critical roles in T-cell apoptosis and memory T-cell development.

INTRODUCTION

To elucidate the molecular mechanisms of T-cell activation and differentiation, we conducted DNA microarray analysis employing the mouse 15,000 cDNA panel of the National Institute of Aging, USA, to compare gene expression patterns of resting versus activated T cells (anti-CD3 and anti-CD28 stimulation for 24 h). Drak2 was one of the genes found to undergo significant changes after activation, and was thus selected for further investigation.

Drak2 is a serine/threonine kinase belonging to a family of death-associated protein kinases (DAP kinases), which consists of DAP (1), DRP-1 (2), ZIP kinase (3), DAPK2 (4), Drak1 and Drak2 (5). Drak1 and Drak2 share 67.1% identy in their kinase domain and 24.2% identy in their non-catalytic regions (5). Drak2 also shares about 50% identity in the kinase domain with other members of the family (2). While DAP, DRP-1 and DAPK2 have a calmodulin regulatory domain in their C-terminal, ZIP, Drak1 and Drak2 do not (1-5). DAP, DAPK2, and DRP-1 are localized in the cytosol (1,2,4), ZIP kinase and Drak1 resides mainly in the nuclei (3,5), and Drak2 is found in both the cytosol and nuclei (5,6), suggesting different mechanisms of action. When DAP family kinases are overexpressed in various cells, apoptosis ensues, either directly, or after cytokine stimulation (1-5), indicating their involvement in apoptosis.

The mechanism of action and regulation of the prototype DAP family kinase, DAP, at the molecular level have been better studied. During apoptosis, DAP can associate with TNFα receptor and Fas-associated death domain, whereas in surviving cells, it binds to 14-3-3 (7). It phosphorylates myosin light chain II in vivo and is necessary for serum-induced stress fibre formation (8); it also phosphorylates $p19^{arf}$ and suppresses fibroblast oncogenic transformation (9). DAP is capable of autophosphorylation, which is inhibitory to its kinase activity (10). It also interacts with DAP-interacting protein-1, which is an E3 ubiquitin ligase and regulates the cellular level of DAP (11). Much less is known about the mechanisms of action of Drak2. It autophosphorylates and phosphorylates myosin light chains as an exogenous substrate (5), although its endogenous substrates have not been identified. Drak2 interacts with a calcineurin homologous protein (6), but the biological significance of this interaction is not clear. According to DNA microarray (12) and real-time reverse transcription/ polymerase chain reaction (RT-PCR) analysis (13) of different tissues, Drak2 is considered exclusively expressed in the T-cell compartment, yet such analyses are not precise, as these methods cannot reveal possible focal Drak2 expression in certain organs.

The immune system of Drak2 null-mutant mice was investigated recently by McGargill et al. (13). Unexpectedly, in vitro, $Drak2^{-/-}$ T cells have no apparent defect in activation-induced apoptosis, after stimulation with anti-CD3 and anti-CD28; this leads to a conclusion by the authors that Drak2 does not play significant roles in T-cell apoptosis. Interestingly, $Drak2^{-/-}$ T cells have a lowered threshold to stimulation, compared to wild type (WT) T cells; the mechanism of such a phenomenon has not been explored.

In this study, we mapped the Drak2 expression pattern during ontogeny, and conducted a detailed *in vitro* and *in vivo* investigation of its functions in the immune system, using transgenic (Tg) mice with actin promoter-driven Drak2 expression. The novelty of our study is as follows. We corrected two misconceptions that Drak was expressed only in the T-cell compartment, and it did not involved T-cell apoptosis. We also provided evidence that Drak2 controlled T-cell memory response.

MATERIALS AND METHODS

In situ hybridization (ISH)

A 1516-bp ApaI/KpnI mouse Drak2 cDNA fragment (positions 1150 to 2676) derived from MGC-6721 (American Type Culture Collection, Rockville, MD) was cloned in pCMV-SPORT6, and was named pCMV-SPORT6-Drak2Δ, which was employed to generate sense and antisense riboprobes, using SP6 and T7 RNA polymerase for both ^{35}S-UTP and ^{35}S-CTP incorporation (14). Tissues were frozen in -35°C isopentane, and kept at -80°C until cut. ISH was performed on 10-μm cryostat sections, as outlined previously (14). Anatomic ISH was conducted with X-ray films. ISH microscopy was undertaken with photographic emulsion followed by 8-day exposure. The slides were developed and then counter-stained with hematoxylin.

Northern blot analysis

A partial Drak2 cDNA fragment (clone H3022H03, National Institute of Aging, mouse 15K cDNA clone set; positions 17-2554, according to the sequence in GeneBank, accession

number NM_133810) was labelled with a digoxin (Dig)-labelling kit from Roche Applied Sciences (Laval, Quebec, Canada). Total RNA was extracted from cultured cells with Trizol (Invitrogen, Burlington, Ontario, Canada). RNA (20 μg/lane) was resolved in 0.9% formaldehyde agarose gels, and transferred to N-Hybond nylon membranes (Amersham Biosciences, Baie d'Urfe, Quebec, Canada). The membranes were hybridized with Dig-labelled probes, and the signals were revealed by a Dig detection kit (Roche Applied Sciences). Band intensities of 18S and 28S ribosome RNA were indicators of even RNA loading.

Generation of Drak2 Tg mice

Mouse full-length Drak2 cDNA (MGC-6721) was excised from the vector with XbaI and SalI, and cloned into XbaI and BamHI sites in vector pAC between the human β-actin promoter and β-actin polyA signals. The resulting construct was named pAC-Drak2. The 4090-kb ClaI/ClaI fragment containing the β-actin promoter, Drak2 cDNA and β-actin polyA signal was excised and injected into fertilized C3HxC57BL/6 eggs. Genotyping of the Tg mice was first performed by Southern blot analysis. Tail DNA of the founders (10 μg/each) was digested with PstI, and resolved by 1% agarose gel electrophoresis. The DNA was transferred onto N^+ Hybond nylon membranes after denaturation. A 2-kb band specific to the transgene was detected by the same Dig-labelled Drak2 probe, as was employed in the Northern blot analysis. PCR was conducted for subsequent genotyping. The 5' and 3' primers were GCTAGGCTTCTGTTGGCTAGC and GAATGCAATTGTTGTTGGTAACTTG, respectively, to detect a 800-bp band. The

following PCR condition was employed: 94^0C x 2 min, 1 cycle; 94^0C x 16 sec, 60^0C x 1 min, 72^0C x 1.5 min, 30 cycles; 72^0C x 5 min, 1 cycle.

Real-time RT-PCR

Drak2 mRNA in Tg and WT cells was measured by real-time RT-PCR; the 5' and 3' primers were CACAGCTGGCCACAGACTTC and CAGAGGACCTGAGAGTCAG, respectively. A 160-bp product was detected with the following amplification program: 95^0C x 15 min, 1 cycle; 94^0C x 15 s, 55^0C x 30 s, 72^0C x 30 s, 40 cycles.

Real-time RT-PCR was also conducted to assess Bcl-2, Bcl-xL and Flip mRNA levels. The 5' and 3' primers for Bcl-2 were CTCGTCGCTACCGTCGTGACTTCG and GTGGCCCAGGTATGCACCCAG, respectively, for the detection of a 380-bp band; the 5' and 3' primers for Bcl-xL were TGGAGTAAACTGGGGTCGCATC and AGCCACAGTCATGCCCGTCAGG, respectively, for the detection of a 264-bp band; the 5' and 3' primers for Flip were GTGGAAGAGTGTCTTGATGAAG and GAGCGAAGCCTGGAGAGTATT, respectively, for the detection of a 480-bp band. The amplification program was the same as that used for Drak2 mRNA.

β-actin mRNA levels were measured as internal controls; the 5' and 3' primers were TGGTACCACAGGCATTGTGAT and TGATGTCACGCACGATTTCCCT, respectively, with the same amplification program as for Drak2 mRNA.

Real-time PCR was performed in triplicate, and the signal ratios of Drak2/β-actin, Bcl-2/β-actin, Bcl-xL/β-actin and Flip/β-actin represented the normalized expression levels of these genes.

Confocal microscopy

Drak2 Tg and WT lymph node cells were placed on slides by Cytospin (Shandon, Pittsburgh, PA), stained with anti-Thy1.2-PE; the cells were subsequently fixed with 4% paraformaldehyde and permeablized with 0.2% Triton x-100. The slides were then stained with rabbit anti-Drak2 Ab (Abgent, San Diego, CA; 1:50 dilution) followed by FITC-conjugated sheep anti-rabbit Ab (Chemicon, Temecula, CA). Such a staining procedure avoided possible failed binding of anti-Thy1.2 mAb to denatured Thy1.2, and prevented entry of anti-Thy1.2 mAb into cytoplasm as background fluorescence. The cells were visualized under a Carl-Ziess confocal microscope, with excitation at 488 nm and emission at 505-550 nm for FITC, and with excitation at 543nm and emission at 560-615 nm for PE. The cell surface Thy1.2 is shown in red, and intracellular Drak2 is in green.

Flow cytometry

T cell, B cell, CD4 cell, and CD8 cell populations in the spleen were analysed by flow cytometry. CD25, CD69 and CD62L expression in T cells was investigated by gating on Thy1.2 cells, as described in our previous publication (15). Annexin-V staining was conducted in Thy1.2-gated T cells or transfected CTEV cells, according to a procedure described before (16).

T-cell lymphokine secretion and proliferation

T cells were purified according to established methods (15). They were stimulated with solid phase anti-CD3, or solid phase anti-CD3 plus anti-CD28. In some experiments, total spleen cells were stimulated with mitomycin-C-treated BALB/c spleen cells in mixed lymphocyte culture. Cell supernatants were collected and assayed for IL-2, IFN-γ and IL-4 by ELISA. Proliferation of T cells and transfected CTEV cells was measured with ^{3}H-thymidine uptake. All these methods have been detailed in our previous publication (15).

Transfection of CTEV cells

CTEV cells (17) were transfected with pCMV-SPORT6-Drak2 (MGC-6721) using Lipofectamine (Invitrogen) according to the manufacturer's instructions; pCMV-SPORT6-Drak2Δ, which contains the Drak2 3' untranslated region served as a control. Twenty-four h after tranfection, dead cells were removed by Lympholyte-M gradient; test and control samples with similar viability of about 80% were cultured overnight, and stained with annexin V to assess cell apoptosis.

The transfected cells were also selected with G-418 for 20 days. Then, a similar number of viable cells ($4x10^5$ cells/200 μl/well) from the test and control samples were cultured for 16 h in the presence of ^{3}H-thymidine, and harvested for the measurement of thymidine uptake.

DTH assay

Mice were first primed by painting their shaved abdominal skin with FITC. On day 6, ear thickness was measured, and then the ears were challenged by FITC painting. Ear thickness

was again measured after 24 h on day 7, and any increases were registered. This method has been described elsewhere (15). To assess the secondary DTH response, these mice were reprimed with FITC on the abdominal skin on day 21; on day 24, ears thickness was measured, and ears were rechallenged by FITC painting; ear thickness was quantified after 24 h on day 25, and any increases were recorded.

RESULTS

Drak2 expression during ontogeny and lymphocyte activation

Drak2 expression during ontogeny is not known. Its expression was studied previously with DNA microarray and with real-time RT-PCR in various tissues (12,13). The limitation of these methods is that they are not able to identify focal expression in a given organ. We, therefore, employed ISH to map the Drak2 expression pattern during ontogeny, starting from embryonic day 12 (e12), and in adult organs, using an antisense probe derived mainly from the Drak2 3' untranslated region, which does not share significant homology with other members of the DAP kinase family.

In the mid-gestation stage on e12 and e14, Drak2 presented ubiquitous expression in most organs (Figs. 1A and 1B). During the perinatal period on e18 and postnatal day 1 (p1), Drak2 expression diminished in most organs but was very high in the thymus (Figs. 1C and 1D). Further expression modulation occurred after birth. On p10 (Fig. 1E) as well as in adulthood (Fig. 1F), Drak2 was prominently expressed in lymphoid organs, such as the thymus, spleen and lymph nodes; in addition, high-level signals were detected in the cerebellum (Cb), skin (Sk), intestine (Int), testes (Tes) and vertebrae (Vb), which probably

reflected the signals from bone marrow. ISH of individual adult organs revealed that in the thymus, Drak2 signals were concentrated in the cortex, whereas in the spleen, in the white pulp (Fig. 2A-H). In the brain (Figs. 2I and 2J), olfactory lobe (OL), ventricular zone (VZ), hippocampal area CA1 (CA1), dentate gyrus (DG), cerebellum (Cb), and pituitary intermediate (IL) and anterior lobes (AL) presented high-level expression. Most interestingly, the suprachiasmatic nuclei were positive for Drak2 mRNA, suggesting Drak2's involvement in the circadian rhythm (Fig. 2K). Drak2 was also expressed in the adrenal gland medulla (Fig. 2L), non-glandular (N Gl) and glandular (Gl) regions of the stomach (Fig. M), and testes spermatocytes (Spc), Sertoli cells and Leydig cells (Fig. N). These results clearly demonstrate that Drak2 expression is not restricted to the T-cells compartment, and its expression in several brain regions, where no active apoptosis occurs, suggests that it has functions other than the regulation of apoptosis.

Drak2 expression during T-cell activation was investigated by Northern blot analysis. Thymocytes and spleen T cells were stimulated with anti-CD3 (clone 2C11), and were harvested at 5 h and 24 h. As shown in Fig. 2O, two discrete bands representing differential splicing products of Drak2 above the 18S ribosome marker were detected in unstimulated cells; their intensity decreased after 5 h and 24 h, indicating downregulation after T-cell activation.

Generation of Drak2 Tg mice

Tg mice expressing human β-actin promoter-driven Drak2 were generated to study Drak2 *in vivo* function in the immune system. The plasmid construct for Tg mice generation is

illustrated in Figure 3A. Three Tg founders were identified by Southern blot analysis, which revealed 2-kb bands specific to Tg mice (lines 877 and 907 were shown in Fig. 3B). Increased Drak2 mRNA expression in mature spleen T cells was confirmed by real-time RT-PCR in line 887 Tg mice (Fig. 3C); similar data were obtained from line 907 (data not presented). Drak2 protein in line 907 Tg and WT lymph node T cells were verified by confocal microscopy employing rabbit anti-Drak2 Ab and anti-thy1.2 mAb double staining (Fig. 3D); Drak2 overexpression (in green) in nuclei and cytosol of Tg T cells (according to cell surface staining of Thy1.2, in red) was obvious compared to WT T cells, in which weak Drak2 signals (in green) were still detectable; control rabbit Ab did not stain the cells (data not shown).

Lines 887 and 907 were expanded for detailed study. These mice were fertile and manifested no gross anomalies upon visual inspection except for their spleen weight. Both lines had a similar phenotype in *vitro* and *in vivo*. Therefore, in most of the cases, unless specified otherwise, representative data for line 887 are reported.

Lymphokine production and proliferation of Drak2 Tg T cells

Spleen weight and cellularity (Fig. 4A) were moderately but consistently reduced in Drak2 Tg mice. T- versus B-cell, and CD4- versus CD8-cell ratios in the spleen of Tg mice were comparable to those of WT controls (Figure 4B). Expression of the T-cell activation markers CD25 and CD69 was normal in Drak2 Tg T cells stimulated by anti-CD3, anti-CD3 plus anti-CD28, or PMA plus ionomycin (Fig. 4C).

We next examined the cytokine production and proliferation of Tg T cells (Fig. 5). Compared to WT T cells, IL-2 and IL-4 but not IFN-γ secretion after anti-CD3 or anti-CD3 plus anti-CD28 stimulation in Tg T cells was augmented (Fig. 5A). On the other hand, despite the augmented IL-2 and IL-4 secretion, Tg T-cell proliferation stimulated by anti-CD3, anti-CD3 plus anti-CD28, or alloantigen was comparable to that of WT T cells, suggesting that IL-2 and IL-4 were not rate-limiting factors for proliferation.

Enhanced apoptosis in activated Drak2 Tg T cells in the presence of exogenous IL-2

Kinases of the DAP family, including Drak2, have been implicated in apoptosis of various cell types, despite a controversial report that Drak2$^{-/-}$ T cells do not seem to undergo abnormal apoptosis after TCR ligation (13). Using Drak2 Tg mice, we set out to examine Drak2's effect on T-cell apoptosis, not only after simple TCR ligation, but also under the influence of IL-2, which is critical for activated T-cell apoptosis (18). WT and Drak2 spleen T cells were activated by solid-phase anti-CD3 and anti-CD28; 24 h later, exogenous IL-2 was added; at 72 h, apoptosis was assessed by annexin V staining. As shown in Fig. 6A, without exogenous IL-2, WT and Tg T cells presented similar rates of apoptosis (37.6% versus 33.5%, first column). In the presence of exogenous IL-2, Tg T cells demonstrated a drastic increase of apoptosis over WT T cells (63.1% versus 27.6%, second column). Persistent TCR ligation is known to favour T-cell apoptosis; under physiological or pathophysiological conditions, TCR ligation is probably a lot shorter than 72 h. We wondered whether the survival of WT and Tg T cells in the presence of IL-2 was still

different if the TCR ligation duration was shortened. To this end, WT and Tg T cells were transferred to uncoated wells after 24-h stimulation with anti-CD3 and anti-CD28, and IL-2 was then added as before. As illustrated in the third column (Fig. 6A), apoptosis was reduced in WT and Tg T cells compared to continuous T-cell ligation (column 2), as expected, but Tg T cells still had a much higher apoptosis rate than WT T cells (48.3% versus 17.5%).

We next employed in vitro Drak2 transfection to confirm our findings on the proapoptotic role of Drak2 in Tg T cells. An IL-2-dependent T cell line CTEV (17) was transfected with a Drak2 expression construct, pSPORT6-Drak2 (MGC-6721, ATCC), in which full-length Drak2 cDNA was placed after a CMV promoter; the majority of dead cells were removed after 24 h with Lympholyte-M gradient. The remaining cells were of similar viability (about 80%) in the test sample (transfected with pSPORT6-Drak2) and the control (transfected with pSPORT6-Drak2Δ). After an additional 16 h culture, cell apoptosis was measured with annexin V staining. Compared to cells transfected with the control construct, CTEV cells transiently transfected with pSPORT6-Drak2 showed significantly increased apoptosis, as measured by annexin V-positive percentage.

We tried to establish stable pSPORT6-Drak2-transfected CTEV cells using standard G418 selection. However, compared to cells transfected with the control construct, pSPORT6-Drak2-transfected cells displayed a significantly slower proliferation rate according to visual inspection, and only a small amount of cells survived after a long-term selection process of about 20 days. These cells constantly had low viability according to trypan blue staining. On day 20 after transfection, an equal number of viable cells from the test and control samples

were pulsed with ^{3}H-thymidine for 16 h, and thymidine uptake was measured to quantify their proliferation. As shown in Fig. 6B, indeed, pSPORT6-Drak2-transfected cells presented drastically reduced growth, most likely due to their high apoptosis rate. Thus, Drak2 overexpression led to augmented CTEV cell apoptosis. It is to be emphasized that in this CTEV cell model, IL-2 was always present, and this model was quite similar to that of Fig. 6A, in which enhanced apoptosis was observed in activated Tg T cells in the presence of IL-2.

To understand the molecular mechanisms of T-cell apoptosis associated with Drak2 overexpression, we surveyed the expression levels of a group of anti-apoptotic factors in Tg versus WT T cells. Bcl-2, Bcl-xL and Flip were expressed at low levels in resting WT and Tg T cells, and were significantly induced 24 h after activation in WT T cells (Fig. 6C); however, such induction was compromised in Tg T cells. In the following 24 h (i.e., from 24 h to 48 h after the initiation of culture), in the presence or absence of IL-2, the difference between WT and Tg T cells was not apparent in terms of Bcl-2, Bcl-xL and Flip expression, although Tg T cells underwent augmented apoptosis in the presence of IL-2 at 72 h. The data suggest that the compromised elevation of these anti-apoptotic factors in activated Tg T cells at an early stage within 24 h of activation rendered the T cells vulnerable to subsequent high-concentration IL-2 insults. The results of this section demonstrate that Drak2 regulates T-cell apoptosis; such an effect is revealed in the presence of higher IL-2 concentration.

Compromised in vivo T-cell memory responses in Drak2 Tg mice

After T-cell clonal expansion in an immune response, IL-2-dependent apoptosis is implicated in the efficacy of memory T-cell development (18). The high apoptosis rate in activated Drak2 Tg T cells in the presence of exogenous IL-2 raised the possibility that

memory T-cell development in these mice might be compromised. Indeed, in middle-aged Tg mice (7 months old), T cells with $CD62L^{lo}$ expression, one of the memory T-cell phenotypes, were increased in percentage, compared to WT mice (Fig. 7A), whereas such a phenotype was not apparent in young Tg mice (3 months old, data not shown). Using T-cell dependent DTH, we assessed memory T-cell development functionally in Drak2 Tg mice. In the primary response measured one week after the first FITC skin priming, Drak2 Tg and WT mice exhibited similar ear thickness increment; however, Tg mice displayed significantly reduced secondary DTH responses (Fig. 7B). These data suggest that memory of the T-cell-mediated immune response is impaired in Drak2 Tg mice.

DISCUSSION

In this study, we investigated the role of Drak2 in mature T-cell apoptosis and memory T-cell development. Several issues are worth discussing.

We have corrected a misconception that Drak2 expression is T-cell-specific. Two previous publications using DNA microarray and RT-PCR failed to detect Drak2 expression outside the T-cell compartment (12,13). The limitation of those methods is that they could not identify localized gene expression in organs; moreover, Drak2 expression during embryonic development was not studied before. Employing ISH, we found that Drak2 was ubiquitously expressed during the mid-gestation stage, around e12 and e14, indicating the participation of this gene in embryonic development. $Drak2^{-/-}$ mice presented no gross anomalies in their

development (13), but this could have been due to the overlapping and rescuing functions of other DAP family kinases. Later, in adult mice, Drak2 expression became more restricted with high levels in the thymus, spleen and lymph nodes; however, many other regions and organs, such as the OL, VZ CA1, IL, AL, SCh in the brain, the Gl and N Gl in the stomach, the adrenal medulla, skin, and testes also showed prominent Drak2 expression, suggesting its broad functions outside the immune system. Drak2 expression in the central nerve system indicates that this molecule has important roles not related to apoptosis, which do not occur significantly in a normal brain. Drak2 expression in the SCh is especially intriguing, as this region is essential in controlling the behavioural circadian rhythm (19); Drak2 is one of a limited number of genes (excluding house keeping genes) with strong expression in the SCh. We monitored the Tg mouse circadian rhythm in 12-h dark/ 12-h light cycles according to their wheel-running activity (20), but abnormalities was not found, compared to WT mice. It would be very interesting to examine whether Drak2$^{-/-}$ mice have an impaired circadian rhythm. The Drak2 gene expression pattern revealed by in situ hybridization provides a useful guidance for further exploration of Drak2 functions in different organs. Actin promoter-driven Drak2 Tg mice were generated for such explorations; however, in this paper, our attention was focus on the role of Drak2 in mature T cells.

Two previous publications failed to discover a role of Drak2 in T-cell apoptosis (13, 21). We have proven that Drak2 served a critical function in T-cell apoptosis, but such an effect was only obvious in the presence of exogenous IL-2. IL-2 is not only a critical lymphokine for T-cell activation, but, paradoxically, it is also essential in activated T-cell apoptosis, as first reported by Lenardo in 1991 (18). Physiologically, IL-2-dependent T-cell apoptosis

could be important in clonal shrinkage after clonal expansion during an immune response, and high in vivo IL-2 concentration could be achieved locally in the vicinity of activated T cells either as an autocrine or paracrine; consequently, the degree of such apoptosis will decide the pool size of surviving T cells, which further differentiate into memory T cells. This could be one of the explanations for the severe autoimmune diseases in mice deficient in IL-2 production (IL-2 gene null mutant) or IL-2 signal reception (IL-2 receptor β gene null mutant) (22,23). Indeed, we have found that secondary but not primary T-cell DTH responses were diminished in Drak2 Tg mice, and middle-aged Drak2 Tg mice had elevated $CD62L^{lo}$ populations; all these observations are consistent with the notion that Drak2 influences memory T-cell development, which was compromised in the presence of Drak2 overexpression. It is noteworthy that Drak2 expression was normally downregulated 24 h after T-cell activation (Fig. 2O), after a surge within 90 min (21). Although the meaning of the rapid surge is not clear, the down regulation after 24 h probably represents a mechanism to prevent excess apoptosis of activated T cells by raising their threshold of vulnerability towards IL-2, and allowing some of the activated T cells to survive and develop into memory cells. Taken together, our data suggest that Drak2 is essential in regulating memory T-cell development.

How Drak2 affects apoptosis is now currently known. We observed that Drak2 Tg T cells had intrinsic defects in upregulation of anti-apoptotic factors, such as Bcl-2, Bcl-xL and Flip, 24 h after activation, although at that time point before addition IL-2, Tg and Wt T cells had not difference in their survival rates. This suggests that Drak2 renders T cells susceptible to IL-2-induced apoptosis induction by reducing their protection by anti-apoptotic factors.

Further studies will be required to elucidate the links between Drak2 and diminished apoptotic factor expression.

In adult Drak2 Tg mice, there was a small but consistent reduction of spleen weight and cellularity, which might reflect compromised ongoing secondary immune responses to environmental antigens. Excessive T cell apoptosis likely contributes to such an anomaly; whether this also involves abnormal B cells apoptosis is currently under investigation.

In summary, our study suggests that Drak2 plays critical roles in mature T-cell apoptosis and memory T-cell development, and this molecule also has functions related and unrelated to apoptosis in a variety of organs. One of its mechanisms in inducing T-cell apoptosis is to downregulate anti-apoptotic factors, which makes the cells vulnerable to apoptotic insults.

ACKNOWLEDGEMENTS

The authors thank Mr. Ovid Da Silva for his editorial assistance, Dr. Martin Marcinkiewicz for *in situ* hybridization analysis, and the Core Facility of the New Emerging Team of Transplantation for DNA microarray analysis.

FOOTNOTES

1. This work was supported by grants from the Canadian Institutes of Health Research (CIHR, MOP57697 and MOP69089), the Kidney Foundation of Canada, the Heart and Stroke Foundation of Quebec, the Juvenile Diabetes Research Foundation USA (1-2005-197), and the J.-Louis Levesque Foundation to J.W. Group grants from the CIHR for New Emerging Teams in Transplantation and from Fonds de la recherche en santé du Québec (FRSQ) for Transfusional and Hemovigilance Medical Research is also acknowledged. J.W. is a National Scholar of the FRSQ.

2. The first two authors contributed equally to this work.

REFERENCES

1. Deiss, L. P., Feinstein, E., Berissi, H., Cohen, O., and Kimchi, A. (1995). *Genes Dev,*9:15-30.

2. Inbal, B., Shani G, Cohen O, Kissil J. L., and Kimchi A.. (2000). *Mol.Cell Biol,* 20:1044-1054.

3. Kawai, T., Matsumoto M, Takeda K, Sanjo H., and Akira S. (1998). *Mol.Cell Biol,*18:1642-1651.

4. Kawai, T., Nomura F, Hoshino K, Copeland N. G., Gilbert D. J., Jenkins N. A., and Akira S. (1999). *Oncogene,* 18:3471-3480.

5. Sanjo, H., Kawai T, and Akira S. (1998). *J.Biol.Chem,* 273:29066-29071.

6. Matsumoto, M., Miyake Y, Nagita M, Inoue H., Shitakubo D., Takemoto K., Ohtsuka C., Murakami H., Nakamura N., and Kanazawa H.. (2001). *J.Bioche,.(Tokyo)* 130:217-225.

7. Henshall, D. C., Araki T, Schindler C. K., Shinoda S., Lan J. Q, and Simon R. P. (2003). *J.Neurochem,* 86:1260-1270.

8. Kuo, J. C., Lin J. R., Staddon J. M., Hosoya H., and Chen R. H. (2003). *J.Cell Sci,* 116:4777-4790.

9. Raveh, T., Droguett G., Horwitz M. S., DePinho R. A., and Kimchi A.. (2001). *Nat.Cell Biol,*3:1-7.

10. Shani, G., Henis-Korenblit S, Jona G, Gileadi O., Eisenstein M., Ziv T., Admon A., and Kimchi A. (2001). *EMBO J,* 20:1099-1113.

11. Jin, Y., Blue E. K, Dixon S, Shao Z., and Gallagher P. J.. (2002) *J.Biol.Chem,* 277:46980-46986.

12. Su, A. I., Cooke M. P., Ching K. A, Hakak Y., Walker J. R., Wiltshire T., Orth A. P., Vega R. G., Sapinoso L. M., Moqrich A., Patapoutian A., Hampton G. M., Schultz P. G. , Hogenesch and J. B. (2002). Proc.Natl.Acad.Sci,U.S.A 99:4465-4470.

13. McGargill, M. A., Wen B. G., Walsh C. M., and Hedrick S. M. (2004). Immunity, 21:781-791.

14. Marcinkiewicz, M. (2002). J.Neuropathol.Exp.Neurol, 61:815-829.

15. Luo, H., Yu G., Tremblay J., and Wu J.. (2004) J.Clin.Invest ,114:1762-1773.

16. Luo, H., Wan X., Wu Y., and Wu J. (2001). J.Immunol, 167:1362-1370.

17. Hu-Li, J., Ohara J., Watson C., Tsang W., and Paul W. E. (1989). J.Immunol, 142:800-807.

18. Lenardo, M. J. (1991) Nature, 353:858-861.

19. Silver, R., LeSauter J., Tresco P. A., and Lehman M. N. (1996). Nature, 382:810-813.

20. Laemle, L. K. and Ottenweller J. E. (1998). Physiol Behav, 64:165-171.

21. Friedrich, M.L., Wen, B.G., Bain, G., Kee, B.L., Katayama, C., Murre, C., Hedrick, S.M., Walsh, C.M. (2005) *Int Immunol.*17:1379-1390.

22. Sadlack, B., Merz H., Schorle H., Schimpl A., Feller A. C., and Horak I. (1993). Cell, 75:253-261.

23. Suzuki, H., Kundig T. M., Furlonger C., Wakeham A., Timms , E. Matsuyama T., Schmits R., Simard J. J., Ohashi P. S., Griesser H., Tniguchi T., Paige C., and Mak T.W. (1995). Science, 268:1472-1476.

FIGURE LEGNEDS

Figure 1. Drak2 expression during ontogeny according to in situ hybridization

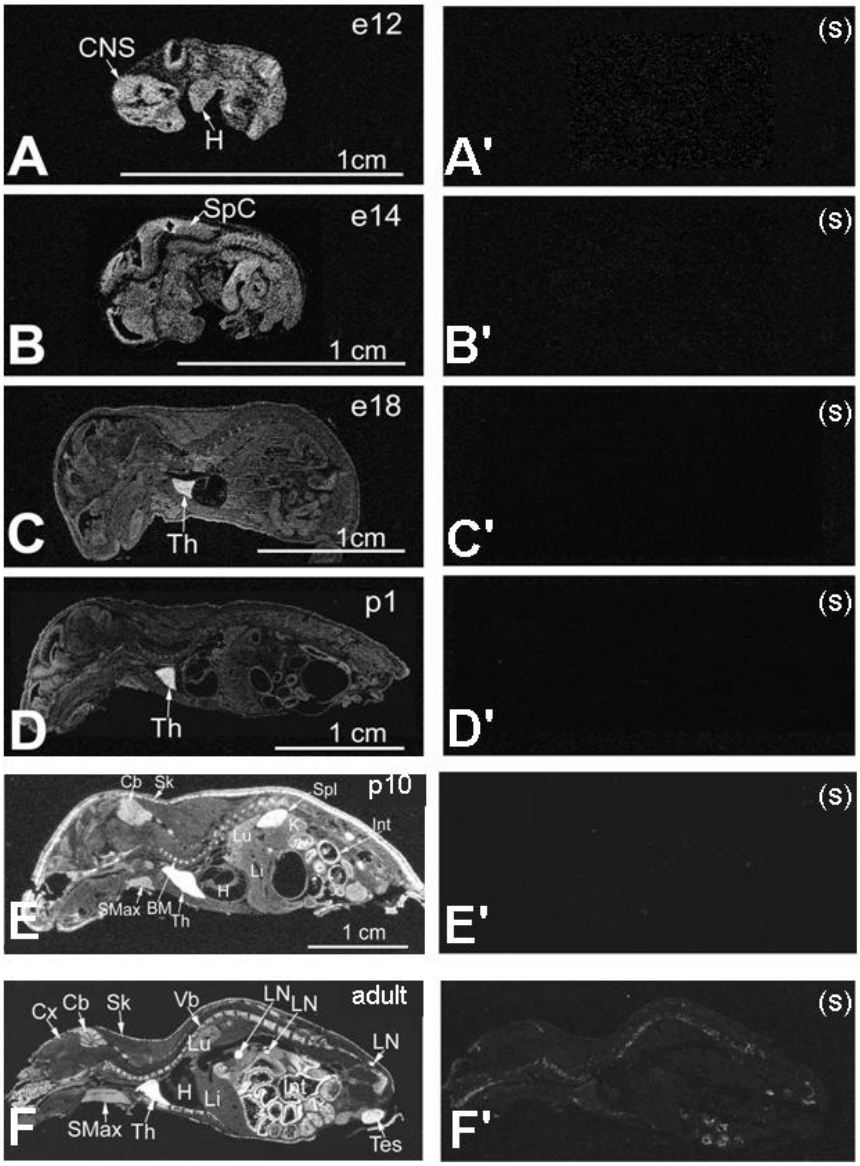

Figure 1

X-ray autoradiography (dark field) of Drak2 *in situ* hybridization in mice from e12 to adulthood, as indicated, is shown (A-F, right column). Hybridization with the sense probe (S) is presented as controls in the left column (A'-F'). Abbreviations are as follows: CNS, central nervous system; SpC, spinal cord; Th, thymus; BM, bone marrow; Cb, cerebellum; H, heart; K, kidney; Int, intestine; Li, liver; Lu, lung; Sk, skin; SMax, submaxillary gland; Spl, spleen; St, stomach. Bar = 1 cm. Ages are indicated.

Figure 2. Drak2 expression in selected adult tissues

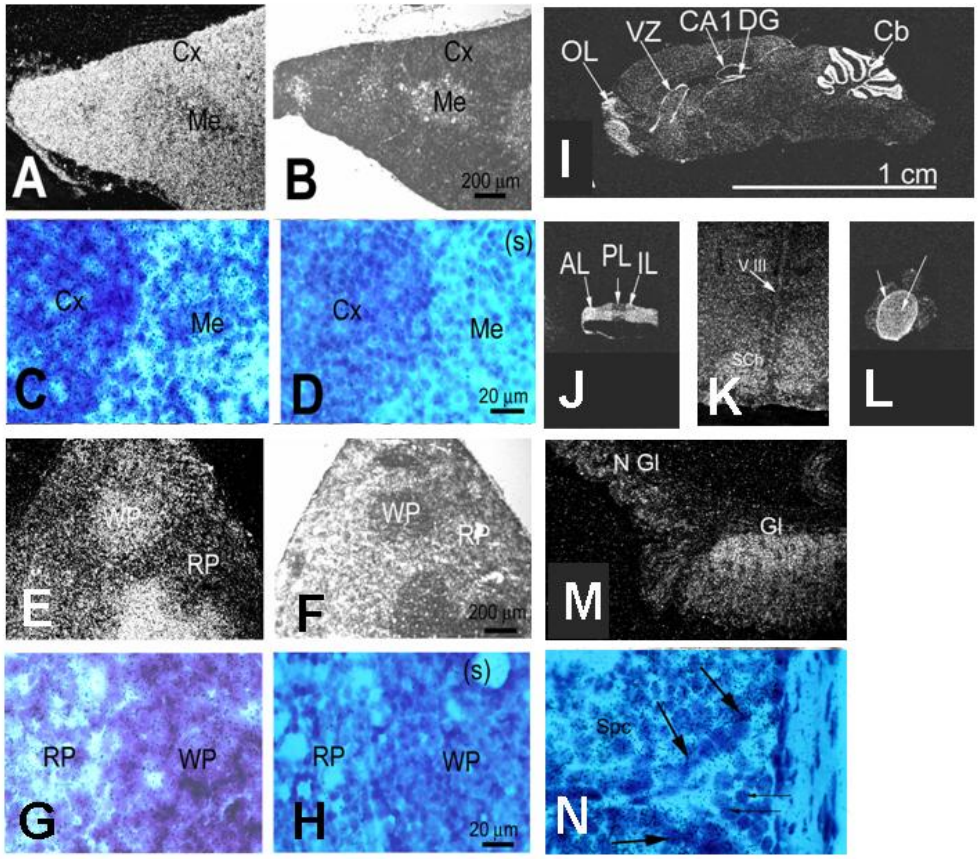

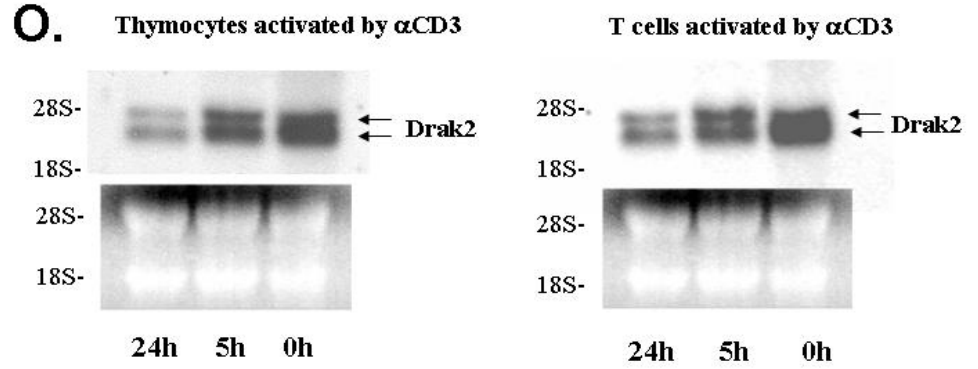

Figure 2

A-N: In situ hybridization of selected adult tissues for Drak2 expression

Hybridization with the sense probe (S) on various tissues (B and D, thymus; F and H, spleen) is included as negative controls. A-D: thymus (Me, medulla; Cx, cortex); E-H: spleen (WP, white pulp; RP, red pulp); I: brain (OL, olfactory lobe; VZ, ventricular zone; CA1, hippocampal area CA1; DG, dentate gyrus; Cb, cerebellum); J: pituitary gland (AL, anterior lobe; IL, intermediate lobe; PL, posterior lobe); K. Brain suprachiasmatic nuclei and vicinity (V III, third ventricle; SCh, suprachasmiatic nuclei); L: adrenal gland (long arrow, medulla; short arrow, cortex); M: stomach (N Gl, non-glandular region; Gl, glandular region); N: testis (large arrows, Sertoli cells; thin arrows, interstitial Leydig cells; Sp, spermatocytes). Panels A, B, E, F, and I-M are dark field X-ray autoradiography; panels C, D, G, H, and N are bright field emulsion autoradiography with hematoxylin counterstaining.

O: Northern blot analysis of Drak2 expression

Thymocytes and spleen T cells were activated by soluble anti-CD3 (0.1 μg/ml, right panel). The duration of activation is indicated. Bands of 28S and 18S ribosomal RNA are presented to show RNA loading.

Figure 3. Generation and characterization of Drak2 Tg mice

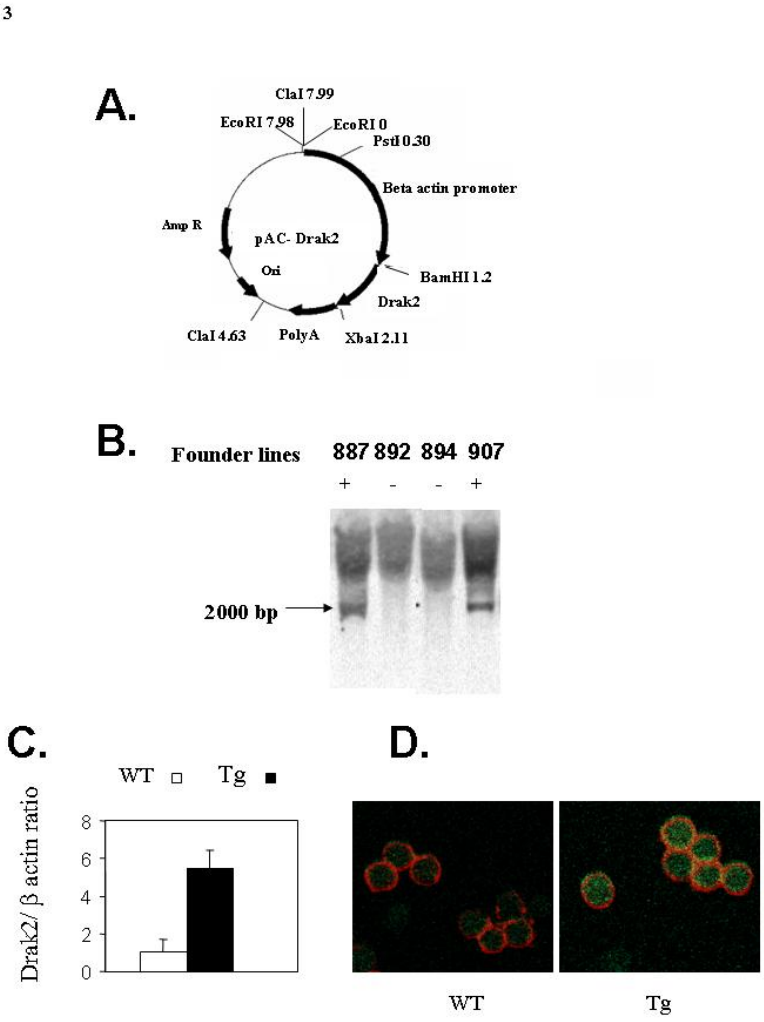

A. pAC-Drak2 construct for Drak2 Tg mice generation

The 4.9-kb ClaI/ClaI fragment was used for microinjection.

B. Southern blot genotyping of Drak2 founder tail DNA

The 2.0-kb band specific to the Drak2 transgene is indicated.

C. *Real-time RT-PCR of Drak2 mRNA from spleen T cells*

Means ± SD of ratios of Drak2 versus β-actin signals are shown; samples are in triplicate.

D. Immunofluorescent staining of Drak2 in WT versus Tg T cells.

Permeablized lymph node T cells were double-stained with rabbit anti-Drak2/sheep anti-rabbit Ig-FITC and anti-Thy1.2-PE mAb, and signals were registered by confocal microscopy. Cell surface Thy1.2 is shown in red, and intracellular Drak2 is in green.

Figure 4. Characterization of Drak2 Tg lymphoid organs and cells

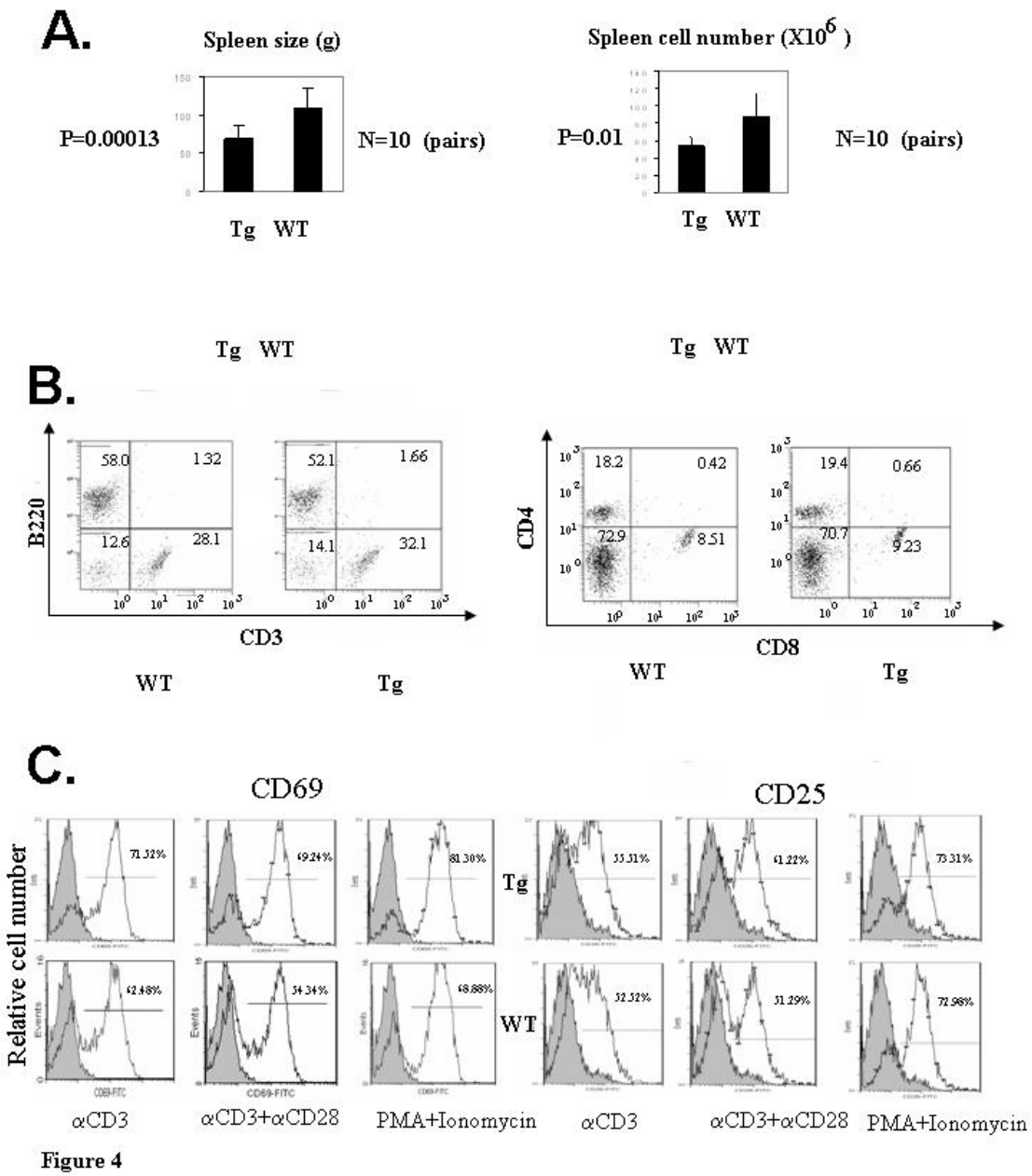

Figure 4

A. Spleen weight and cellularity in Drak2 Tg mice

Ten pairs of Tg mice and their WT littermates were compared for their spleen weight and cellularity. The difference was highly significant ($p=0.0003$ for weight, and $p=0.01$ for cellularity, paired Student's t test).

B. Spleen cell subpopulations for Drak2 Tg mice

T-cell ($CD3^+$) and B-cell ($B220^+$) populations, and CD4 and CD8 T-cell populations in Drak2 Tg and WT spleens were analyzed by 2-color flow cytometry. The percentages are indicated in the histograms.

C. C69 and CD25 expression on activated Drak2 Tg T cells

Drak2 Tg and WT T cells were stimulated overnight by solid phase anti-CD3 (4 μg/ml), or anti-CD3 plus anti-CD28 (0.57 μg/ml and 2.86 μg/ml, respectively) (concentration used during coating). CD69 and CD25 expression on Thy-1.2-gated T cells was measured by 2-color flow cytometry (CD69/Thy1.2 and CD25/Thy1.2).

The experiments described in Figures 4B and 4C were repeated more than 3 times, and representative data are shown.

Figure 5. Lymphokine production and proliferation of Drak2 Tg T cells

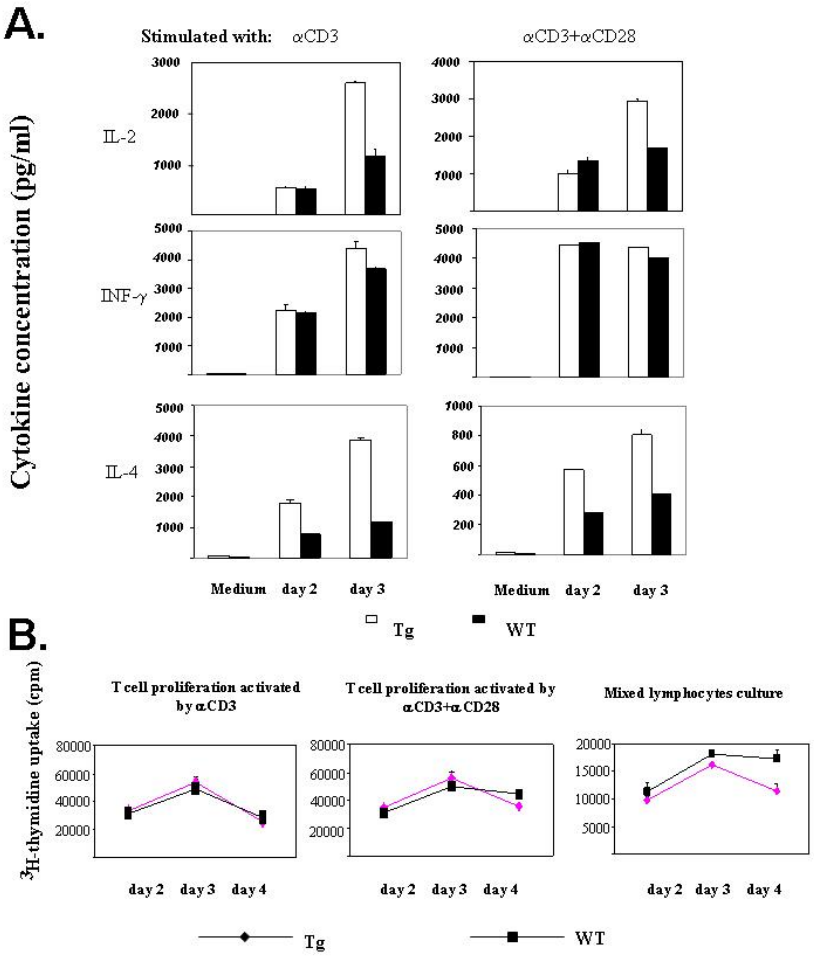

Figure 5

Drak2 Tg and WT spleen T cells were stimulated by solid phase anti-CD3 (4 µg/ml), or solid phase anti-CD3 (0.57 µg/ml) plus anti-CD28 (2.86 µg/ml) (concentrations used during plate coating) as indicated. In mixed lymphocyte culture, total spleen cells from Drak2 Tg or WT mice were stimulated by mitomycin C-treated allogeneic BALB/c spleen cells. Supernatants were harvested on the days indicated, and assayed for lymphokines by ELISA (Fig. 5A). ^{3}H-thymidine uptake of the remaining cells was

measured in triplicate (Fig. 5B). The experiments were repeated more than 3 times, and representative data with means ± SD are shown.

Figure 6. Drak2 T cells are prone to apoptosis

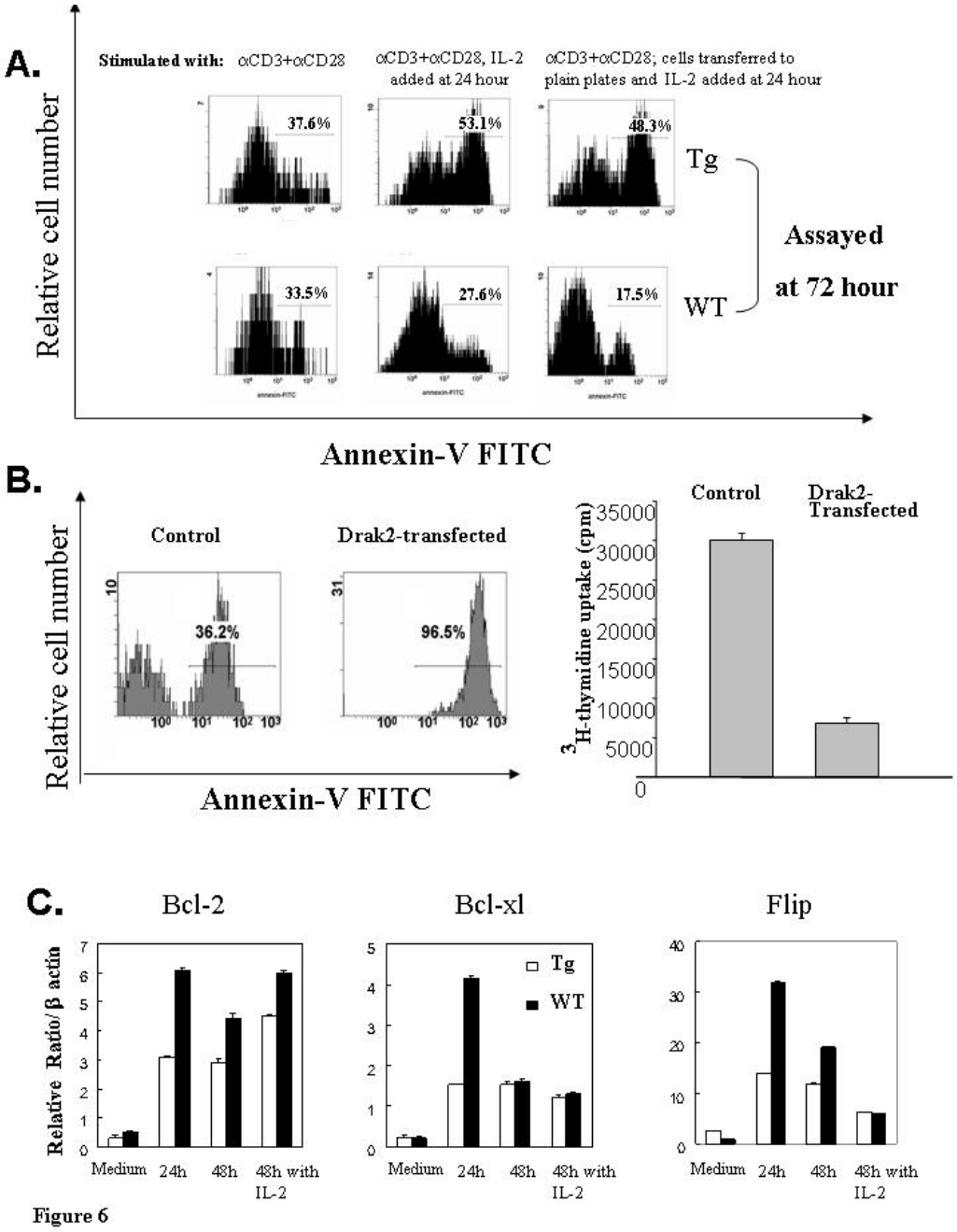

Figure 6

A. Augmented apoptosis of activated Drak2 Tg T cells in the presence of exogenous IL-2

Drak2 Tg and WT spleen T cells were stimulated with solid phase anti-CD3 plus anti-CD28, as described in Fig. 5, in the absence (first column) or presence (second column) of exogenous IL-2 (50 U/ml), which was added to the culture at 24 h. Some T cells (third column) were transferred from anti-CD3- and anti-CD28-coated wells to uncoated wells at 24 h, and exogenous IL-2 was then added to the culture. The cells were harvested at 72 h, and their annexin V expression was assessed by flow cytometry.

B. Increased apoptosis and reduced proliferation of Drak2-transfected CTEV cells

IL-2-dependent CTEV T cell line was transfected with pSPORT-Drak2 or a control construct pSPORT-Drak2Δ. After overnight culture, dead cells were removed by Lympholyte-M gradient, Test and control samples of similar viability (80%) were cultured for an additional 16 h, and their apoptosis was assessed by annexin V staining (right panel). The transfected cells were also selected by G418 for 20 days; then, a similar number of viable cells (according to trypan blue staining) from test and control samples ($4x10^5$/200 μg/well) were pulsed with ^{3}H-thymidine for 16 h for the measurement of thymidine uptake (right panel).

C. Compromised anti-apoptotic factor upregulation in activated Drak2 Tg T cells

Drak2 and WT spleen T cells were activated by solid phase anti-CD3 and anti-CD28 as described in Fig. 5. The cells were harvested, and their Bcl-2, Bcl-xL and Flip mRNA was measured by real-time RT-PCR. The samples were in triplicate, and

means ± SD of the ratios of signals of these molecules versus those of β-actin are shown.

All experiments were conducted more than 3 times, and data from representative experiments are shown.

Figure 7. In vivo cellular and humoral immune responses of Drak2 Tg

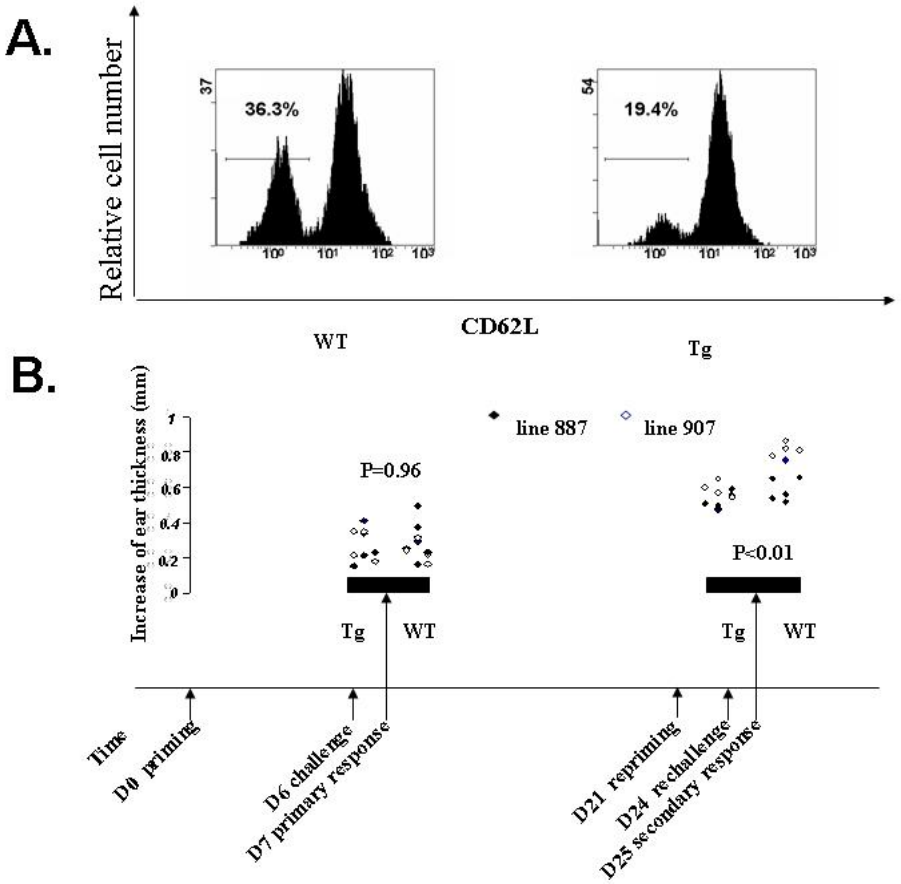

Figure 7

mice

A. Increased CD62L^{lo} T-cell population in middle-aged Drak2 mice

Peripheral blood T cells from Drak2 Tg or WT mice (6-8 months old) were double-stained with Thy-1.2-PE and CD62L-FITC. The histograms showed CD62L expression on Thy1.2-gated cells; percentages of CD62L^{lo} populations are indicated. Four pairs of Tg and WT mice were examined, and data from a representative pair are presented.

B. Normal primary but compromised secondary DTH responses in Drak2 Tg mice

Drak2 transgenic mice (total n=9; n=5 for line 887, and n=4 for line 907) and their WT littermates (total n=10; n=6 for line 887, and n=4 for line 907) were primed by FITC painting on abdominal skin on day 0, and challenged by FITC painting of the ear on day 6. Primary DTH was determined on day 7 by measuring the increase of ear thickness. The mice was reprimed on day 21 on abdominal skin, and rechallenged on the ear on day 24. Secondary DTH was measured on day 25 according to the increase of ear thickness. The increase in ear thickness of each mouse is presented. The difference between the 2 groups is not significant in their primary response ($p=0.96$), but highly significant ($p<0.01$, 2-tailed Student's t test) in their secondary response.

Article 2.

DRAK2 OVEREXPRESSION RESULTS IN INCREASED β-CELL APOPTOSIS AFTER FREE FATTY ACID STIMULATION

Jianning Mao, Hongyu Luo, and Jiangping Wu

J.Cell Biochem. 105 (4):1073-1080, 2008.

Note: **Jianning Mao performed all the experiments in this paper.**

DRAK2 OVEREXPRESSION RESULTS IN INCREASED β-CELL APOPTOSIS AFTER FREE FATTY ACID STIMULATION

Jianning Mao, Hongyu Luo, and Jiangping Wu

Running title: Drak2 in free fatty acid-induced β-cell apoptosis

From [*]the Laboratory of Immunology and [+]Nephrology Service, Centre hospitalier de l'Université de Montréal (CHUM), Notre Dame Hospital, Montreal, Quebec, Canada

Correspondence may be addressed to: Dr. Jiangping Wu, Laboratory of Immunology, Research Centre, CHUM, Notre Dame Hospital, Pavilion DeSève, Room Y-5616, 1560 Sherbrooke Street East, Montreal, Quebec H2L 4M1, Canada. Telephone: (514) 890-8000 ext. 25164; Fax: (514) 412-7596.

ABSTRACT

Drak2 is a serine threonine kinase in the death-associated protein family. In this study, we investigated its role in free fatty acid (FFA)-induced islet apoptosis. Drak2 mRNA and protein were rapidly induced in islet β-cells after FFA stimulation. Such Drak2 upregulation was accompanied by increased β-cell apoptosis, which was inhibited by Drak2 knockdown using siRNA. Conversely, transgenic (Tg) Drak2 overexpression led to aggravated β-cell apoptosis triggered by FFA. Drak2 overexpression in islets compromised the increase of anti-apoptotic factors, such as Bcl-2, Bcl-xL and Flip, upon FFA assault. Further in vivo experiments demonstrated that Drak2 Tg mice presented compromised glucose tolerance in a diet-induced obesity model. Our data show that Drak2 is detrimental to islet survival in the presence of excessive lipid.

INTRODUCTION

Due to calorie-rich diet and sedative life-style, obesity is epidemic in industrialized countries. Taking the US as an example, 30% of its population are obese and 50% are overweight (1) Obesity favours the development of the metabolic syndrome, of which type 2 diabetes (T2D) is one manifestation. In T2D, reduced insulin sensitivity is the major problem (2) initially, but at a later stage, islet apoptosis is also involved.

Blood free fatty acids (FFA) are generated mainly from lipolysis occurring in adipose tissues (3). They are the main energy source for non-glucose dependent tissues such as the liver, heart and muscles. In obesity, the blood FFA level is permanently increased (3), and such increase causes insulin resistance in the liver and skeleton muscles. This is then set the condition for the T2D development. The chronic elevation of blood FFA, especially saturated FFA such as palmitate has been shown to cause β-cell endoplasmic reticulum stress and apoptosis (4).

Recent research has also revealed that adipose and other tissues in T2D release harmful inflammatory cytokines, which are detrimental to islet function and survival (5). In the late stage of T2D, increased blood glucose in combination of elevated FFA contribute to β-cell apoptosis (6).

It is, therefore, conceivable that genes controlling β-cell apoptosis and survival are important in determining susceptibility to islet destruction and T2D risks.

Drak2 is a serine/threonine kinase belonging to a family of death-associated protein kinases (DAP kinases), which consists of DAP (7), DRP-1 (8), ZIP kinase (9), DAPK2 (10), Drak1 and Drak2 (11). Drak2 shares about 50% identity in the kinase domain with other members of the family (7). While DAP, DRP-1 and DAPK2 have a calmodulin regulatory domain in their C-terminal, ZIP, Drak1 and Drak2 do not (7-11). DAP, DAPK2, and DRP-1 are localized in the cytosol (7,8,10), ZIP kinase and Drak1 reside mainly in the nuclei (9,11), whereas Drak2 is found in both the cytosol and nuclei (11,12), suggesting different mechanisms of action. Drak2 autophosphorylates itself, and phosphorylates myosin light chain as an exogenous substrate (11). Its endogenous substrates, other than itself, have not been identified. Drak2 interacts with a calcineurin homologous protein (12), but the biological significance of this interaction is not clear.

When DAP family kinases are overexpressed in various cells, apoptosis ensues (7-11), indicating their involvement in apoptosis. In Drak2 transgenic (Tg) mice, Tg T cells manifest augmented apoptosis after TCR stimulation followed by culture in the presence of IL-2; as a consequence, the memory T-cell pool is diminished, and the Tg mice incur compromised secondary but not primary in vivo T-cell responses (13).

In this study, we discovered that Drak2 expression in islets was rapidly induced by FFA. The induction was accompanied by islet apoptosis. Truncation of such Drak2 upregulation protected β-cells from apoptosis thus induced. Drak2 overexpression in Tg islets resulted in increased β-cell death in vitro upon FFA stimulation, and Drak2 Tg mice developed glucose intolerance after diet-induced obesity. The implications of these findings are discussed.

MATERIALS AND METHODS

Islet purification

Islet purification is performed as we described before (14,15). Briefly, 2-ml of digestion solution (Hanks' balanced salt solution [HBSS] containing 20 mM HEPES and 2 mg/ml collagenase IV (Worthington Biochemical, Lakewood, NJ) were injected into the common bile duct of Tg or wild type (WT) mice (20-24 g) after the distal end of the duct was ligated. The distended pancreas was isolated and put into a 15-ml tube containing an additional 0.5 ml of digestion solution. The pancreas was digested at 37^0C for exactly 28 min, and the digestion process was stopped by the addition of 10 ml of cold HBSS containing 20 mM HEPES. The islet suspension was filtered through No. 7880 cheesecloth gauze (Tyco Healthcare, Mansfield, MA) and centrifuged at 500g for 1-2 min. The pellet was washed with cold HBSS once at 500g for 1-2 min, and the supernatant was removed completely. The pellet was then resuspended in 3 ml of 25% Ficoll, and 2-ml layers of 23, 20, and 11% Ficoll were added sequentially. The Ficoll gradient was centrifuged at 700g for 5 min. Most of the islets were in the interface between the 20 and 23% Ficoll layers and were handpicked with Pasteur pipettes. They were then washed twice with cold HBSS. The islets were cultured overnight in RPMI 1640 containing 10% FCS, and then used for experimentation.

Real time RT-PCR

Drak2 mRNA in Tg and WT cells was measured by real-time RT-PCR; the 5' and 3' primers were CACAGCTGGCCACAGACTTC and CAGAGGACCTGAGAGTCAG, respectively. A 160-bp product was detected with the following amplification program: 95^0C x 15 min, 1 cycle; 94^0C x 15 s, 55^0C x 30 s, 72^0C x 30 s, 40 cycles.

Real-time RT-PCR was also conducted to assess Bcl-2, Bcl-xL and Flip mRNA levels. The 5' and 3' primers for Bcl-2 were CTCGTCGCTACCGTCGTGACTTCG and GTGGCCCAGGTATGCACCCAG, respectively, for the detection of a 380-bp band; the 5' and 3' primers for Bcl-xL were TGGAGTAAACTGGGGTCGCATC and AGCCACAGTCATGCCCGTCAGG, respectively, for the detection of a 264-bp band; the 5' and 3' primers for Flip were GTGGAAGAGTGTCTTGATGAAG and GAGCGAAGCCTGGAGAGTATT, respectively, for the detection of a 480-bp band. The amplification program was the same as that used for Drak2 mRNA.

β-actin mRNA levels were measured as internal controls; the 5' and 3' primers were TGGTACCACAGGCATTGTGAT and TGATGTCACGCACGATTTCCCT, respectively, with the same amplification program as for Drak2 mRNA.

Real-time PCR was performed in triplicate, and the signal ratios of Drak2/β-actin, Bcl-2/β-actin, Bcl-xL/β-actin and Flip/β-actin represented the normalized expression levels of these genes.

Flow cytometry

Drak2 Tg and WT islets were digested with 0.05% trypsin-EDTA to obtain single cell suspensions. The cells were fixed with 4% paraformaldehyde and permeabilized with 0.2% Triton X-100. They were stained with rabbit anti-Drak2 Ab (Abgent, San Diego, CA; 1:50 dilution) and anti-insulin mAb (Sigma, St. Louis, MO; 1:500 dilution). Subsequently, they were stained with FITC-conjugated sheep anti-rabbit antibody (Chemicon, Temecula, CA), and PE-conjugated goat anti-mouse antibody (Jackson Immunoresearch, West Grove, PA), and analyzed by 2-color flow cytometry. Dispersed islet cells or small interfering RNA (siRNA)-transfected NIT-1 cells were also analyzed for apoptosis by flow cytometry using FITC-annexin V staining (16).

Drak2 knockdown by siRNA in NIT-1 cells

NIT-1 cells, derived from mouse insulinoma, were transfected with siRNA using Lipofectamine 2000 (Invitrogen, Burlington, Ontario) according to the manufacturer's instructions. For Drak2 siRNA, the oligonucleotide RNA sequences were CAUCCCUGAAGAUGGCAGCtt and GCUGCCAUCUUCAGGGAUGtt. The control was the scrambled sequence of said siRNA with following sequences: 5'CCCUAAGUGUAGGACGCACtt and 3'GUGCGUCCUACACUUAGGGtt. Single stranded RNA pairs were annealed by being incubated for 1 min at 90^0C, and then cooled down to room temperature over 45 min. The final concentration of double-stranded siRNA was 20 μM for transfection.

Insulin release assay

After 48 h culture in complete F-12K medium with 10% FCS in the absence or presence of various stimulants, the islets were transferred to 12-well plates at a density of 10 islets/well. The islets were gently washed twice with 1 ml Kreb's buffer (NaCl, 135 mM; KCl, 3.6 mM; NaH_2PO_4, 5 mM; $MgCl_2$, 0.5 mM; $CaCl_2$, 1.5 mM; $NaHCO_3$, 2 mM; HEPES, pH 7.4, 10 mM; BSA, 0.07%), and then incubated in Kreb's buffer containing 2.8 mM glucose for 5 min at 37^0C. Two hundred micro litres of supernatant were removed for determination of basal insulin levels. The islets were cultured for additional 40 min, and all the supernatants were harvested for determination of insulin levels as 2.8 mM glucose-stimulated release. The islets were then cultured in Kreb's buffer containing 16.7 mM glucose for 45 min at 37 ^{0}C, and the supernatants were harvested for determination of insulin levels as 16.7 mM glucose-stimulated release. The insulin was assayed by ELISA (Linco Research, St. Charles, MO). The basal insulin levels, which were near zero, were deducted from the 2.8 mM and 16.7 mM glucose-stimulated levels in final data presentation, which was the fold increase of insulin levels of high glucose versus low glucose stimulation.

Glucose tolerance tests

Tg and WT mice were fed a high-fat diet (45% of total calories in the form of fat; Research Diets Inc. New Brunswick, NJ) from age 9 weeks for 6 weeks. They were then fasted for 16 h and injected i.p. with D-glucose (2 mg/g body weight) in PBS. Blood samples from the tail vein were taken at 15, 30, 60, 90, and 120 min after injection for glucose measurements with a glucose meter (Bayer, Toronto, Ontario).

FFA measurements

Serum samples were collected and stored at −20°C until analysis. Their FFA concentrations were determined utilizing the nonesterified fatty acid assay kit (Wako, Richmond, VA) following a modified version of the manufacturer's protocol to accommodate a 96-well microplate. This method utilizes the acylation of coenzyme A by fatty acids in the presence of added acyl-CoA synthetase. Briefly, reagents A and B were prepared as directed by the protocol and then diluted with 13.3 ml of 0.05 M phosphate buffer. Seven standards, ranging from 0 to 1 mEq/L, were prepared from the supplied stock (1 mEq/L). The samples, standards, controls, and blanks were then added to a 96-well microplate in duplicate (10 µl/well). At that time, 100 µl of reagent A was added to each well and mixed prior to a 30-min incubation at room temperature. Finally, reagent B was added (200 µl per well), and mixed followed by an additional 30-min incubation at room temperature, after which the plate was read at 550 nm. Utilizing the standard curve, sample values were expressed as mEq/L.

RESULTS

Rapid induction of Drak2 expression in islet β-cells and its association with islet apoptosis

In obesity and T2D, high serum lipid is known to jeopardize islet function and survival (17). When isolated islets were exposed to FFA in vitro, Drak2 mRNA was drastically induced within 24 h (Fig. 1A). When FFA was injected into mice i.p., within 1 hour, serum FFA levels were increased (Fig. 1B). Such a FFA concentration increase was accompanied by a significant augmentation of Drak2 expression at 1 h (Fig. 1A; time shown was the duration between FFA injection and mouse sacrifice; the time of islet

isolation was not calculated in). The in vivo response was much faster than in vitro response. A likely explanation was that β-cells in vivo in the pancreas were in their natural environment with full viability and function, while isolated islets in vitro had experienced traumatic isolation procedures, and were slow to respond to additional stimuli.

We next assessed Drak2 protein levels in β-cells, employing anti-insulin mAb and anti-Drak2 Ab in 2-color flow cytometry. When the islets were stimulated with FFA, Drak2 protein levels in insulin-positive β-cells were significantly augmented at 48h after FFA assault, as shown in histogram 1C; a summary of 3 independent experiments is illustrated in Fig. 1D. The finding on Drak2 protein increase was consistent with the heightened Drak2 mRNA expression at 24h. FFA induced islet cell apoptosis (Fig. 2A, top row, WT islets). Taken together, our data indicate that Drak2 overexpression in islets leads to their apoptosis.

Drak2 knockdown by siRNA protected NIT-1 insulinoma cells from FFA-triggered apoptosis

To prove that Drak2 was indeed critical to FFA-induced β-cell apoptosis, we employed siRNA to prevent Drak2 upregulation in NIT-1 insulinoma cells. NIT-1 cells were derived from a transgenic NOD mouse harbouring a hybrid rat insulin-promoter/SV40 large T-antigen gene (18). As shown in Fig. 3A, similarly to normal β–cells, Drak2 protein was induced in NIT-1 cells by FFA according to flow cytometry. Two different Drak2 siRNAs (#592 and #1162) significantly truncated Drak2 protein upregulation

stimulated by FFA, but a control siRNA had no effect on the Drak2 level. As in normal islet cells, FFA induced NIT-1 cell apoptosis after 24 h (Fig. 3B). However, with protection by the 2 Drak2 siRNAs #592 and #1162, but not the control siRNA, such apoptosis induction was truncated. We noticed that FFA-induced apoptosis in NIT-1 cells occurred at 24 h after the FFA assault, compared with 48 h needed for normal islet cells. The faster apoptosis kinetics in NIT-1 cells was probably due to that they were transformed cells with more active cellular machinery for live and death decisions.

Drak2 overexpression in Tg islets aggravated FFA-triggered apoptosis

To further validate the role of Drak2 in islet survival, actin promoter-driven Drak2 Tg mice, as described in our previous publication (13), were studied. These mice are viable, fertile, and have no gross anomalies. They had comparable body weight with WT littermates from 6 wks to 22 wks old (Fig. 4A). Their serum inflammatory cytokine IL-6 levels were similarly low as that of WT mice (Fig. 4B). There was no significant difference in fasting blood glucose levels between Tg and WT mice (Fig. 4C). We demonstrated in Fig. 4D that Drak2 protein expression in insulin-positive Tg islet cells was augmented both in terms of Drak2 mean fluorescent intensity (MFI) and percentage of Drak2 positive cells, compared with WT islet cells (MFI 22.1 in Tg β-cells versus MFI 13.3 in WT β-cells; 97.2% versus 74.4% Drak2 positive Tg β-cells versus WT β-cells), according to Drak2/insulin two-colour flow cytometry.

When Tg islets were stimulated with FFA for 24 h, their apoptosis was significantly increased, compared to WT islets (41.8% versus 20.2%; Fig. 2A, 2nd column). At 48 h,

WT islets also started to suffer from apoptosis, but Tg islets were inflicted with more damage (57.6% versus 42.2%, Tg versus WT; Fig. 2A, 3rd column; a summary of 3 independent experiments with data collected at 48 h is illustrated in Fig. 2B).

To assess the function of β-cells under FFA assault, we evaluated islet insulin release after 16.7 mM glucose stimulation. At 48 h after FFA assault, insulin released by the Tg β-cells was significantly lower than by WT β-cells (Fig. 2C). This confirmed that augmented Drak2 expression was harmful to β-cell function.

Drak2 overexpression compromised anti-apoptotic molecule induction

To understand the molecular mechanisms of β-cell apoptosis associated with Drak2 overexpression, we surveyed the expression levels of a group of anti-apoptotic factors in Tg versus WT β-cells. Anti-apoptotic factors Bcl-2, Bcl-xL and Flip were expressed at low levels in WT and Tg β-cells, but were significantly induced 24 h after FFA stimulation in WT β-cells (Fig. 5); however, such induction was compromised in Tg β-cells. The data indicate that Drak2 overexpression in islets reduce the elevation of anti-apoptotic factors upon detrimental stimulation, and suggests that such compromise might be one of the reasons that renders β-cells prone apoptotic.

Drak2 overexpression led to glucose intolerance in mice under high fat diet

With a regular diet, Tg mice in the C57BL/6 background at 9 weeks of age had a moderate elevation of serum FFA, compared with WT mice, although the difference did not reach statistical significance (Fig. 6A). The Tg mouse serum fasting insulin level at

this stage was significantly higher than that of WT (Fig. 6B), probably due to insulin resistance caused by the higher serum FFA levels; such FFA-related insulin resistance and the subsequence insulin level increase has been reported previously (19). When the mice were fed a high fat-diet for 6 weeks to mimic a pre-T2D condition, i.e., diet-induced obesity (20), both Tg and WT animals became overweight, on average 10 g heavier than mice on a normal diet (data not shown). After the high-fat diet, both groups maintained normal fasting blood glucose levels (Fig. 6C). However, Tg mouse serum FFA levels were significantly higher than those of WT mice (Fig. 6A); Tg mouse fasting insulin levels were significantly lower than those of WT mice. Moreover, in the glucose tolerance test, Tg mice manifested statistically significantly higher blood glucose levels at 30, 60 and 90 min after glucose injection (Fig. 6C). The interpretation of these results is given in the section of Discussion.

DISCUSSION

In this study, we have demonstrated that Drak2 is critical in β-cell apoptosis triggered by FFA. Further in vivo experiments proved that enhanced Drak2 expression reduced glucose tolerance after high-fat diet. It seems that Drak2 is in the pathway downstream of harmful signals received by islets upon FFA stimulation.

We showed that Drak2 was upregulated in islet β-cells upon FFA stimulation, and such upregulation was correlated to decreased islet function and survival. Interestingly, although Tg islets had higher Drak2 expression, such over expression by itself did not manifest harmful effects on the islets, as Tg mice did not develop diabetes, and Tg

islets culture in medium did not suffer from increased apoptosis, compared to WT islets, until an exogenous detrimental factor FFA was present. This suggests that Drak2 might act on a two-hit mode, in which signalling event(s) (hit 1) derived from FFA stimulation as well as Drak2 (hit 2) are both required to results in β-cell damage and/or dysfunction. For normal islets, high Drak2 expression (hit 2) could be a consequence of FFA (hit 1). We hypothesize that in individuals with abnormally high basal Drak2 expression in islets, less hit 1 might be sufficient to cause excessive islet damage or dysfunction, and thus these individuals are more prone to T2D development when facing increased serum lipid. In humans, Drak2 gene is located in 2q33.2, and is 14.8 Mbp away from a type 2 diabetes risk region at 2q32.1 (http://www.ncbi.nlm.nih.gov/entrez/dispomim.cgi?cmd=entry&id=601724). An epidemiological study on T2D prevalence in individuals having enhanced Drak2 expression will answer the question whether Drak2 is a bona fide diabetes risk gene in humans.

We found Tg mice had a moderately increased serum FFA level compared with WT mice under a normal diet. The mechanism of such an increase is not clear at the present time. It is quite likely that such a FFA increase caused insulin resistance, which in turn was responsible for the elevated serum insulin levels. It was somewhat surprising that after a high-fat diet, in the presence of prolonged higher serum FFA levels in Tg mice, the fasting insulin levels of Tg mice were significantly lower than those of WT mice. A possible explanation is that the prolonged high FFA levels in Tg mice compromised islet β-cells in terms of insulin release and/or survival. When these mice underwent the

glucose tolerance test, they could not cope with the transient surge of blood glucose by providing sufficient insulin, and manifested a prolonged high glucose levels, compared to WT mice.

Currently, our knowledge about the Drak2 activation pathway and Drak2 substrates is limited. We only know that Drak2 is a genuine substrate of itself. Obviously, genes in the Drak2 pathway could all be involved in FFA-induced islet dysfunction and apoptosis, which are critical factors in type 2 diabetes development.

ACKNOWLEDGEMENT

The authors thank Mr. Ovid Da Silva for his editorial assistance.

FOOTNOTE

1. This work was supported by grants from the Canadian Institutes of Health Research (CIHR, MOP57697, MOP69089 and PPP85159 to J.W., and MOP79565 to H.L), the Kidney Foundation of Canada, the Heart and Stroke Foundation of Quebec, the Juvenile Diabetes Research Foundation USA (1-2005-197), and the J.-Louis Levesque Foundation to J.W. Group grants from the CIHR for New Emerging Teams in Transplantation, Fonds de la recherche en santé du Québec (FRSQ) for Transfusional and Hemovigilance Medical Research, and Genome Canada/Genome Quebec are also acknowledged. J.W. was a National Scholar of the FRSQ.

REFERENCES

1. Wild,S, Roglic,G, Green,A, Sicree,R, King,H. 2004. Global prevalence of diabetes: estimates for the year 2000 and projections for 2030. Diabetes Care 27:1047-1053.

2. Lockwood,DH, Amatruda,JM. 1983. Cellular alterations responsible for insulin resistance in obesity and type II diabetes mellitus. Am.J Med. 75:23-31.

3. Delarue,J, Magnan,C. 2007. Free fatty acids and insulin resistance. Curr.Opin.Clin.Nutr.Metab Care 10:142-148.

4. Lai,E, Bikopoulos,G, Wheeler,MB, Rozakis-Adcock,M, Volchuk,A. 2008. Differential activation of ER stress and apoptosis in response to chronically elevated free fatty acids in pancreatic beta-cells. Am.J.Physiol Endocrinol.Metab 294:E540-E550.

5. Kahn,SE, Hull,RL, Utzschneider,KM. 2006. Mechanisms linking obesity to insulin resistance and type 2 diabetes. Nature 444:840-846.

6. Rhodes,CJ. 2005. Type 2 Diabetes-a Matter of {beta}-Cell Life and Death? Science 307:380-384.

7. Deiss,LP, Feinstein,E, Berissi,H, Cohen,O, Kimchi,A. 1995. Identification of a novel serine/threonine kinase and a novel 15-kD protein as potential mediators of the gamma interferon-induced cell death. Genes Dev. 9:15-30.

8. Inbal,B, Shani,G, Cohen,O, Kissil,JL, Kimchi,A. 2000. Death-associated protein kinase-related protein 1, a novel serine/threonine kinase involved in apoptosis. Mol.Cell Biol. 20:1044-1054.

9. Kawai,T, Matsumoto,M, Takeda,K, Sanjo,H, Akira,S. 1998. ZIP kinase, a novel serine/threonine kinase which mediates apoptosis. Mol.Cell Biol. 18:1642-1651.

10. Kawai,T, Nomura,F, Hoshino,K, Copeland,NG, Gilbert,DJ, Jenkins,NA, Akira,S. 1999. Death-associated protein kinase 2 is a new calcium/calmodulin-dependent protein kinase that signals apoptosis through its catalytic activity. Oncogene 18:3471-3480.

11. Sanjo,H, Kawai,T, Akira,S. 1998. DRAKs, novel serine/threonine kinases related to death-associated protein kinase that trigger apoptosis. J.Biol.Chem. 273:29066-29071.

12. Matsumoto,M, Miyake,Y, Nagita,M, Inoue,H, Shitakubo,D, Takemoto,K, Ohtsuka,C, Murakami,H, Nakamura,N, Kanazawa,H. 2001. A serine/threonine kinase which causes apoptosis-like cell death interacts with a calcineurin B-like protein capable of binding Na(+)/H(+) exchanger. J.Biochem.(Tokyo) 130:217-225.

13. Mao,J, Qiao,X, Luo,H, Wu,J. 2006. Transgenic drak2 overexpression in mice leads to increased T cell apoptosis and compromised memory T cell development. J.Biol.Chem. 281:12587-12595.

14. Wu,Y, Han,B, Luo,H, Shi,G, Wu,J. 2004. Dipeptide boronic acid, a novel proteasome inhibitor, prevents islet-allograft rejection. Transplantation 78:360-366.

15. Wu,Y, Han,B, Luo,H, Roduit,R, Salcedo,TW, Moore,PA, Zhang,J, Wu,J. 2003. DcR3/TR6 effectively prevents islet primary nonfunction after transplantation. Diabetes 52:2279-2286.

16. Murakami,Y, Takamatsu,H, Taki,J, Tatsumi,M, Noda,A, Ichise,R, Tait,JF, Nishimura,S. 2004. 18F-labelled annexin V: a PET tracer for apoptosis imaging. Eur.J.Nucl.Med.Mol.Imaging 31:469-474.

17. Ahren,B. 2005. Type 2 diabetes,insulin secretion and beta-cell mass. Curr.Mol.Med. 5:275-286.

18. Hamaguchi,K, Gaskins,HR, Leiter,EH. 1991. NIT-1, a pancreatic beta-cell line established from a transgenic NOD/Lt mouse. Diabetes 40:842-849.

19. Jiao,K, Liu,H, Chen,J, Tian,D, Hou,J, Kaye,AD. 2008. Roles of plasma interleukin-6 and tumor necrosis factor-alpha and FFA and TG in the development of insulin resistance induced by high-fat diet. Cytokine 42:161-169.

20. Winzell,MS, Ahren,B. 2004. The high-fat diet-fed mouse: a model for studying mechanisms and treatment of impaired glucose tolerance and type 2 diabetes. Diabetes 53 Suppl 3:S215-S219.

FIGURE LEGNEDS

Figure 1. Drak2 was rapidly augmented in islets treated with FFA

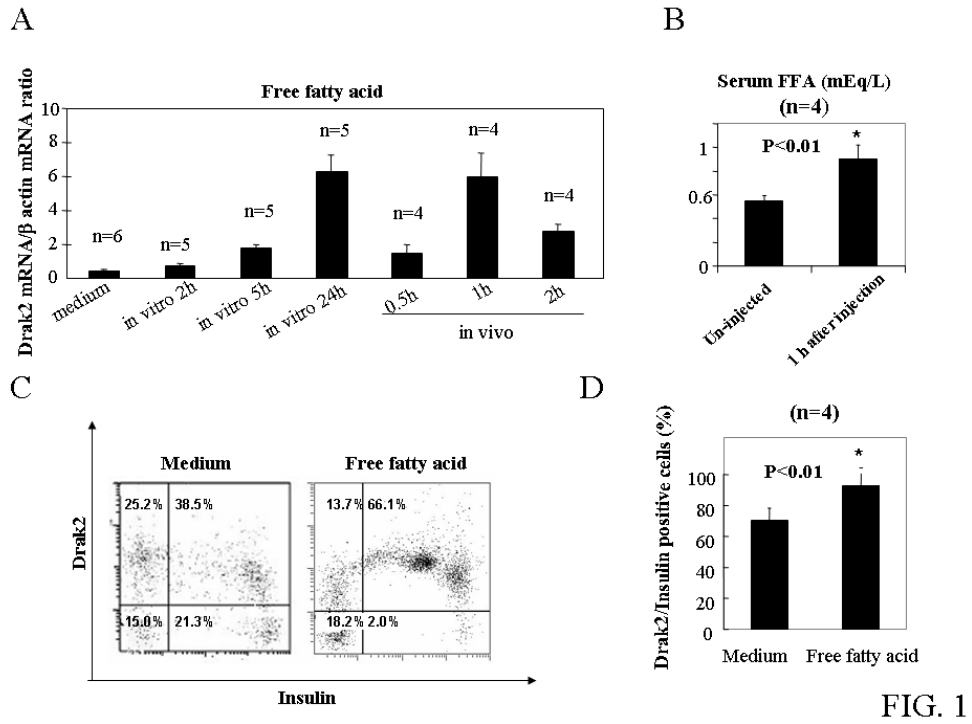

FIG. 1

A. Drak2 mRNA expression according to real time RT-PCR

Islets were stimulated by FFA (0.7 mM oleate and palmitate mixed in a 2:1 ratio) in vitro, or C57BL/6 mice were injected with 15mM FFA 0.5ml (oleate and palmitate mixed in a 2:1 ratio) i.v. in PBS at the indicated time before sacrifice of the mice. For the in vivo experiment, the time indicated was from the time of FFA injection until the sacrifice; the duration of islet isolation (about 1 h) was not calculated in. Drak2 mRNA expression in islet cells was measured by real time RT-PCR. The ratio of Drak2 mRNA and β-actin mRNA was taken as a measure of Drak2 mRNA levels. The samples were in triplicate, and the means $\pm$ SD of 4-6 independent experiments (as indicated) are shown.

B. Plasma FFA levels after FFA injection

C57BL/6 mice were injected i.p. with 0.5 ml of 15mM FFA (oleate and palmitate mixed in a 2:1 ratio), and their plasma FFA levels 1 h after the injection were measured by ELISA. Samples were in duplicate. Means ± SD of the injected and control groups are shown (n=4 for each group). The difference is statistically significant ($p<0.01$, Student's t test).

C. and D. Drak2 protein expression according to flow cytometry

C57BL/6 islets were cultured for 48 h in the absence or presence of FFA as described in Fig. 1A. The islets were dispersed after the culture and analyzed by 2-color flow cytometry for intracellular insulin and Drak2 staining. The experiment was repeated 4 times. A representative set of histograms is shown in Fig. 1B and the summary of all 4 experiments is illustrated in Fig. 1C. The asterisk indicates a p value of <0.01 according to Student's t test.

Figure 2. Drak2 Tg islets were prone to apoptosis upon FFA stimulation

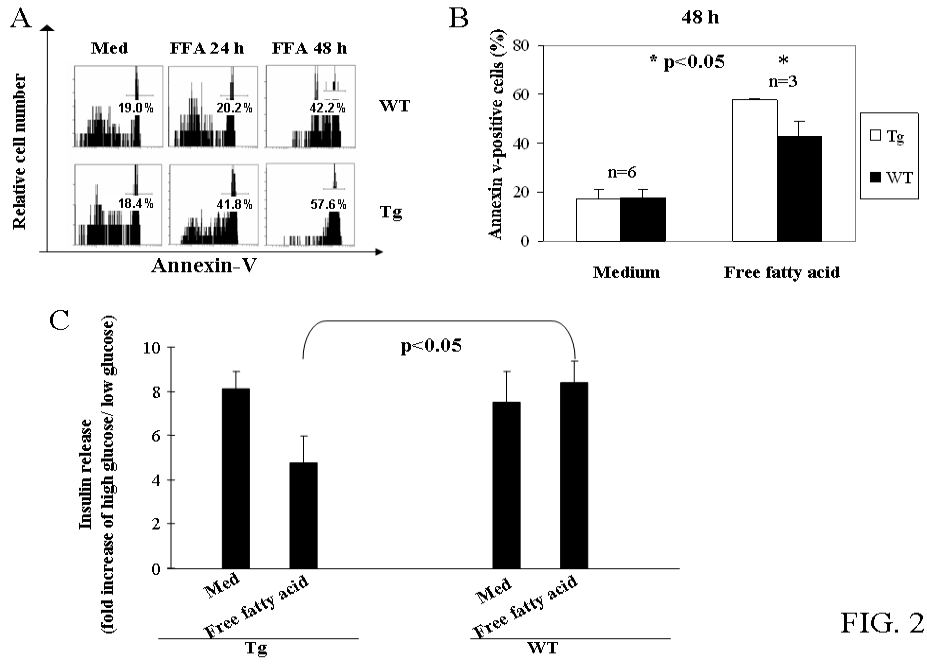

FIG. 2

A and B. Flow cytometry analysis of islet cell apoptosis

Drak2 Tg and WT islets were cultured in RPMI 1640 with 10% FCS and stimulated with FFA as described in Fig. 1. After 24 h or 48 h, as indicated, the islets were dispersed and analyzed by flow cytometry with annexin V staining. The percentage of annexin V-positive cells is shown in the histograms (Fig. 2A). The experiment was repeated 3-6 times and the mean $\pm$ SD of data at 48 h of all these experiments are illustrated in Fig. 2B. The asterisk indicates $p<0.05$, according to Student's t test.

C. Islet insulin release after FFA stimulation

Islets from Tg or WT mice were cultured in F-12K medium with 10% FCS in the presence or absence of FFA as described in Fig. 1. Insulin release by these cells was conducted after 48 h. For each treatment, the fold increase between low glucose and high glucose stimuli was presented. Insulin release by Tg islets after FFA stimulation was significantly lower than that by WT islets ($p<0.05$, Student's t test).

Figure 3. Drak2 siRNA inhibited Drak2 protein upregulation and reduced apoptosis in NIT-1 cells upon FFA stimulation

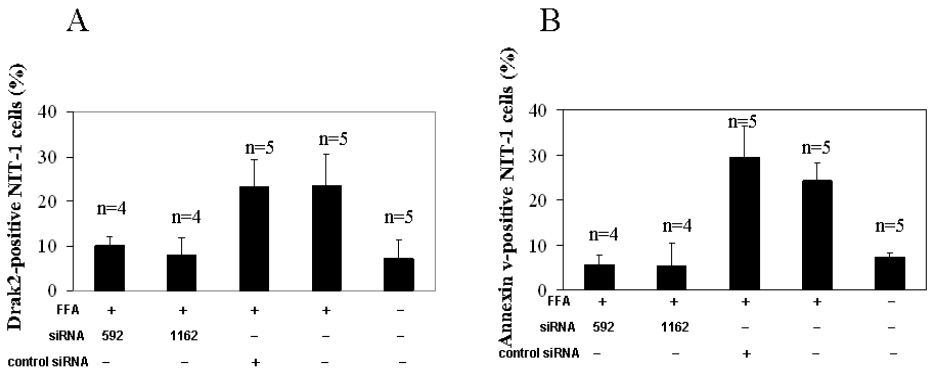

FIG. 3

A. Drak2 protein levels in NIT-1 cells

NIT-1 cells were transfected with 2 Drak2 siRNAs (#592 and #1162), or a control siRNA, which is with a scrambled sequence of #1162. The cells were cultured for 24 h in the absence or presence of FFA, as indicated, and then analyzed for intracellular Drak2 protein levels by flow cytometry. The experiment was repeated 4-5 times, as indicated, and means $\pm$ SD of these experiments are shown.

B. Drak2 siRNA prevented FFA-induced apoptosis in NIT-1 cells

NIT-1 cells were transfected with 2 different Drak2 siRNAs (#592 and #1162), or a control siRNA, as described in Fig. 3A. The cells were cultured for 24 h in the absence or presence of

FFA, as indicated, and analyzed for apoptosis by flow cytometry with annexin V staining. The experiment was repeated 4-5 times, as indicated, and means ± SD of percentage apoptosis of all of these experiments are shown.

Figure 4. Features of Drak2 Tg mice

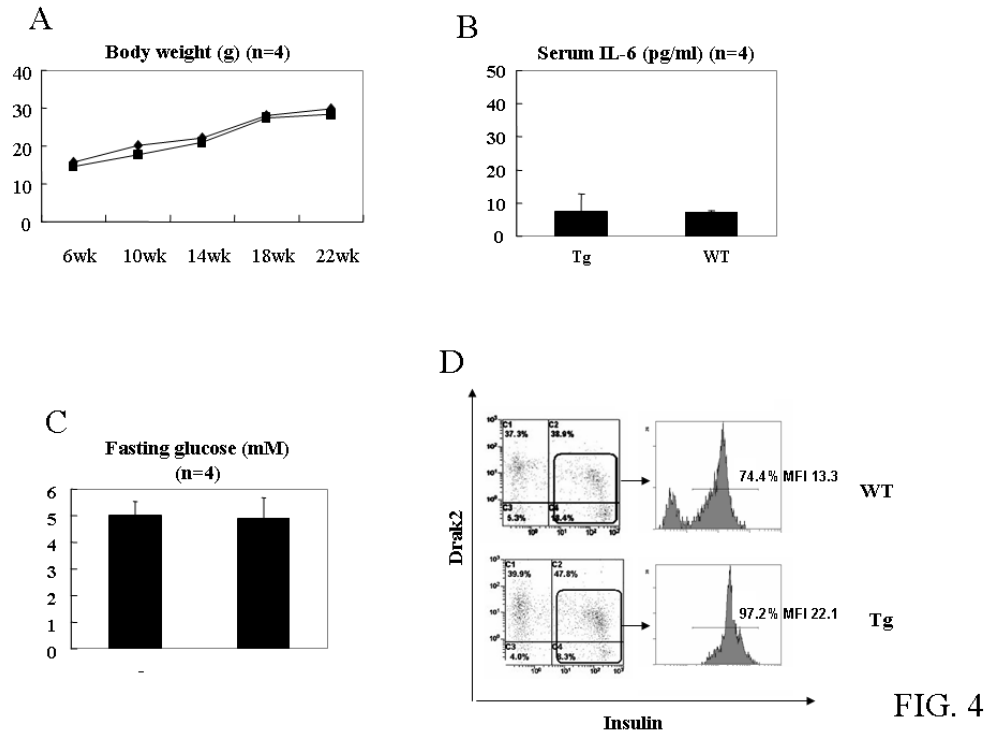

FIG. 4

A. Body weight of Tg and WT mice

The body weight (means ± SD) of Tg and WT littermates (n=4 for each group) from 6 wks to 22 wks of age are illustrated. No significant difference in any time point is found ($p>0.05$, Student's t test).

B. Serum IL-6 levels of Tg and WT mice

Serum IL6 of Tg and WT mice (n=4 for each group) were measured by ELISA. The ELISA samples were in duplicate. Means ± SD of IL-6 levels are shown. There is no statistical difference between the two groups ($p>0.05$, Student's t test).

C. Fasting serum glucose levels of Tg and WT mice

Blood glucose of Tg and WT mice (n=4 for each group) were measured after overnight fasting. Means ± SD of the glucose levels are shown. There is no statistical difference in the blood glucose levels of the two groups ($p>0.05$, Student's t test).

D. Drak2 overexpression in Tg β-cells

Drak2 Tg or WT islets were analyzed by 2-color flow cytometry for Drak2 and insulin expression (right column). The percentage of Drak2 positive cells among insulin-positive cells and their mean fluorescent intensity (MFI) are indicated in the left column. Upper row, WT; bottom row, Drak2 Tg.

Figure 5. Compromised anti-apoptotic factor upregulation in Drak2 Tg islets

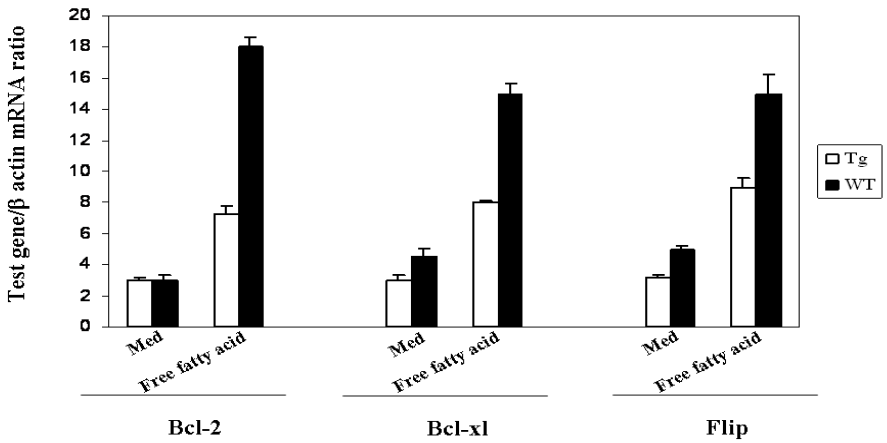

FIG. 5

Drak2 and WT islets were stimulated by FFA as described in Fig. 1. The islets were harvested after 24 h, and their Bcl-2, Bcl-xL and Flip mRNA was measured by real-time RT-PCR. The samples were in triplicate. Means ± SD of the ratios of signals of these molecules versus those of β-actin from 2 independent experiments are shown.

Figure 6. Features of Drak2Tg mice after diet-induced obesity

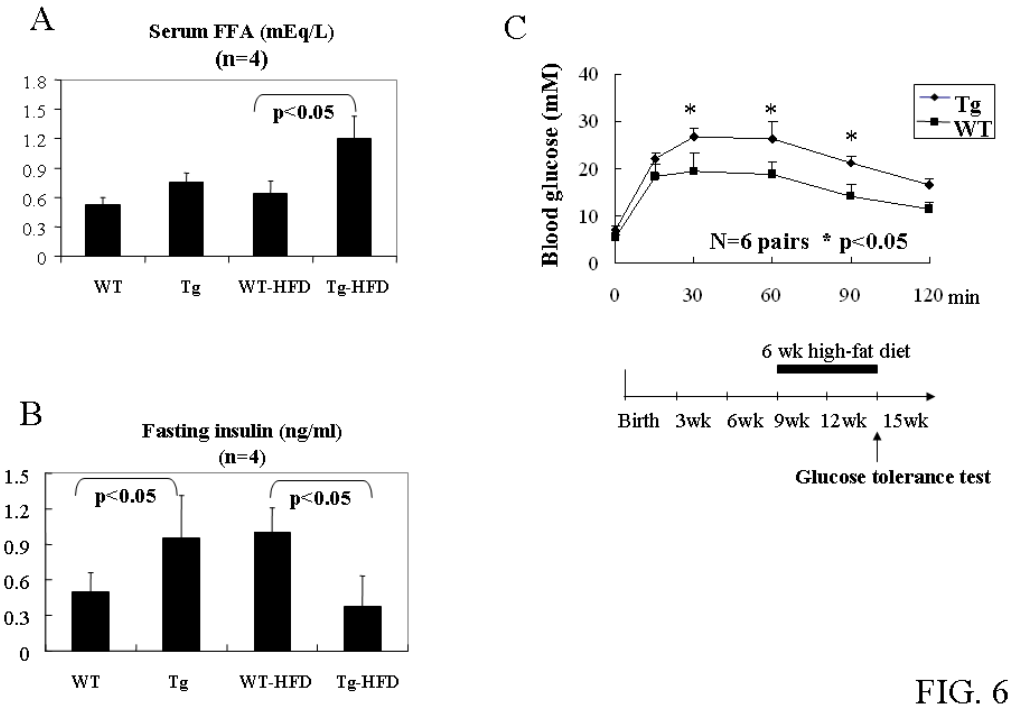

FIG. 6

A. Serum FFA levels of Tg and WT mice before and after high-fat diet

Tg and WT mouse serum FFA levels were measured by ELISA before and after a 6-wk high-fat diet (HFD). The ELISA samples were in duplicate. Means ± SD of the FFA levels of the two groups (n=4 for each group) are shown. The serum FFA levels of the Tg and WT groups were significantly different after HFD ($p<0.05$, Student's t test).

B. Fasting serum insulin levels of Tg and WT mice before and after high-fat diet

Tg and WT mouse fasting serum insulin levels were measured by ELISA before and after 6-wk HFD. The ELISA samples were in duplicate. Means $\pm$ SD of the insulin levels of the two groups (n=4 for each group) are shown. The insulin levels of the Tg mice were significantly higher than those of WT mice before HFD, and were significantly lower than those of WT mice after HFD ($p<0.05$ in both cases, Student's t test).

C. Reduced glucose tolerance in Drak2 Tg mice after diet-induced obesity

Drak2 Tg and WT mice were fed a high-fat diet for 6 weeks from 9 weeks of age. Both groups became obese at age 15 weeks when the glucose tolerance test was conducted. Tg mice on a high-fat diet presented significantly higher blood glucose at 30, 60, and 90 min after i.p. glucose injection, compared to WT mice (n=6 pairs, $p<0.05$, Student's t test).

Article 3.

DRAK2 IS UPSTREAM OF p70S6 KINASE: IT IMPLICATION IN CYTOKINE-INDUCED ISLET APOPTOSIS, TYPE I DIABETES AND ISLET TRANSPLANTATION

Jianning Mao, Hongyu Luo, Bing Han, Richard Bertrand, and Jiangping Wu

J.Immunol. 182 (8):4762-4770, 2009.

Note: In this paper, Bing Han performed β-cell intracellular staining as shown in Figure 2. All the remaining works were performed by Jianning Mao.

DRAK2 IS UPSTREAM OF P70S6 KINASE: IT IMPLICATION IN CYTOKINE-INDUCED ISLET APOPTOSIS, DIABETES AND ISLET TRANSPLANTATION

Jianning Mao*, Hongyu Luo*, Bing Han*, Richard Bertrand#, and Jiangping Wu*+

From *the Laboratory of Immunology, #Laboratory of Oncology and +Nephrology Service, Centre hospitalier de l'Université de Montréal (CRCHUM), Notre Dame Hospital, Montreal, Quebec, Canada

Correspondence should be addressed to: Dr. Jiangping Wu, Laboratory of Immunology, Research Centre, CHUM, Notre-Dame Hospital, Pavilion DeSève, Room Y-5616, 1560 Sherbrooke Street East, Montreal, Quebec H2L 4M1, Canada. Telephone: (514) 890-8000 ext. 25164; Fax: (514) 412-7596;

Drak2, apoptosis, islets, type 1 diabetes, rapamycin

ABSTRACT

Drak2 is a member of the death-associated protein family and a serine threonine kinase. In this study, we investigated its role in β-cell survival and diabetes. Drak2 mRNA and protein were rapidly induced in islet β-cells after stimulation by inflammatory lymphokines known to be present in type 1 diabetes. Drak2 upregulation was accompanied by increased β-cell apoptosis. β-cell apoptosis caused by the said stimuli was inhibited by Drak2 knockdown using siRNA. Conversely, transgenic (Tg) Drak2 overexpression led to aggravated β-cell apoptosis triggered by the stimuli. Further in vivo experiments demonstrated that Drak2 overexpressed in Tg islets was responsible for a diabetes-prone phenotype. We established that inducible nitric oxide synthase was upstream and caspase-9 was down stream of Drak2 in its signalling pathway. Purified Drak2 could phosphorylate ribosomal protein S6 (p70S6) kinase in an in vitro kinase assay. Drak2 overexpression in NIT-1 cells led to enhanced p70S6 kinase phosphorylation, while Drak2 knockdown in these cells reduced it. These mechanistic studies proved that p70S6 kinase was a bona fide Drak2 substrate.

INTRODUCTION

Diabetes is a metabolic disorder in which pancreatic islets fail to produce sufficient insulin to prevent blood glucose from rising beyond a normal range. Type 1 diabetes is an autoimmune disease normally starting at a young age. In type 1 diabetes, insufficient insulin production is caused by the destruction of islets by T cells either directly or indirectly by inflammatory cytokines, such as IFNγ and/or TNFα plus IL-β (1, 2). It is conceivable that genes controlling islet apoptosis and survival are important in determining susceptibility to islet destruction, and, consequently, in determining diabetes risk as well as its onset tempo (3). Such genes can, therefore, be characterized as type 1 diabetes risk genes.

Drak2 is a serine/threonine kinase belonging to a family of death-associated protein kinases (DAP kinases), which consists of DAP (4) , DRP-1 (5), ZIP kinase (6), DAPK2 (7), Drak1 and Drak2 (8). Drak2 shares about 50% identity in the kinase domain with other members of the family (4). While DAP, DRP-1 and DAPK2 have a calmodulin regulatory domain in their C-terminal, ZIP, Drak1 and Drak2 do not (4, 5, 6, 7, 8). DAP, DAPK2, and DRP-1 are localized in the cytosol (4, 5, 7), ZIP kinase and Drak1 reside mainly in the nuclei (6, 8), whereas Drak2 is found in both the cytosol and nuclei (8, 9), suggesting different mechanisms of action. Drak2 autophosphorylates itself, and phosphorylates myosin light chain as an exogenous substrate (8).

Its endogenous substrates, other than itself, have not been identified. Drak2 interacts with a calcineurin homologous protein (4), but the biological significance of this interaction is not clear.

Our in situ hybridization analysis has revealed that Drak2 expression is ubiquitous at the mid-gestation stage in embryos, followed by more focal expression in various organs in the perinatal period and adulthood, notably in the thymus, spleen, lymph nodes, cerebellum, suprachiasmatic nuclei, pituitary, olfactory lobes, adrenal medulla, stomach, skin and testes (10). Such an expression pattern suggests that Drak2 has a fundamental function in cell biology, and previous notion that Drak2 was a T-cell-specific gene is erroneous.

When DAP family kinases are overexpressed in various cells, apoptosis ensues (4-8), indicating their involvement in apoptosis. In Drak2 transgenic (Tg) mice, Tg T cells manifest augmented apoptosis after TCR stimulation followed by culture in the presence of IL-2; as a consequence, the memory T-cell pool is diminished, and these Tg mice incur compromised secondary but not primary in vivo T-cell responses (10). The results reveal that Drak2 is important in regulating T-cell apoptosis both in vitro and in vivo.

In the course of our search for genes affecting islet survival, we discovered that Drak2 expression in islets was rapidly induced by inflammatory stimuli. The induction was accompanied by islet apoptosis. Prevention of such Drak2 upregulation protected β-cells from apoptosis; conversely, Drak2 overexpression in Tg islets resulted in increased β-cell death. Mice with transplanted Drak2 Tg islets were prone to chronic cytokine stress in vivo. We further

identified ribosomal protein S6 p70S6 kinase as a substrate of Drak2. The implications of these findings are discussed.

MATERIALS AND METHODS

Islet purification

Islets were purified from pancreas of Tg and WT mice, which were in the C57BL/6 background, as we described earlier (11, 12). Briefly, 2-ml of digestion solution (Hanks' balanced salt solution [HBSS] containing 20 mM HEPES and 2 mg/ml collagenase IV (Worthington Biochemical, Lakewood, NJ) were injected into the common bile duct of Tg or wild type (WT) mice (20-24 g) after the distal end of the duct was ligated. The distended pancreas was isolated and put into a 15-ml tube containing an additional 0.5 ml of digestion solution. The pancreas was digested at 37^0C for exactly 28 min, and the digestion process was stopped by the addition of 10 ml of cold HBSS containing 20 mM HEPES. The islet suspension was filtered through No. 7880 cheesecloth gauze (Tyco Healthcare, Mansfield, MA) and centrifuged at 500 g for 1-2 min. The pellet was washed with cold HBSS once at 500 g for 1-2 min, and the supernatant was removed completely. The pellet was then resuspended in 3 ml of 25% Ficoll, and 2-ml layers of 23, 20, and 11% Ficoll were added sequentially. The Ficoll gradient was centrifuged at 700g for 5 min. Most of the islets were in the interface between the 20 and 23% Ficoll layers and were handpicked with Pasteur pipettes. They were then washed twice with cold HBSS. The islets were cultured overnight in RPMI 1640 containing 10% FCS, and then used for experimentation.

Treatment of islets with cytokines

Isolated islets were cultured in 24-well plates at approximately 200 islets per well in RPMI 1640 with 10% FCS. IFN-γ (1000 U/ml, TNF-α (200 ng/ml), IL-β (0.5 ng/ml) (R & D Research (Burlington, Ontario, Canada), or N^G-Methyl-L-arginine acetate salt (L-NMMA; 1 mM) (Sigma, Oakville, Ontario, Canada), were added to the wells at the beginning of the culture, as indicated in each experiment.

Flow cytometry

Islets were dispersed into single cells with 0.05% trypsin before flow cytometry. For Drak2 and insulin detection, the dispersed islet cells were fixed with 4% paraformaldehyde and permeabilized with 0.2% Triton X-100. The cells were stained with rabbit anti-Drak2 Ab (Abgent, San Diego, CA) and anti-insulin mAb (Sigma). After wash, the cells were stained with FITC-conjugated sheep anti-rabbit antibody (Ab) (Chemicon, Temecula, CA), and PE-conjugated goat anti-mouse antibody (Jackson Immunoresearch, West Grove, PA), and analyzed by 2-color flow cytometry. Dispersed islet cells or small interfering RNA (siRNA)-transfected NIT-1 cells were also analyzed for apoptosis by flow cytometry with FITC-annexin V (BD Pharmingen, Mississauga, Ontario, Canada) staining (13). Briefly, 5 μl of FITC-annexin V was added to each sample of cells in binding buffer (0.01 M HEPES, pH 7.4; 0.14 M NaCl, 2.5 mM $CaCl_2$). After 15 min incubation at room temperature, the cells were washed and analyzed by flow cytometry. For all flow cytometry, the major population in forward and side scatter histograms was gated for further 1- or 2-color analysis, and 5,000 gated events were registered.

Drak2 knockdown by siRNA in NIT-1 cells

NIT-1 cells, derived from mouse insulinoma, were transfected with siRNA using Lipofectamine 2000 (Invitrogen, Burlington, Ontario) according to the manufacturer's instructions. Two siRNAs specific for Drak2 were employed. For Drak2 siRNA #1162, the oligonucleotide RNA sequences were CAUCCCUGAAGAUGGCAGCtt and GCUGCCAUCUUCAGGGAUGtt. For Drak2 siRNA #592, the oligonucleotide RNA sequences were UAACAUUGUUCACCUUGAUtt and AUCAAGGUGAACAAUGUUAtt. The control siRNA was scrambled #1162 with the following sequences: 5'CCCUAAGUGUAGGACGCACtt and 3'GUGCGUCCUACACUUAGGGtt. Single-stranded RNA pairs were annealed by incubation for 1 min at 90^0C, and then cooled down to room temperature over 45 min. The final concentration of double-stranded siRNA was 10 nM for transfection. In some cases, a mixture of #1162 and #592 at 5 nM each was used for transfection.

Confocal microscopy

Drak2 Tg and WT islets were digested with 0.05% trypsin-EDTA to obtain single cell suspensions. The cells were placed on slides by Cytospin (Shandon, Pittsburgh, PA), fixed with 4% paraformaldehyde and permeabilized with 0.2% Triton X-100. The slides were stained with rabbit anti-Drak2 Ab (Abgent, San Diego, CA; 1:50 dilution) and anti-insulin mAb (Sigma, St. Louis, MO; 1:500 dilution). Subsequently, the slides were stained with FITC-conjugated sheep anti-rabbit antibody (Ab) (Chemicon, Temecula, CA), and PE-conjugated goat anti-mouse antibody (Jackson Immunoresearch, West Grove, PA). The cells were visualized under a Carl Zeiss confocal microscope, with excitation at 488 nm and emission at 505-550 nm for FITC, and with excitation at 543 nm and emission at 560-615 nm for PE. Intracellular Drak2 is shown in green, and intracellular insulin is in red.

Insulin release assay

Islets were cultured for 48 h in complete RPMI 1640 medium with 10% FCS in the absence or presence of various stimulants; they were then transferred to 12-well plates at a density of 10 islets/well. The islets were gently washed twice with 1 ml Kreb's buffer (NaCl, 135 mM; KCl, 3.6 mM; NaH_2PO_4, 5 mM; $MgCl_2$, 0.5 mM; $CaCl_2$, 1.5 mM; $NaHCO_3$, 2 mM; HEPES, pH 7.4, 10 mM; BSA, 0.07%), and then incubated in Kreb's buffer containing 2.8 mM glucose for 5 min at 37^0C. Two hundred micro litres of supernatant were removed for determination of basal insulin levels. The islets were cultured for an additional 40 min, and all the supernatants were harvested for the measurement of insulin levels as 2.8 mM glucose-stimulated release. The islets were then cultured in Kreb's buffer containing 16.7 mM glucose for 45 min at 37^0C, and the supernatants were harvested to assess insulin levels as 16.7 mM glucose-stimulated release. Insulin was assayed by ELISA (Linco Research, St. Charles, MO). Basal insulin levels, which were near zero, were deducted from the 2.8 mM and 16.7 mM glucose-stimulated levels. The fold increase in insulin release between 16.7 mM glucose and 2.8 mM glucose stimulation was calculated.

Islet transplantation

Diabetes was induced in C57BL/6 mice by streptozocin (STZ) (200 mg/kg body weight, i.p.). After 14 days, syngeneic Tg or WT islets were transplanted into the peritoneal cavity of these diabetic mice (400 islets per mouse) to render the recipients euglycemic. Two weeks after islet transplantation, glucose tolerance tests were performed to ascertain if the islet reserve capacities

of these Tg and WT islet recipients were comparable. The transplanted mice were then injected i.v. with multiple low doses of STZ (40 mg/kg/day x 5 days) to assess the incidence of diabetes.

Generation of recombinant proteins

Full-length cDNAs of Drak2 and p70S6 kinase were cloned into pGEX-4T-1 in-frame downstream of the GST coding sequence. These constructs were named pGEX-4T-1-Drak2 and pGEX-4T-1-S6K, respectively, and were used to generate GST-tagged Drak2 and p70S6 kinase in E. coli. The recombinant proteins were purified with a size exclusion column (Superdex, 2 cm in diameter x75 cm in length,) followed by a glutathione-agarose column (GE Healthcare, Piscataway, NJ). Drak2 cDNA was also cloned into pCEP4-HA in-frame downstream of a coding sequence of 3 HA repeats. The construct was called pCEP4-HA-Drak2 and was employed to transfect NIT-1 cells. In some experiments, HA-Drak2 was purified with Sepharose conjugated with anti-HA Ab (Covance, Berkeley, CA)

Protein kinase substrate array

Mouse recombinant Drak2 protein (95% pure according to silver staining) produced from *E. coli* was used as a kinase in the Protoarray Kinase Substrate Identification Kit, which contains 5000 human protein kinase substrates (Invitrogen, Carlsbad, CA). The reaction was conducted according to manufacturer's instructions. Proteins with a Z-score above 3 (indicating a confidence level above 99.9%) are considered potential Drak2 substrates.

Z-score = (the signal value from a given protein minus the mean signal value for all proteins in the array)/the signal value of standard deviation for all proteins.

In vitro kinase assay

The autophosphorylation of Drak2 were performed by incubating 0.3 μg HA-Drak2 or GST-Drak2 protein in kinase buffer (10 mM Tris-HCl [pH 7.5], 10 mM $MgCl_2$, 3 mM $MnCl_2$, 0.5 mM $CaCl_2$ and 0.1 mM [γ–^{32}P]-ATP (111 GBq/mmol)(GE Healthcare) in a total volume of 30 μl at 30°C for 15 min. In some experiments, GST of GST-Drak2 and GST-p70S6 kinase was cleaved by thrombin (GE Healthcare) and then used in the in vitro kinase assay. The kinase reactions were terminated by adding 10 μl of 3x SDS-polyacrylamide gel electrophoresis (PAGE) loading buffer. The proteins were resolved by SDS-PAGE, transferred to nitrocellulose membrane, and autoradiographed.

Immunoblotting

NIT-1 cells were transiently transfected with pCEP4-HA-Drak2 or empty vector pCEP4-HA. After 48 h, the cells were lysed and resolved in 10% SDS-PAGE (60 μg/lane) followed by immunoblotting. For HA-Drak2 expression, membrane was blotted with mouse anti-HA mAb (Santa Cruz, Santa Cruz, CA; 1:1000 dilution) followed by horse radish peroxidase (HRP)-conjugated sheep anti-mouse IgG (GE Healthcare; 1:2000 dilution). To assess p70S6 kinase phosphorylation, the membrane was blotted with mouse anti-phospho-p70S6 kinase (Thr389) Ab (Cell Signaling, Danvers, MA; 1:1000 dilution) followed by HRP-conjugated sheep anti-mouse IgG (GE Health; 1:2000 dilution). The membrane was also blotted with rabbit anti-p70S6 kinase Ab (Cell Signaling, Danvers, MA; 1:1000 dilution) followed by HRP-conjugated donkey anti-rabbit IgG to show similar total p70S6 kinase protein. In some experiments, NIT-1 cells were stimulated with IFN-γ (1000U/ml) plus IL-1β (0.5 ng/ml), or TNF-α (200ng/ml) plus IL-1β (0.5

ng/ml). Twenty four hours later, they were transfected with two different Drak2 siRNAs (#592 and #1162), or with a control siRNA. After additional 24 h, phospho-p70S6 kinase and total p70S6 kinase in the cell lysates were detected in immunoblotting. For caspase-9 detection, NIT-1 cells were stimulated with cytokines and transfected with a mixture of 2 Drak2 siRNAs (#592 and #1162; 5 nM each) or with a control siRNA to #1162 (10 nM) at the beginning of culture. Twenty-four hours later, the cells were lysed and resolved in 10% SDS-PAGE (60 μg protein /lane). The membranes were blotted with anti-caspase-9 Ab (Cell Signaling; 1:1000 dilution) followed by HRP-conjugated donkey anti-rabbit IgG (GE Health; 1:2000 dilution). After that the membrane was stripped and blotted with anti-β-actin Ab (Cell Signaling; 1:1000 dilution) as a loading control.

RESULTS

Rapid induction of Drak2 expression in islet β-cells

We treated islets with a combination of IFN-γ and IL-1β or TNF-α and IL-1β, which are reported to cause islet apoptosis in type 1 diabetes (14,15). The islets were harvested 2 h, 6 h and 24 h after the cytokine stimulation. We found that these cytokines induced Drak2 mRNA expression in isolated islets within 24 h (Figs. 1A and 1B). We next assessed Drak2 protein levels in β-cells stimulated with IFN-γ plus IL-1β, or TNF-α plus IL-1β, employing anti-insulin mAb and anti-Drak2 Ab in 2-color flow cytometry. Histograms of a representative kinetics study at 0 h, 6 h, 24 h and 48 h was shown in Fig. 2. In islets culture in medium, Drak2 protein levels in insulin-positive β-cells were nearly constant for 24 h (44.7-47.2%), but then it increased to 63.8% at 48 h (first row). The presence of inflammatory cytokines, i.e., IFN-γ plus IL-1β, or

TNF-α plus IL-1β, induced rapid upregulation of Drak2 as early as 6 h; the elevated cytokine-stimulated expression last until 48 h, compared to that of cells in plain medium.

Drak2 knockdown by siRNA protected NIT-1 insulinoma cells from cytokine-triggered apoptosis

To prove that Drak2 was indeed critical to cytokine-induced β-cell apoptosis, we employed siRNA to prevent Drak2 upregulation in NIT-1 insulinoma cells. As shown in Fig. 3A, similarly to normal β-cells, Drak2 protein was induced in NIT-1 cells by IFN-γ plus IL-1β (3rd column, top panel) or TNF-α plus IL-1β (3rd column, lower panel). siRNA prevented Drak2 protein upregulation stimulated by IFN-γ plus IL-1β and TNF-α plus IL-1β (1st column, Fig. 3A). Control siRNA had no effect on Drak2 levels (2nd column, Fig. 3A). A bar graph summarizing 4-5 independent experiments is shown in Fig. 3B. As in normal islet cells, these stimuli induced NIT-1 cell apoptosis after 24 h (3rd column, Fig. 3C). However, with protection by Drak2 siRNA (1st column) but not control siRNA (2nd column), such apoptosis induction by IFN-γ plus IL-1β (top panel) or TNF-α plus IL-1β (lower panel) was dampened. A bar graph summarizing data from 4-5 independent experiments is shown in Fig. 3D. These results confirmed the detrimental role of Drak2 in islet β-cell survival.

The position of Drak2 in the INF-γ/IL-1β-triggered β-cell apoptosis pathway

It is known that INF-γ/IL-1β-mediated β-cell apoptosis is mediated by nitric oxide (NO) (2). To locate the position of Drak2 in relation to NO in this model, we assessed Drak2 induction in the presence of L-NMMA, an inhibitor of inducible nitric oxide synthase (iNOS). As shown in Fig. 3E, L-NMMA potently inhibited INF-γ plus IL-1β–induced Drak2 augmentation, and this clearly

placed Drak2 downstream of NO in this apoptosis pathway. We further detected procaspase-9 cleavage in NIT-1 cells after IFN-γ plus IL-1β or TNF-α plus IL-1β stimulation, and such cleavage was reduced (Fig. 3F), accompanied by reduced NIT-1 cell apoptosis (Figs. 3C and 3D) when Drak2 expression was knocked down by Drak2 siRNA. This indicated that caspase-9 was downstream of the cytokine/NO/Drak2 pathway in β-cell apoptosis.

Transgenic Drak2 overexpression in Tg islets aggravated cytokine-triggered apoptosis

The role of Drak2 in islet survival was further validated using actin promoter-driven Drak2 Tg mice which we generated recently (10). These mice are viable, fertile, and have no gross anomalies (10). The WT and Drak2 Tg pancreases had similar islets number and size, according to histological examination and number of islets isolated (data not shown). We demonstrated (Fig. 4A) that Drak2 mRNA was about 4 times higher in Tg islets than in WT islets. Immunofluorescence study revealed elevated Drak2 protein levels in insulin-positive Tg β-cells (Fig. 4B), although their forward and side scatter (representing size and granularity of islet cells) in flow cytometry were similar (left column, Fig. 5A). The inflammatory cytokines (IFN-γ plus IL-1β or TNF-α plus IL-1β) induced WT islet cell apoptosis after 48 h (Figs. 5A and 5B, top rows), as expected. However, Tg islet cells underwent increased apoptosis compared with WT islet cells when stimulated with IFN-γ plus IL-1β or TNF-α plus IL-1β (bottom rows, Figs. 5A and 5B). A summary of data from 4-6 experiments are given in Fig. 5C. Insulin release assay demonstrated that the β-cell function of Tg islets assaulted by cytokines was significantly lower than that of WT islets (Fig. 5D). Since Tg islets treated with cytokines had significantly increased apoptosis compared with WT islets, the compromised β-cells function seen in insulin release assay pinpointing the apoptotic islet cells to β-cells, although we cannot exclude the

possibility that the cytokines also damaged the function of live β-cells. These in vitro experiments confirmed that augmented Drak2 expression was harmful to β-cell survival.

Drak2 overexpression led to increased diabetes incidence in vivo

The proapoptotic effect of Drak2 in β-cells in vitro raised a logical question as to whether its overexpression would render mice prone to diabetes. In our Tg mice, Drak2 expression was not restricted to islets as it was driven by the actin promoter (10). To pin-point the in vivo phenotype to islets, we transplanted Tg or WT islets to full-dose STZ (200 mg/kg)-induced diabetic mice, which were syngeneic to the donors. Once the recipients became normoglycemic, glucose tolerance tests were performed to ascertain that they had similar reserve islet capacity (data not shown). These recipients were then injected with multiple low-doses of STZ to induce borderline diabetes in WT islet recipients. Islet damage by such a STZ regimen is reported to cause chronic inflammatory environment in the pancreas (16, 17). After STZ injection, the blood glucose levels of WT mice hovered around 12 mM (Fig. 5E). However, such treatment caused full-blown diabetes in Tg islet recipients from days 15 to 18 post STZ treatment (Fig. 5E), with their blood glucose rising above 20 mM. This finding clearly indicates that Drak2 overexpressed in Tg islets is responsible for the diabetes-prone phenotype in the recipients.

Identification of p70S6 kinase as a Drak2 substrate in vitro

To understand the mechanism of Drak2 action, we attempted to discover the substrate of Drak2. Recombinant mouse GST-Drak2 was generated with the construct pGEX-4T-1-Drak2, and was prepared to more than 95% purity after size fractionation followed by affinity purification (Fig. 6A, 1st and 2nd lanes). Its kinase activity was confirmed by autophosphorylation in an in vitro

kinase assay (Fig. 6B). It was then employed as the kinase in an assay with the Invitrogen Protoarray Kinase Substrate Identification Kit, which contained 5,000 potential kinase substrate proteins of human origin. Five proteins showed a Z-score above 3, a threshold indicating more than 99.9% confidence. Among the 5 proteins, one was p70S6 kinase.

To confirm that mouse Drak2 could phosphorylate mouse p70S6 kinase, GST-tagged mouse p70S6 kinase was generated with the construct pGEX-4T-1-p70S6K, and processed to more that 95% purity after affinity purification followed by cleavage of GST by thrombin (Fig. 6C). Mouse Drak2, which was also more than 95% pure (Fig. 6A, 3rd lane) after affinity purification followed by cleavage of GST by thrombin, served as a kinase in an in vitro kinase assay, using mouse p70S6 kinase as a substrate. As illustrated in Fig. 6D, Drak2 could autophosphorylate itself, as expected (lane 1). It also phosphorylated mouse p70S6 kinase (lane 1). On the other hand, p70S6 kinase could not autophosphorylate (lane 2) in the kinase assay. Thus, the phosphorylation on mouse p70S6 kinase was caused by Drak2, and p70S6 kinase was a bona fide Drak2 substrate in vitro.

Identification of p70S6 kinase as a Drak2 substrate in vivo

Next, we attempted to demonstrate that p70S6 kinase was a Drak2 substrate inside the cells (in vivo). NIT-1 cells were transiently transfected with a HA-tagged Drak2 expression construct pCEP4-HA-Drak2. HA-tagged Drak2 was affinity-purified, and it showed the expected size in immunoblotting (Fig. 7A). It was tested in an in vitro kinase assay and could autophosphorylate itself, as illustrated in Fig. 7B, proving that the recombinant protein possessed active kinase activity. When NIT-1 cells were transiently transfected with pCEP4-HA-Drak2 or an empty

vector, recombinant HA-Drak2 expression at the size of 45 kD could be detected by anti-HA Ab in immunoblotting in the former but not in the latter transfected cells, as seen in Fig. 7C (lane 1 versus lane 2, top panel). In pCEP4-HA-Drak2-transfected cells (lane 1, middle panel, Fig. 7C) but not empty vector-transfected cells (lane 2, middle panel, Fig. 7C), p70S6 kinase phosphorylation was augmented, while total p70S6 kinase protein remained constant (bottom panel, Fig. 7C). This indicates that Drak2 overexpression in vivo led to increased p70S6 kinase phosphorylation, and corroborates our in vitro kinase assay that p70S6 kinase was a Drak2 substrate.

Further in vivo verification of the relationship between Drak2 and p70S6 kinase phosphorylation was undertaken by knocking down Drak2 expression with siRNA. As depicted in Fig. 8, IFN-γ plus IL-1β or TNF-α plus IL-1β induced Drak2 protein expression (the 2nd and 3rd columns, compared with the 1st column; Fig. 8A). This was accompanied by increased p70S6 kinase phosphorylation (the 2nd and 3rd lanes, compared with the 1st lane, Fig. 8B; the 2nd and 3rd columns, compared with the 1st column, Fig. 8C). Control siRNA had no effect on Drak2 induction (the last 2 columns compared with the 2nd and 3rd columns, Fig. 8A), nor did it on p70S6 kinase phosphorylation (the last 2 lanes compared with the 2nd and 3rd lanes, Fig. 8B; last the 2 columns compared with the 2nd and 3rd columns, Fig. 8C). However, 2 different Drak2 siRNAs knocked down cytokine-induced Drak2 expression (columns 5, 6, 8, and 9, compared with columns 2 and 3, Fig. 8A), and this was accompanied by reduced cytokine-induced p70S6 kinase phosphorylation (lanes 5, 6, 8 and 9, compared with lanes 2 and 3, Fig. 8B; columns 5, 6, 8, and 9, compared with columns 2 and 3, Fig. 8C). This further confirms that p70S6 kinase was a Drak2 substrate in vivo.

To study the relevance of p70S6 kinase in β-cell apoptosis, we used rapamycin to inhibit mTORC1, which is another kinase capable of phosphorylating p70S6 kinase. NIT-1 cells under rapamycin protection showed reduced apoptosis upon IFN-γ plus IL-1β or TNF-α plus IL-1β exposure (Fig. 8D), and a bar graph summarizing data from 2 independent experiments is shown in Fig. 8E. Taking our Drak2 and rapamycin results together, we believe that p70S6 kinase activity is required for β-cell apoptosis.

DISCUSSION

In this study, we demonstrated that Drak2 is critical for β-cell apoptosis triggered by inflammatory cytokines. Further in vivo experiments proved that enhanced Drak2 expression in islets rendered mice prone to diabetes in a model of STZ-induced islet stress. We further discovered that p70S6 kinase was a substrate of Drak2.

Drak2 Tg islets manifested increased apoptosis after cytokine assaults (Figs. 5A and 5B). However, without such assaults, apoptosis of Tg islets cultured in medium was not different from that of WT islets. This suggests that Drak2 overexpression, by itself, is not sufficient to cause β-cell apoptosis, but rather the overexpression renders β-cells vulnerable to signalling from other detrimental factors. Indeed, islet β-cell apoptosis often needs concerted signals from different pathways. For example, single cytokine such as TNFα, IFNγ or IL-1β does not have a significant effect on β-cells, but a combination of 2 or 3 of them potently induces their apoptosis (2). It is to be noted that while it took 24 h to reach peak Drak2 induction by a combination of two cytokines

such as IFN-γ plus IL-1β or TNF-α plus IL-1β, Drak2 expression peaked faster at 5 h after the stimulation of IFN-γ, TNF-α and IL-1β in combination, accompanied by a higher degree of apoptosis (data not shown). This indicates that 1) multiple detrimental factors are additive to islet apoptosis, and 2) Drak2 is a common mediator in multiple cytokine signalling pathways. The latter notion is further supported by a finding that another detrimental factor, FasL, could also induce Drak2 expression in islets (data not shown), and that Drak2 Tg islets treated with FasL in combination with IFN-γ presented increased apoptosis compared with WT islets. Our finding is also consistent with the fact that type 1 diabetes is under polygenic control, and abnormal expression of a single gene rarely induces diabetes.

In humans, the Drak2 gene is located in 2q33.2, and is 7.2 Mbp from a type 1 diabetes risk locus IDDM12 at 2q33.2. Although CTLA-4 has been identified in this locus (18), whether there are additional type 1 diabetes risk genes in this area needs to be assessed. Single nucleotide polymorphism analysis of Drak2 gene and genes that regulate Drak2 expression in type 1 diabetes versus normal individuals will answer the question whether Drak2 is a bona fide type 1 diabetes risk gene in humans.

Obviously, if Drak2 is a diabetes risk factor, genes in the Drak2 pathway could all be involved in such a risk, and genetic studies aimed at validating Drak2 as a diabetes risk factor should include genes in its signalling pathway.

Our prior knowledge about the Drak2 activation pathway and Drak2 substrates is limited. In this study, we found that an iNOS inhibitor L-NMMA could effective block IFN-γ/IL-1β induced

Drak2 expression, and thus placed NO upstream of Drak2 in this particular cytokine pathway. We also demonstrated Drak2 acted through caspase-9 in apoptosis, although our study on caspase-8 activation was not conclusive (data not shown). Concerning the direct Drak2 substrate(s), we only knew before that Drak2 is a genuine substrate of itself. In this study, we identified 5 putative Drak2 substrates, and proved that p70S6 kinase was a bona fide Drak2 substrate in vitro and in vivo. Verification of the other 4 substrates is ongoing, and it is quite possible that Drak2 has multiple substrates.

p70S6 kinase plays a critical role in protein synthesis, and is a key regulator in cell size and cell cycle progression. It is activated through phosphorylation, which is triggered by a wide range of growth factors, cytokines and nutrients (19). mTORC1 and PDK1 are 2 known kinases which work in concert to phosphorylate and activate p70S6 kinase. We have identified a novel p70S6 kinase signalling pathway in which Drak2 was an additional upstream kinase capable of phosphorylating p70S6 kinase. According to our data, the inflammatory cytokine/Drak2/p70S6 kinase pathway seems to be critical in islet apoptosis, because the action of all these 3 components was correlated to islet apoptosis, and they were sequentially linked. Inhibitors of components of this pathway should have protective effects on β-cells.

Interestingly, islet transplantation efficiency has been greatly improved after rapamycin, a mTORC1 inhibitor, replaced the calcineurin inhibitor cyclosporin A in the islet transplantation regimen (20). It is possible that p70S6 kinase is critical in islet apoptosis and that inhibition of p70S6 kinase phosphorylation by rapamycin contributes to the reduction of islet apoptosis after transplantation; hence, this is partially responsible for the increase in transplantation efficiency.

We have further in vitro evidence that rapamycin rendered β-cells partially resistant to apoptosis induced by cytokines, suggesting that p70S6 kinase is relevant to islet survival. It is possible that inflammatory cytokines activate both the Drak2/p70S6 kinase and mTORC1/p70S6 kinase pathways, and that inhibiting one of them is only partially effective in reducing β-cell apoptosis. Indeed, when Drak2 upregulation stimulated by cytokines was prevented by siRNA, islet apoptosis was decreased, but was not totally prevented. Similarly, rapamycin only partially protected islet apoptosis from the cytokines. Dual inhibition of mTORC1 (with rapamycin) and Drak2 (with Drak2 inhibitors that are to be developed) might achieve better results in islet protection in terms of cytokine-induced β-cell apoptosis.

With that said, we read with interest a recent report by Freankel et al., in which the authors demonstrated that mTOR inhibition by rapamycin exacerbates type 2 diabetes, and reduced islet mass in diabetes *P. obesus* (21). This result seems to be in conflict with our findings that rapamycin protected β-cells from apoptosis, and previous reports showing that p70S6 kinase gene knockout leads to increased insulin sensitivity (22) and that overactivation of mTOR/p70S6 kinase is responsible for impaired insulin action (23). A possible explanation is that rapamycin's effect on other targets such as mTORC2, and/or 4EBP1 via mTORC1 might be detrimental to β-cell viability in a type 2 diabetes environment. If this is the case, Drak2 inhibitors which target p70S kinase activation alone without affecting mTORC2 and 4EBP1 might have advantage over rapamycin in protecting islets from apoptosis.

ACKNOWLEDGEMENTS

This work was supported by grants from the Canadian Institutes of Health Research (CIHR, MOP57697, MOP69089 and PPP85159 to J.W., and MOP79565 to H.L), the Kidney Foundation of Canada, the Heart and Stroke Foundation of Quebec, the Juvenile Diabetes Research Foundation USA (1-2005-197), and the J.-Louis Levesque Foundation to J.W. Group grants from the CIHR for New Emerging Teams in Transplantation and from Fonds de la recherche en santé du Québec (FRSQ) for Transfusional and Hemovigilance Medical Research, and Genome Canada/Genome Quebec are also acknowledged.

The authors thank Dr. John A. Di Battista for helpful discussions, and Mr. Ovid Da Silva for his editorial assistance.

References

1. Hohmeier HE, Tran VV, Chen G, Gasa R, Newgard CB. 2003. Inflammatory mechanisms in diabetes: lessons from the beta-cell *Int. J. Obes. Relat Metab Disord.* 27 Suppl 3:S12-S16

2. Cnop M, Welsh N, Jonas JC, Jorns A, Lenzen S, Eizirik DL. 2005. Mechanisms of pancreatic beta-cell death in type 1 and type 2 diabetes: many differences, few similarities *Diabetes* 54 Suppl 2:S97-107

3. Chacon MR, Vendrell J, Miranda M, Ceperuelo-Mallafre V, Megia A, Gutierrrez C, Fernandez-Real JM, Richart C, Garcia-Espana A. 2007. Different TNFalpha expression elicited by glucose in monocytes from type 2 diabetes mellitus patients *Atherosclerosis*

4. Deiss LP, Feinstein E, Berissi H, Cohen O, Kimchi A. 1995. Identification of a novel serine/threonine kinase and a novel 15-kD protein as potential mediators of the gamma interferon-induced cell death *Genes Dev.* 9:15-30

5. Inbal B, Shani G, Cohen O, Kissil JL, Kimchi A. 2000. Death-associated protein kinase-related protein 1, a novel serine/threonine kinase involved in apoptosis *Mol. Cell Biol.* 20:1044-54

6. Kawai T, Matsumoto M, Takeda K, Sanjo H, Akira S. 1998. ZIP kinase, a novel serine/threonine kinase which mediates apoptosis *Mol. Cell Biol.* 18:1642-51

7. Kawai T, Nomura F, Hoshino K, Copeland NG, Gilbert DJ, Jenkins NA, Akira S. 1999. Death-associated protein kinase 2 is a new calcium/calmodulin-dependent protein kinase that signals apoptosis through its catalytic activity *Oncogene* 18:3471-80

8. Sanjo H, Kawai T, Akira S. 1998. DRAKs, novel serine/threonine kinases related to death-associated protein kinase that trigger apoptosis *J. Biol. Chem.* 273:29066-71

9. Matsumoto M, Miyake Y, Nagita M, Inoue H, Shitakubo D, Takemoto K, Ohtsuka C, Murakami H, Nakamura N, Kanazawa H. 2001. A serine/threonine kinase which causes apoptosis-like cell death interacts with a calcineurin B-like protein capable of binding Na(+)/H(+) exchanger *J. Biochem. (Tokyo)* 130:217-25

10. Mao J, Qiao X, Luo H, Wu J. 2006. Transgenic drak2 overexpression in mice leads to increased T cell apoptosis and compromised memory T cell development *J. Biol. Chem.* 281:12587-95

11. Wu Y, Han B, Luo H, Roduit R, Salcedo TW, Moore PA, Zhang J, Wu J. 2003. DcR3/TR6 effectively prevents islet primary nonfunction after transplantation *Diabetes* 52:2279-86

12. Wu Y, Han B, Luo H, Shi G, Wu J. 2004. Dipeptide boronic acid, a novel proteasome inhibitor, prevents islet-allograft rejection *Transplantation* 78:360-6

13. Murakami Y, Takamatsu H, Taki J, Tatsumi M, Noda A, Ichise R, Tait JF, Nishimura S. 2004. 18F-labelled annexin V: a PET tracer for apoptosis imaging *Eur. J. Nucl. Med. Mol. Imaging* 31:469-74

14. Alizadeh BZ, Hanifi-Moghaddam P, Eerligh P, van der Slik AR, Kolb H, Kharagjitsingh AV, Pereira Arias AM, Ronkainen M, Knip M, Bonfanti R, Bonifacio E, Devendra D, Wilkin T, Giphart MJ, Koeleman BP, Nolsoe R, Mandrup PT, Schloot NC, Roep BO. 2006. Association of interferon-gamma and interleukin 10 genotypes and serum levels with partial clinical remission in type 1 diabetes *Clin. Exp. Immunol.* 145:480-4

15. Lee MS, Chang I, Kim S. 2004. Death effectors of beta-cell apoptosis in type 1 diabetes *Mol. Genet. Metab* 83:82-92

16. Liadis N, Murakami K, Eweida M, Elford AR, Sheu L, Gaisano HY, Hakem R, Ohashi PS, Woo M. 2005. Caspase-3-dependent beta-cell apoptosis in the initiation of autoimmune diabetes mellitus *Mol. Cell Biol.* 25:3620-9

17. Pighin D, Karabatas L, Pastorale C, Dascal E, Carbone C, Chicco A, Lombardo YB, Basabe JC. 2005. Role of lipids in the early developmental stages of experimental immune diabetes induced by multiple low-dose streptozotocin *J. Appl. Physiol* 98:1064-9

18. Turpeinen H, Laine AP, Hermann R, Simell O, Veijola R, Knip M, Ilonen J. 2003. A linkage analysis of the CTLA4 gene region in Finnish patients with type 1 diabetes *Eur. J. Immunogenet.* 30:289-93

19. Jastrzebski K, Hannan KM, Tchoubrieva EB, Hannan RD, Pearson RB. 2007. Coordinate regulation of ribosome biogenesis and function by the ribosomal protein S6 kinase, a key mediator of mTOR function *Growth Factors* 25:209-26

20. Marcelli-Tourvieille S, Hubert T, Moerman E, Gmyr V, Kerr-Conte J, Nunes B, Dherbomez M, Vandewalle B, Pattou F, Vantyghem MC. 2007. In vivo and in vitro effect of sirolimus on insulin secretion *Transplantation* 83:532-8

21. Fraenkel M, Ketzinel-Gilad M, Ariav Y, Pappo O, Karaca M, Castel J, Berthault MF, Magnan C, Cerasi E, Kaiser N, Leibowitz G. 2008. mTOR inhibition by rapamycin prevents beta-cell adaptation to hyperglycemia and exacerbates the metabolic state in type 2 diabetes *Diabetes* 57:945-57

22. Um SH, Frigerio F, Watanabe M, Picard F, Joaquin M, Sticker M, Fumagalli S, Allegrini PR, Kozma SC, Auwerx J, Thomas G. 2004. Absence of S6K1 protects against age- and diet-induced obesity while enhancing insulin sensitivity *Nature* 431:200-5

23. Khamzina L, Veilleux A, Bergeron S, Marette A. 2005. Increased activation of the mammalian target of rapamycin pathway in liver and skeletal muscle of obese rats: possible involvement in obesity-linked insulin resistance *Endocrinology* 146:1473-81

FIGURE LEGEMDS

Figure 1. Drak2 mRNA was rapidly augmented in islets encountering inflammatory stimulation

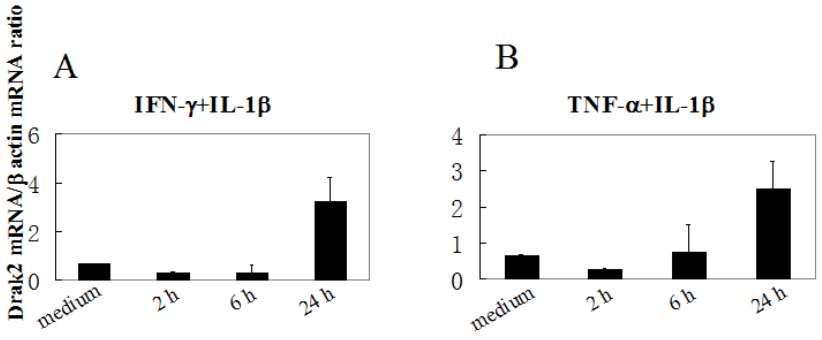

FIG. 1

Drak2 mRNA expression in C57BL/6 islet cells was measured by real time RT-PCR. The ratio of Drak2 mRNA and β-actin mRNA was taken as a measure of Drak2 mRNA levels. The samples were in triplicate, and the means ± SD of 5 to 6 independent experiments are shown.

A. Islets were stimulated by IFN-γ (1,000 U/ml) plus IL-1β (0.5 ng/ml) in vitro for 24 h.

B. Islets were stimulated by TNF-α (200 ng/ml) plus IL-1β (0.5 ng/ml) in vitro for 24 h.

Figure 2. Flow cytometry analysis of Drak2 protein upregulation in β-cells upon inflammatory stimuli

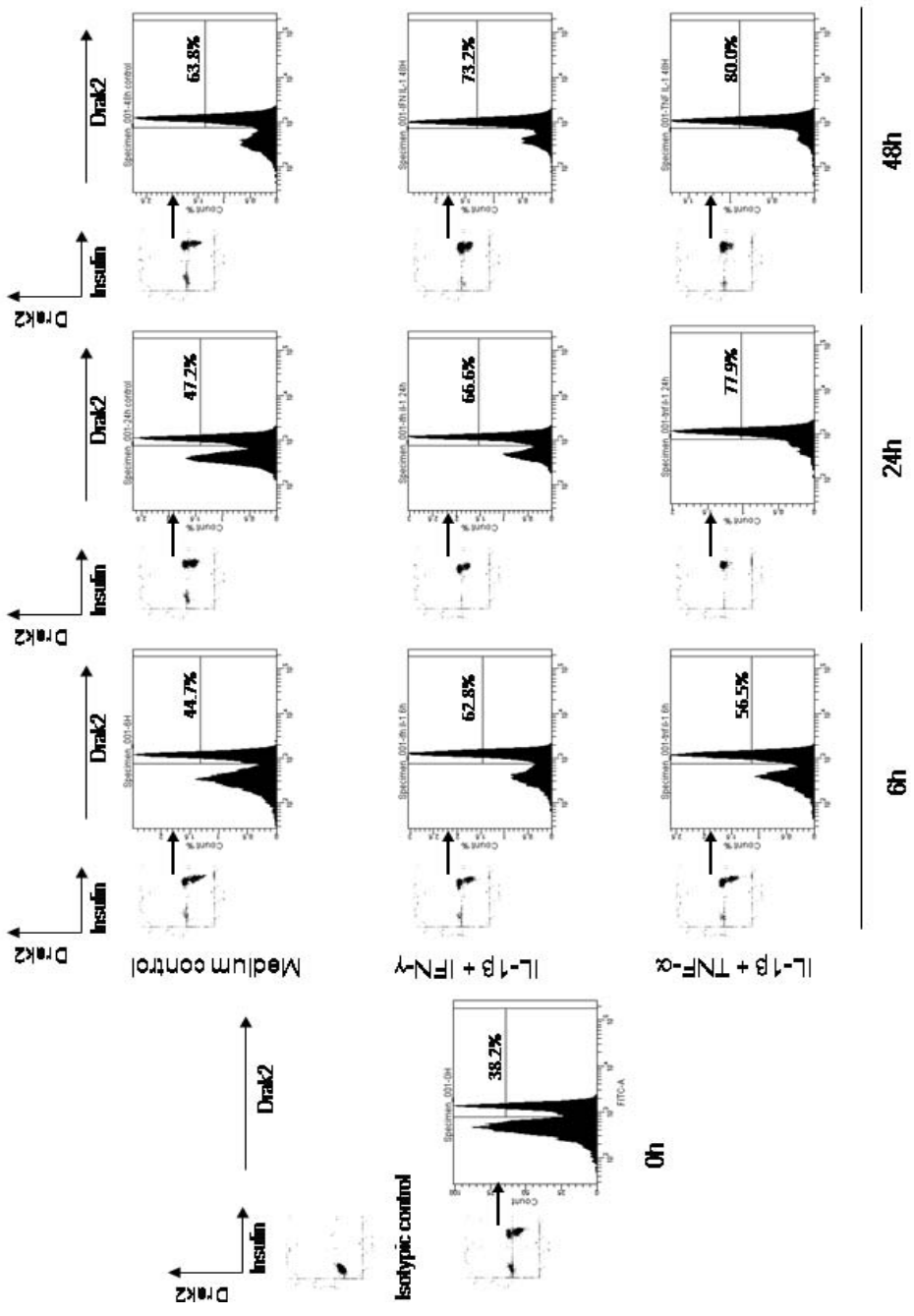

FIG. 2

C57BL/6 islets were cultured for 0, 6 24 and 48 h in the absence or presence of IFN-γ plus IL-1β, or TNF-α plus IL-1β, as described in Fig. 1. The islets were dispersed after culture and analyzed by 2-color flow cytometry for intracellular insulin and Drak2. The experiment was repeated twice. Histograms from a representative experiment are shown. The first column showed the isotypic control for Drak2 and insulin staining (upper panel), and Drak2 expression at 0 h (lower panel). Insulin positive cells were gated and their Drak2 expression was presented in one-color histograms. The staining background according to isotypic control has been deducted from all percentages shown.

Figure 3. Drak 2 signalling is responsible for β-cell apoptosis

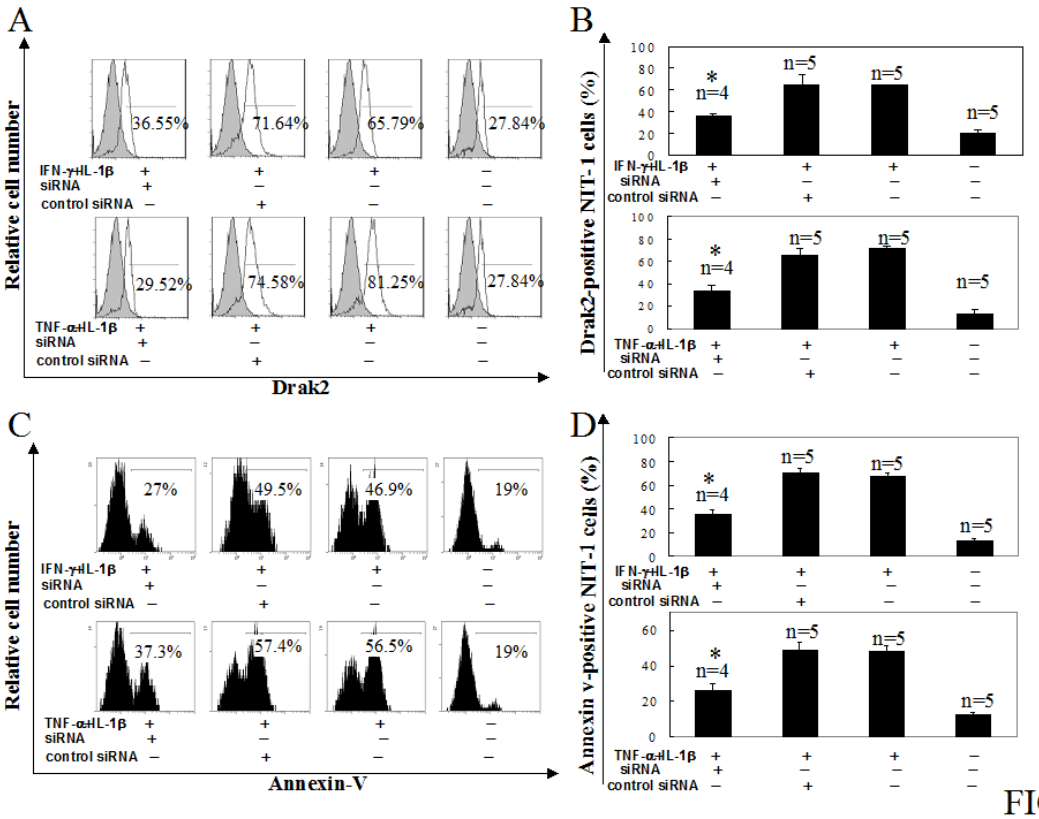

FIG. 3

A and B. Drak2 siRNA inhibited Drak2 protein upregulation in NIT-1 insulinoma cells

NIT-1 insulinoma cells were cultured in the absence or presence of IFN-γ plus IL-1β, or TNF-α plus IL-1β, as described in Fig. 1. Twenty-four hours after the initiation of incubation, the cells were transfected with Drak2 siRNA (#1162) or control siRNA (scrambled #1162). The cells were harvested at 48 h and analyzed for intracellular Drak2 protein levels by flow cytometry. The experiment was repeated 4 to 5 times.

Histograms of a representative experiment are shown in (A). Shaded areas are isotypic controls. The staining background (isotypic control) has been deducted from all percentages shown. Means ± SD of these 4-5 experiments are shown in (B) (n=4 or n=5, as indicated). Asterisks indicate p values (<0.05) of siRNA- versus control siRNA-treated cells, according to Student's t test.

C and D. Drak2 siRNA prevented cytokine-induced apoptosis in NIT-1 cells

NIT-1 cells were cultured in the absence or presence of IFN-γ plus IL-1β, or TNF-α plus IL-1β, as described in Fig. 1. Twenty-four hours after the initiation of incubation, the cells were transfected with Drak2 siRNA (#1162) or control siRNA. The cells were harvested at 48 h and analyzed for apoptosis by flow cytometry with annexin V staining. The experiment was repeated 4 to 5 times. Histograms of a representative experiment are shown in (C). Means ± SD of percentage of apoptosis in all these independent experiments (n=4 or n=5, as indicated) are shown in (D). Asterisks indicate p values (<0.05) of siRNA- versus control siRNA-treated cells, according to Student's t test.

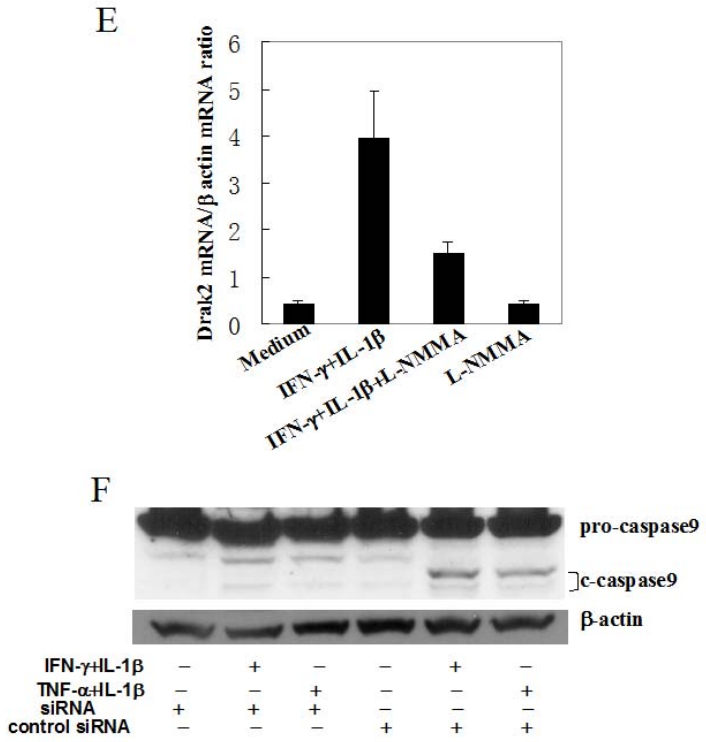

FIG. 3

E. iNOS inhibitor L-NMMA blocks Drak2 cytokine-induced Drak2 upregulation

Islets were cultured in the absence or presence of IFN-γ plus IL-1β and 1 mM L-NMMA. After 24 h, the islets were harvested and their Drak2 mRNA was measured by real-time RT-PCR. The ratio of Drak2 mRNA and β-actin mRNA was taken as a measure of Drak2 mRNA levels. The samples were in duplicate, and the means ± SD of 3 independent experiments are shown.

F. Drak2-induced apoptosis utilized the caspase-9 pathway

NIT-1 insulinoma cells were simply cultured or transfected with Drak2 siRNA (a mixture of #592 and #1162 at 5 nM each) or control siRNA (10 nM), and stimulated by IFN-γ plus IL-1β, or TNF-α plus IL-1β, as indicated. After 24 h, the cells were

harvested, and pro-caspase-9 cleavage was detected by Western blotting (upper panel). The positions of pro-caspase-9 and cleaved caspase-9 (c-caspase-9) are indicated. The same membrane was blotted with anti-β-actin (lower panel) to show even protein loading.

Figure 4. Drak2 overexpression in Tg islet β-cells

FIG. 4

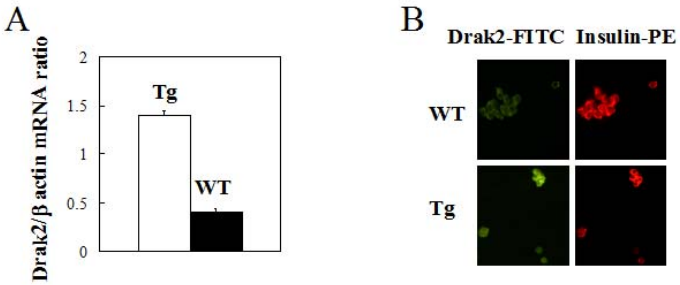

A. Drak2 mRNA overexpression in Tg islets

Islets from actin promoter-driven Drak2 Tg mice or their WT littermates were isolated and Drak2 mRNA levels were measured by real time RT-PCR. The samples were in duplicate. Means ± SD of Drak2/β-actin mRNA ratios of 2 independent experiments are shown.

B. Drak2 protein overexpression in Tg β-cells

Drak2 Tg or WT islets were analyzed by confocal microscopy for Drak2 and insulin expression. The Drak2 signal is in green, and insulin, in red. Representative data from 2 experiments are shown.

Figure 5. Drak2 Tg islets were prone to apoptosis upon inflammatory cytokine stimulation

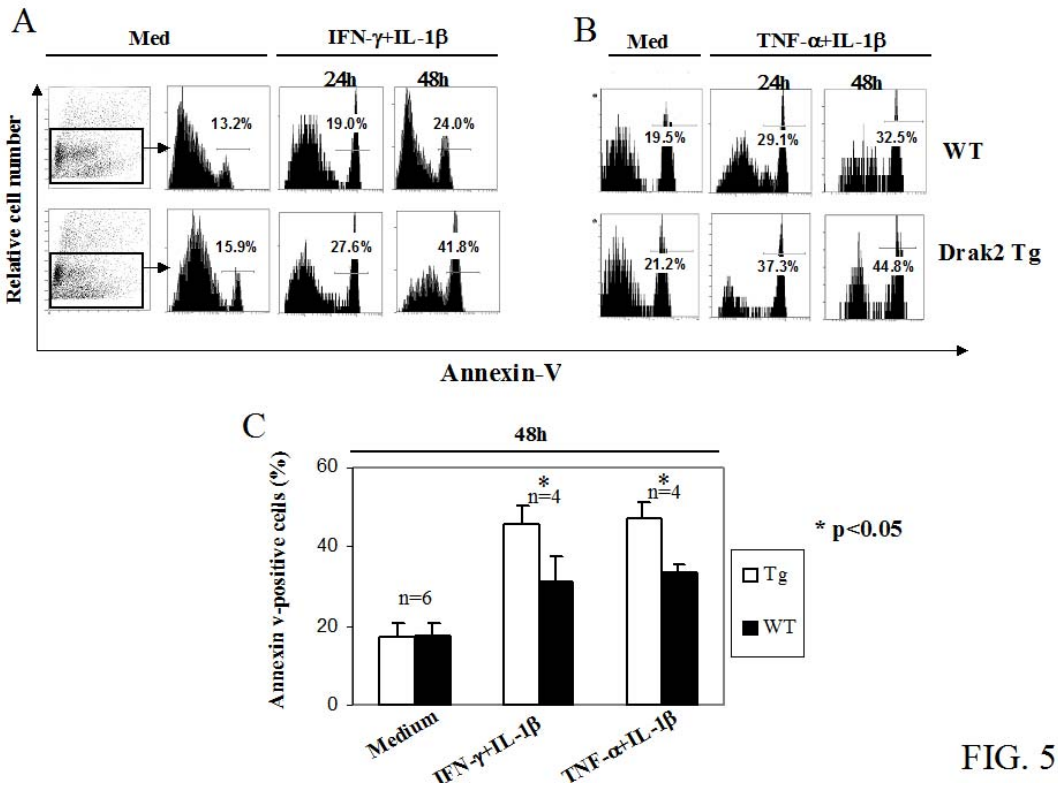

FIG. 5

A-C. Flow cytometry analysis of islet cell apoptosis

Drak2 Tg and WT islets were cultured in RPMI 1640 medium with 10% FCS and stimulated with IFN-γ (1000 U/ml) plus IL-1β (0.5 ng/ml) or TNF-α (200 ng/ml) plus

IL-1β (0.5 ng/ml). After 24 and 48 h, the islets were dispersed and analyzed by flow cytometry with annexin V staining. The percentage of annexin V-positive cells is shown in the histograms. The experiment was repeated more than 4-6 times. A representative set of data is shown in Figs. 4A and 4B, and a data summary from 48-h cultures appears in Fig. 4C, with the number of experiments (n) indicated. Asterisks indicate $p<0.05$ according to paired Student's t test.

FIG. 5

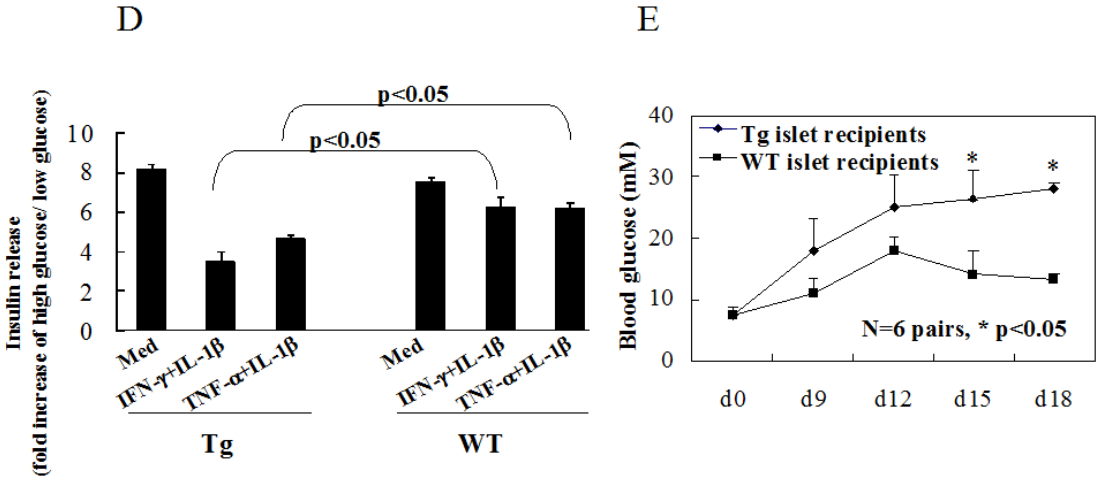

D. Insulin release assay of islets after cytokine stimulation

Islets from Tg or WT mice were cultured in the presence or absence of IFN-γ (1000 U/ml) plus IL-1β (0.5 ng/ml), or TNF-α (200 ng/ml) plus IL-1β (0.5 ng/ml). Insulin release by these islets (10 islets/treatment/well) was measured after 48 h. Samples were in duplicate. Means ± SD of the results of 4 determinants from 2 independent

experiments are shown in terms of fold increase in insulin release stimulated by 16.7 mM versus 2.8 mM glucose.

E. Increased STZ-induced diabetes incidence in mice with transplanted Drak2 Tg islets

Diabetes was induced in C57BL/6 mice by a single i.p. STZ injection (200 mg/kg body weight). After 14 days, the diabetes status of these mice was confirmed according to blood glucose levels. WT or Tg islets were then transplanted i.p. to these diabetic mice to achieve euglycemia. After another 14 days, the glucose tolerance of these mice was verified to be similar (data now shown). Multiple low doses of STZ (40 mg/kg body weight/day x 5 days) were subsequently given i.v. to these islet transplant recipients. Their blood glucose levels from day 0 (the day after multiple low doses of STZ injection was terminated) to day 18 are shown. From days 15 on, the blood glucose levels of the Tg and WT islet recipients are significantly different ($p<0.05$, Student's t test).

Figure 6. p70S6 kinase phosphorylation by Drak 2 in vitro

FIG. 6

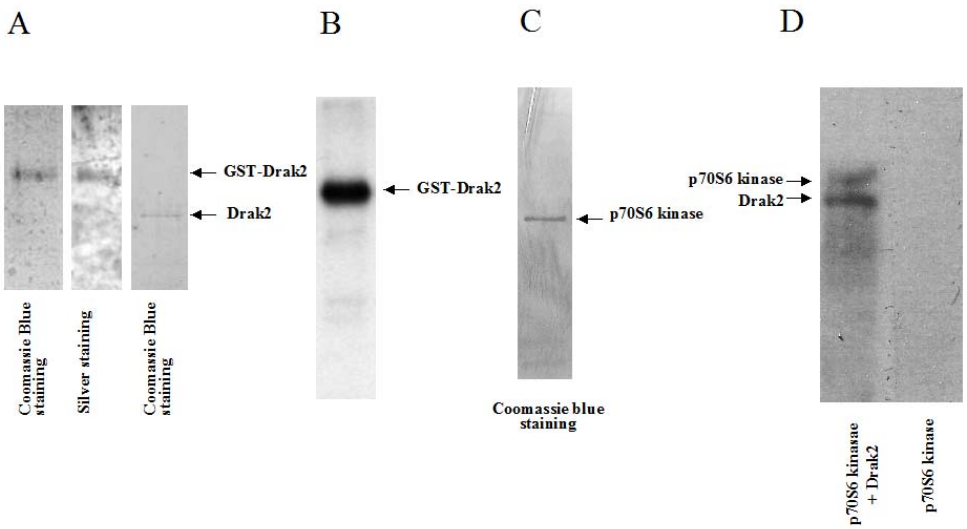

A. Generation of recombinant GST-Drak2

GST-Drak2 was produced in E. coli with the construct pGEX-4T-1-Drak2. The recombinant protein was first affinity-purified with glutathione-agarose beads, followed by size-exclusion chromatography. The purified protein appeared at the expected size (71 kD) and was more that 95% pure according to Coomassie Blue (1st lane) and silver staining (2ndlane). In some experiments, the GST tag of GST-Drak2 was cleaved by thrombin during affinity purification, and the purity of the untagged Drak2 was more than 95%, according to Coomassie Blue staining (3rd lane).

B. GST-Drak2 was kinase-active

GST-Drak2 was employed in an in vitro kinase assay. The product of the assay was resolved by 12% SDS-PAGE, followed by autoradiography. A distinct radio-labeled band at the expected size of GST-Drak2 (71 kD) was detected.

C. Generation of recombinant GST-p70S6 kinase

GST-p70S6 kinase was produced in *E. coli* with the construct pGEX-4T-1-p70S6K. The recombinant protein was first affinity purified with glutathione-agarose beads, followed cleavage of the GST-tag by thrombin. The purified protein appeared at the expected size (53 kD) with more than 95% purity, according to Coomassie Blue staining.

D. p70S6 kinase phosphorylated by Drak2 in vitro

Mouse recombinant Drak2 and p70S6 kinase were reacted in an in vitro kinase assay. The product of the reaction was resolved by 12% SDS-PAGE, followed by autoradiography. Distinct radio-labeled bands at the expected sizes of Drak2 (45 kD) and S6 kinase (53 kD) were detected (lane 1). In lane 2, p70S6 kinase alone was present in the in vitro kinase assay without Drak2, and no radioactive band was detected.

Figure 7. Drak 2 phosphorylated p70S6 kinase in vivo

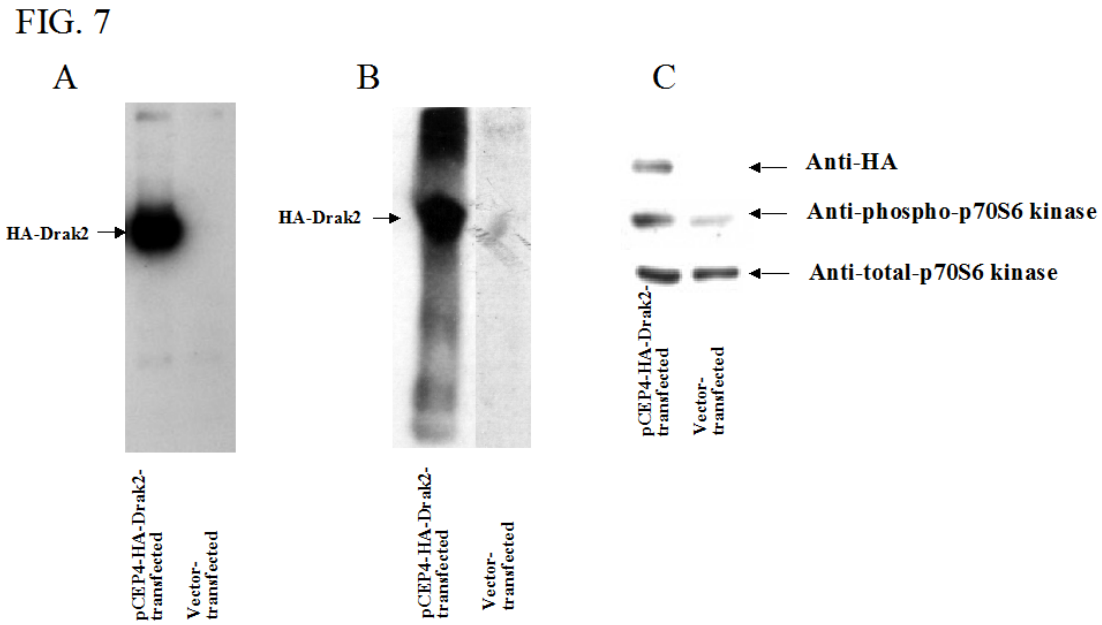

A. Expression of HA-Drak2 in NIT-1 cells

NIT-1 cells were transiently transfected with pCEP4-HA-Drak2. After 48 h, recombinant HA-Drak2 was affinity-purified from the cell lysates with anti-HA agarose, followed by HA peptide elution. The purified protein was resolved in 12% SDS-PAGE, and immunoblotted with anti-HA Ab. Left lane: protein purified from pCEP4-HA-Drak2-transfected NIT-1 cells; right lane: protein purified from empty vector pCEP4-HA transfected NIT-1 cells using the same procedure.

B. Recombinant HA-Drak2 was kinase-active

HA-Drak2, affinity-purified from in pCEP4-HA-Drak2-transfected NIT-1 cells, was employed in an in vitro kinase assay. The product of the assay was resolved by 12% SDS-PAGE, followed by autoradiography. A distinct radio-labeled band at the expected size of HA-Drak2 (45 kD) was detected (left lane). No radio-labeled band was detected using a sample purified from empty vector-transfected NIT-1 cells (right lane).

C. Drak2 overexpression led to enhanced p70S6 kinase phosphorylation in vivo

NIT-1 cells were transiently transfected with pCEP4-HA-Drak2 (left lane) or empty vector pCEP4-HA (right lane). After 48 h, the cells were harvested, and the lysates were analyzed with immunoblotting. Upper panel: the membrane was blotted with anti-HA to ascertain the HA-Drak2 overexpression; middle panel: the membrane was blotted with anti-phospho-p70S6 kinase to assess p70S6 kinase phosphorylation; bottom panel: the membrane was blotted with anti-p70S6 kinase to ascertain the similar total p70S6 kinase levels in NIT-1 cells transfected with pCEP4-HA-Drak2 or the empty vector pCEP4-HA.

Figure 8. Effect of Drak2 siRNA on p70S6 kinase phosphorylation and of rapamycin on β-cell apoptosis

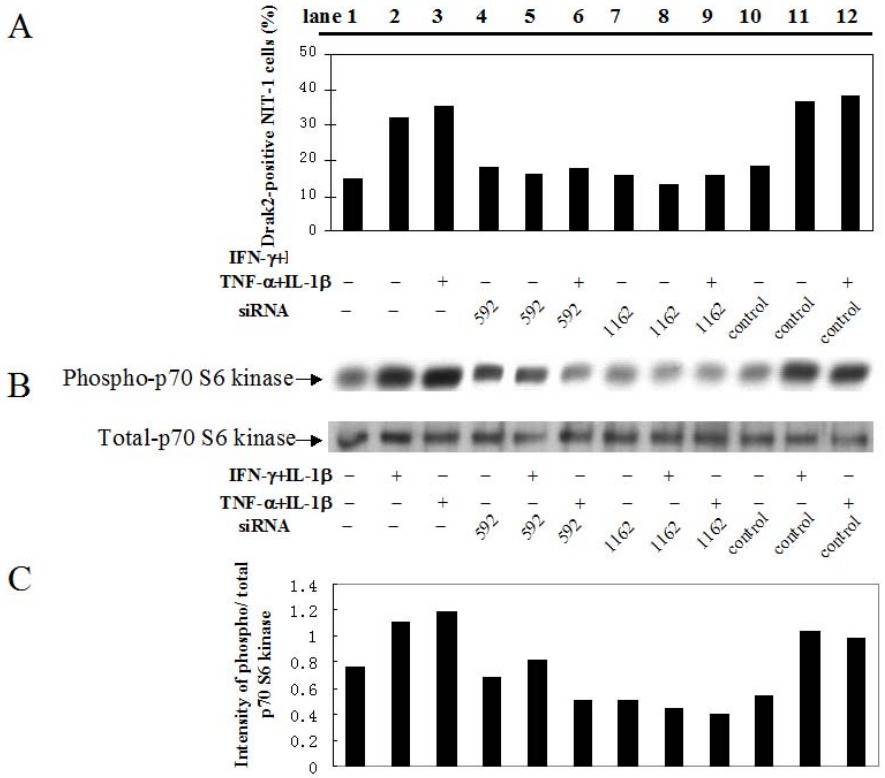

FIG. 8

A-C. Drak2 siRNA inhibited p70S6 kinase phosphorylation in vivo

NIT-1 cells were stimulated with IFN-γ (1000 U/ml) plus IL-1β (0.5 ng/ml), or TNF-α (200 ng/ml) plus IL-1β (0.5 ng/ml). After 24 h, they were transfected with 2 different Drak2 siRNAs (#592 and #1162), or with a control siRNA, which had a scrambled sequence of siRNA #1162. Drak2 protein expression at 48 h was assayed by flow cytometry (Fig. 8A). Phospho-p70S6 kinase (upper panel) and total p70S6 kinase (lower panel) in the cell lysates were detected by immunoblotting (Fig. 8B). The ratio of phospho-p70S6 kinase and total p70S6 kinase signals according to densitometry

were expressed in a bar graph (Fig. 8C). The experiment was conducted twice, and a representative one is shown.

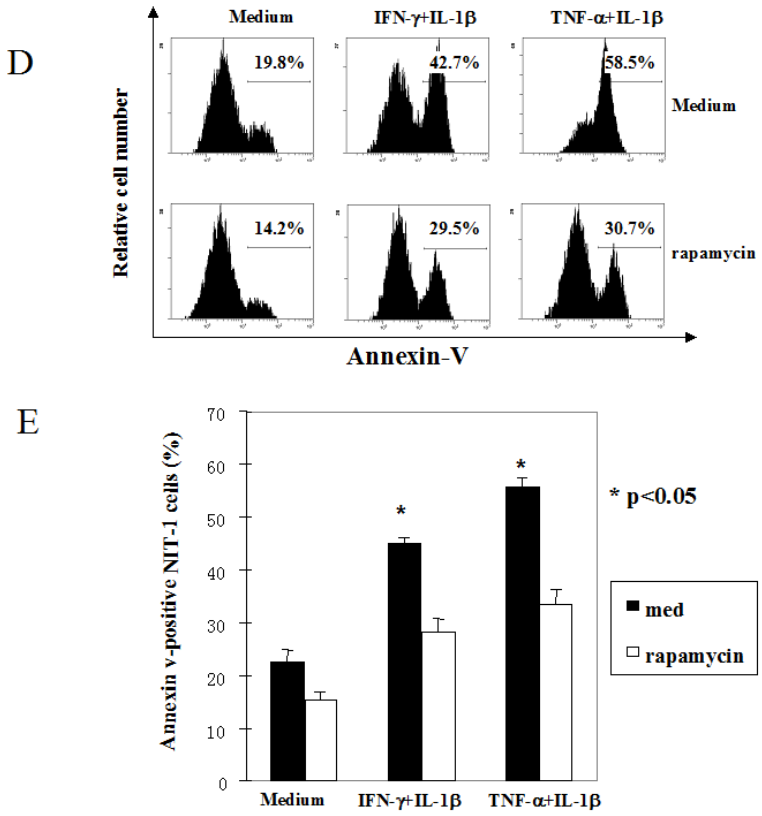

FIG. 8

D and E. Rapamycin protected NIT-1 cells from cytokine-induced apoptosis

NIT-1 cells were stimulated with IFN-γ (1000 U/ml) plus IL-1β (0.5 ng/ml), or TNF-α (200 ng/ml) plus IL-1β (0.5 ng/ml) for 48 h in the presence or absence of rapamycin (250 nM). Their apoptosis was assessed by annexin V staining followed by flow cytometry. The experiment was conducted twice. Histograms of a representative experiment are shown in (D), and the means ± SD of 2 indepent experiments are shown in (E). The asterisks indicate highly significant difference ($p<0.05$, Student's t test).

III. DISCUSSION

III. Discussion

As a part of my Ph.D. program, I and my collaborators mapped the expression pattern of Drak2 during ontogeny, found that Drak2 was critical in T-cell apoptosis and memory T-cell development, discovered that Drak2 was a T1D and T2D risk factor, and revealed that p70S6 kinase was a substrate of Drak2. The results of our study are discussed below.

1. Expression of Drak2

In our study, firstly we checked the Drak2 expression level. Although previous report claims that Drak2 expression is T cell-specific (1), employing ISH, we found that Drak2 was ubiquitously expressed during the mid-gestation stage. Later, in adult mice, Drak2 expression became more restricted with high levels in the thymus, spleen, and lymph nodes; however, many other regions and organs, such as the olfactory lobe, ventricular zone, hippocampal area CA1, intermediate lobe, anterior lobe, suprachasmiatic nuclei in the brain, the glandular and nonglandular regions in the stomach, the adrenal medulla, skin, and testes also showed prominent Drak2 expression. The signal of Drak2 in the adult brain probably suggests that it play an important role other than apoptosis. The ubiquitous expression of Drak2 in the mid-gestation stage also indicates that Drak2 participates in embryonic development. The broad expression pattern of Drak2 indicates that it is an important kinase whose function is not restricted in lymphoid organs. Till now, the studies on Drak2 have been mainly focused on the immune system (1-4), and we are the first ones who have discovered the role of Drak2 in islet beta cell function and survival.

2. The physiological role of Drak2 in T cell homeostasis

Previously, study on Drak2 knockout mouse claims that Drak2 is not involved in T cell apoptosis (1). They found *Drak2*$^{-/-}$ mice have enhanced T cell activation and are resistant to experimental autoimmune encephalomyelitis, an autoimmune demyelinating disease that resembles multiple sclerosis (1). Recent study by the same group on knockout mouse show that *Drak2*$^{-/-}$ T cells require greater tonic signaling for maintenance during clonal expansion. Following stimulation, *Drak2*$^{-/-}$ T cells were more sensitive to an intrinsic form of apoptosis that was prevented by CD28 ligation, homeostatic cytokines, or enforced Bcl-x_L expression. T cell-specific Bcl-x_L expression also restored the susceptibility of *Drak2*$^{-/-}$ mice to experimental autoimmune encephalomyelitis (3).

How do we reconcile the two opposite findings, one with KO null mutation showing that Drak2 is not important or even anti-apoptotic, and one with Tg overexpression showing that it is proapoptotic? We are almost sure that McGargill et. al. did not conduct a careful investigation and hastly made their conclusion that Drak2 has no role in T-cell apoptosis (1). Their second study demonstrating that drak2$^{-/-}$ T cells are more sensitive to an intrinsic form of apoptosis seems to be better conducted. It's known that after an infection is cleared, there are two forms of apoptosis in clonal contraction: activation-induced cell death (AICD) and activated cell autonomous death (ACAD) (5). AICD is thought to depend on an extrinsic form of apoptosis induced by the ligation of death receptors such as Fas on the surface of the T cell (6). Which program is activated

is largely depended on the antigen. AICD is the prevailing mechanism if antigens are present at higher concentrations at the early stage of immune response. ACAD, in contrast, might be the dominating mechanism at the end of the immune response when foreign antigen is present only at very low concentrations (5).

We found that Drak2 mRNA level in activated T cell showed a peak at 90 minute, followed by a decrease after 24 hour. Although the meaning of the rapid surge is not clear, this probably suggests that Drak2's level needs to be precisely regulated during an immune response. It's possible at the early stage of T-cell activation, the up-regulation of Drak2, which happens within hours, instructs the apoptosis of activated T cells by AICD; the overexpression of Drak2 in Tg mouse at this stage leads to increased cell death. On the other hand, after 24 hour, Drak2 is down-regulated and kept at a low level. The low level of Drak2 probably prevents excessive apoptosis of AICD by raising their threshold of vulnerability toward IL-2. Also, a certain low level of Drak2 is needed at this stage to prevent excessive apoptosis caused by ACAD. The complete deletion of Drak2 in knockout mouse leads to increased ACAD in T cells, which can be rescued by CD28 ligation or enforced Bcl-$_{XL}$ expression.

3. Drak2 might work on a two-hit model

The expression of Drak2 increases when WT T cells are activated or when WT islet β cells are under treatment. However, Drak2 transgenic T cells didn't show the tendency of apoptosis until exogenous IL-2 was added. Also, the difference between transgenic and WT islets apoptosis can only be found under cytokine or free fatty acid treatment.

This suggests that Drak2 might act on a two-hit mode, in which other signalling events (hit 1) derived from stimulation as well as Drak2 (hit 2) are both required to results in cell damage and/or dysfucntion. We hypothesize that in individuals with abnormally high basal Drak2 expression (hit 2), less hit 1 might be sufficient to cause excessive cell damage or dysfunction.

4. The signalling pathway of Drak2

4.1 Pathways upstream of Drak2

In islet β cells, Drak2 expression was increased after TNFα, IFNγ, IL-1β or free fatty acid treatment. Recent study shows the cytotoxic effect of IL-1β/IFNγ was associated with the expression of inducible nitric oxide synthase (iNOS) and production of nitric oxide. NG-monomethyl-L-arginine (L-NMMA) is an inhibitor of inducible nitric oxide synthase (iNOS) and production of nitric oxide. It can block the β cells death induced by IL-1β and IFNγ (7). In our study, when islets are treated with IL-1β and IFNγ in the presence of L-NMMA, the induced Drak2 expression by IL-1β and IFNγ is diminished by L-NNMA. This proved that iNOS is upstream of Drak2 in cytokine induced β cell apoptosis.

4.2 Downstream of Drak2

Previously, we only know that Drak2 is a genuine substrate of itself. In this study, we identified 5 putative Drak2 substrates, and proved that p70S6 kinase (p70S6K) was Drak2 substrate in vitro and in vivo.

The S6 kinases are members of the AGC family of serine/threonine protein kinases and are involved in the regulation of cell growth, survival and metabolism (8).

Nowadays, there is increased interest of p70S6K's role in diabetes. The pancreatic β-cell has a unique ability to secrete insulin and also express a functional insulin receptor. The docking proteins of this receptor are insulin receptor substrate (IRS)-1 and -2, and the downstream signaling elements are mTOR and translational regulators PHAS-I and p70S6 kinase. Thus, p70S6K is the necessary component of the insulin signaling cascade to regulate insulin-mediated gene expression and protein translation in an autocrine manner (9). However, in parallel studies, it has become increasingly evident that p70S6K may also be implicated in a negative feedback loop to suppress insulin signaling. p70S6K may lead to insulin resistance by affecting IRS1 serine phosphorylation. In a homeostatic setting, as nutrients and amino acids are consumed, p70S6K activity participates in mediating cell growth. In contrast, under conditions of nutrient overload associated with the obese state, constitutive activation of p70S6K signaling leads to desensitization of insulin signaling through IRS1 serine phosphorylation and inhibition of IRS1 transcription. Thus, p70S6K may mediate insulin resistance, and potentially type 2 diabetes in the face of nutrient excess (10).

In our study, we found that Drak2 mice are prone to type 2 diabetes when they are fed with high fat diet. It is possible that Drak2 overexpression leads to p70S6K constitutive activation and under conditions of nutrient overload; subsequently, the activation of

p70S6K signalling leads to insulin resistance. Our data also suggest that the activation of this pathway will lead to β cell apoptosis.

By activating p70S6K through direct phosphorylation, mTOR is an important element in the activation scheme of p70S6K. Rapamycin prevents the phosphorylation of mTOR. It is a potent immunosuppressant that interferes with T-cell activation at the level of translation, and it has been, in part, responsible for the success of the Edmonton protocol in islet transplantation in type 1 diabetes (11). Moreover, recent study suggests that rapamycin increases basal and stimulated insulin levels in vivo and insulin content in vitro and reduce apoptosis in islet (12). Interestingly, islet transplantation efficiency has been greatly improved after rapamycin is introduced into the immunosuppressant regimen. It is conceivable that inhibition of p70S6K phosphorylation by rapamycin contributes to reduction of islet apoptosis after transplantation, and hence, is partially responsible for the increase in transplantation efficiency. We have further in vitro evidence that rapamycin renders β cells partially resistant to apoptosis, validating that p70S6K is indeed relevant to islet survival. It is possible that inflammatory cytokines activate both the Drak2/p70S6K and mTORC1/p70S6K pathways (Fig.2), and that inhibiting one of them is only partially effective in reducing β cell apoptosis. Indeed, when Drak2 upregulation stimulated by cytokines was prevented by siRNA, islet apoptosis was decreased, but was not totally prevented. Similarly, rapamycin only partially protected islet apoptosis from the cytokines. We tried rapamycin and Drak2 siRNA combination, they showed a synergy in protecting human islet from apoptosis caused by cytokine treatment. Hence dual inhibition of mTORC1 (with rapamycin) and

Drak2 (with Drak2 inhibitors that are to be developed) might achieve better results in islet protection in terms of cytokine-induced β cell apoposis.

Full activation of p70S6K requires multiple coordinated phosphorylation events. The first step in the phosphorylation sequence leading to activation is the mTOR-dependent phosphorylation of Ser 371 in the linker domain, as well as Ser 411, Ser 418, Thr 421 and Ser 424, located in the carboxy-terminal autoinhibitory domain (13-16). The analogous residues in mouse p70S6k are Ser 394, Ser 434, Ser 441, Thr 444 and Ser 447. Phosphorylation of Thr389 within a hydrophobic motif by the mTOR-Raptor complex allows docking of phosphoinoside-dependent kinase1 PDK1 (17;18), which phosphorylate Thr 229 (in the catalytic domain). This is the final phosphorylation event (19;20). Since Drak2 phosphorylates p70s6K, it will be interesting to know which p70S6k amino acid residues are the substrates of Drak2, and whether Drak2 and mTORC1 have overlapping phosphorylation repertoire on p70S6K.

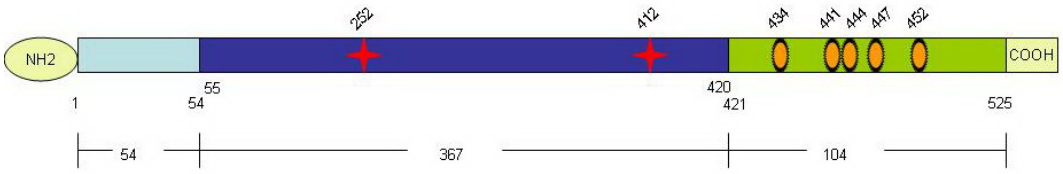

The phosphorilation sites of mouse p70s6 kinase

5. A proposed model of Drak2 signalling

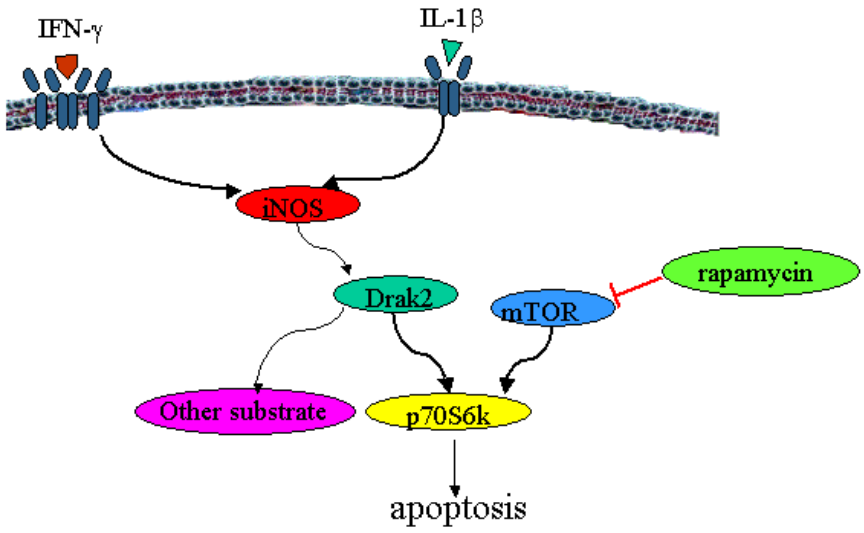

Fig. 2

Based on our data, we propose the following pathways involving Drak2 (Fig.2).

In islet β cell, IFN-γ and IL-1β induce apoptosis by activating iNOS. Drak2 is downstream of iNOS, and it can phosphorylate p70S6k. mTOR activate p70S6K. Rapamycin, an inhibitor of mTOR, renders β-cells partially resistant to apoptosis induced by cytokines, suggesting that p70S6 kinase is relevant to islet apoptosis.

We also found that FasL induced Drak2 expression in islets, and Drak2 Tg islets treated with FasL plus IFN-γ presented increased apoptosis, compared to WT islets (data not shown). It is known that islet β-cell apoptosis often needs concerted signals from different pathways. It is possible that Drak2 signaling pathway interacts with several

other apoptotic pathways, and these signalling pathways play a concerted effort on β-cell apoptosis. We found that Drak2 acts through caspase-9 in apoptosis induced by cytokines. However, our study on the involvement caspase 8 and Bid cleavage in Drak2-mediated apoptosis was not conclusive. Further elucidating the relationship amongh these factors will be needed to better understand the full cascade of Drak2 signaling in apoptosis induction.

We found that p70S6 kinase, a key regulator of cell size and cell cycle, is a substrate of Drak2. In the future, we will validate other 4 putative Drak2 substrates identified by our protein kinase substrate array. Considering the multiple substrates of Drak2 and its broad expression pattern in the embryonic stage and non-lymphoid organs, it's possible that further study on Drak2 will show us a more complicated network of Drak2 signaling in various cells and organs.

6. Summary and further perspectives

Our study demonstrates that Drak2 is a pro-apoptotic factor in both T cells and islet β cells. It plays important roles in memory T-cell development and diabetes pathogenesis. We have identified 5 putative Drak2 substrates, and proved that p70S6K is a bona fide Drak2 substrate in vitro and in vivo.

For the further investigation, firstly, we plan to identify which amino acid residue(s) of p70S6K is phosphorylated by Drak2. p70S6K has multiple functions in cell growth, survival, apoptosis and protein translation. Finding out its residue(s) phosphorylated by

Drak2 will help us better understand the function of Drak2 in comparison to mTOR, another kinase capable of phosphorylating p70S6K. We will know then whether they have overlaping or different effect on p70S6K activation.

Secondly, it's intriguing that both Tg and KO mice of Drak2 have increased T-cell apoptosis. It's possible that Drak2 plays different roles in extrinsic and intrinsic apoptosis pathways, which were tested separately in Tg and KO T cells by us and the group in San Diego. To confirm our hypothesis, we could using the Tg and KO T cells in the same experiment of extrinsic or intrinsic apoptosis induction, to ascertain that they behave differently.

We will also try to validate other 4 putative Drak2 substrates identified by our protein kinase substrate array. It is possible that Drak2 has different functions when it phosphorylates different sustrates. Cyclin dependent kinase 3 (CDK3) is among the 4 other putative Drak2 substrates identified by the array. CDKs are a family of serine/threonine kinases involved in the regulation of cell cycle. Little is known about CDK3, which is a homolog of CDK2 and cell division cycle kinase 2 (CDC2). Previous studies using ectopic expression of human CDK3 suggest a role for this kinase in the G(1)/S-phase transition (21;22). If CDK3 is confirmed to be another substrate of Drak2, we might discover additional Drak2 function in cell cycle progression.

Lastly, we are very much intereated in developping Drak2 inhibitors, as they could be used as therapeutic agents/drugs for preventing or delaying the onset of T1D and T2D. Since we have produced recombinant Drak2 and identified p70S6K as its substrate, the screening of Drak2 inhibitors from a suitable small molecule compound bank is a quite feasible task.

7. Contributions to science

1) We have corrected a previous misconception that Drak2's expression is restricted in the T-cell compartment. We have found broad expression of Drak2 at embryo stage and prominent signal in non-lymphoind organs in adult such as brain, stomach, skin and testis. This could provide a valuable guidance in the future to investigate the complete physiological role of Drak2.

2) With the transgenic mouse model, we found activated Drak2 Tg T cells demonstrated significantly enhanced apoptosis in the presence of exogenous IL-2, which is accompanied with a compromised memory T-cell response. This also corrected an erroneous conclusion by another group that Drak2 is not involved in apoptosis at that time.

3) We also found that Drak2 overexpression in Tg mouse led to aggravated β-cell apoptosis triggered by cytokine or free fatty acid stimuli. Further in vivo experiments demonstrated that Drak2 Tg mice were prone to T1D in a multiple-low-dose STZ-induced diabetes model, and prone to T2D in a diet-induced obesity model, indicating that Drak2 is a contributing risk factor to T1D and T2D.

4) We established that inducible nitric oxide synthase was upstream and caspase-9 was down stream of Drak2. We also identified p70S6K as a novel substrate of

Drak2. These findings illustrated the signalling pathway of Drak2 and are essential in developping therapeutic compounds for diabetes.

Reference List

(1) McGargill MA, Wen BG, Walsh CM, Hedrick SM. A deficiency in Drak2 results in a T cell hypersensitivity and an unexpected resistance to autoimmunity. Immunity 2004 Dec;21(6):781-91.

(2) Schaumburg CS, Gatzka M, Walsh CM, Lane TE. DRAK2 regulates memory T cell responses following murine coronavirus infection. Autoimmunity 2007 Nov;40(7):483-8.

(3) Ramos SJ, Hernandez JB, Gatzka M, Walsh CM. Enhanced T cell apoptosis within Drak2-deficient mice promotes resistance to autoimmunity. J Immunol 2008 Dec 1;181(11):7606-16.

(4) McGargill MA, Choy C, Wen BG, Hedrick SM. Drak2 regulates the survival of activated T cells and is required for organ-specific autoimmune disease. J Immunol 2008 Dec 1;181(11):7593-605.

(5) Rathmell JC, Thompson CB. Pathways of apoptosis in lymphocyte development, homeostasis, and disease. Cell 2002 Apr;109 Suppl:S97-107.

(6) Hildeman DA, Zhu Y, Mitchell TC, Kappler J, Marrack P. Molecular mechanisms of activated T cell death in vivo. Curr Opin Immunol 2002 Jun;14(3):354-9.

(7) Jeong IK, Oh SH, Chung JH, Min YK, Lee MS, Lee MK, et al. The stimulatory effect of IL-1beta on the insulin secretion of rat pancreatic islet is not related with iNOS pathway. Exp Mol Med 2002 Mar 31;34(1):12-7.

(8) Grammer TC, Cheatham L, Chou MM, Blenis J. The p70S6K signalling pathway: a novel signalling system involved in growth regulation. Cancer Surv 1996;27:271-92.

(9) McDaniel ML, Marshall CA, Pappan KL, Kwon G. Metabolic and autocrine regulation of the mammalian target of rapamycin by pancreatic beta-cells. Diabetes 2002 Oct;51(10):2877-85.

(10) Um SH, Frigerio F, Watanabe M, Picard F, Joaquin M, Sticker M, et al. Absence of S6K1 protects against age- and diet-induced obesity while enhancing insulin sensitivity. Nature 2004 Sep 9;431(7005):200-5.

(11) Ryan EA, Lakey JR, Rajotte RV, Korbutt GS, Kin T, Imes S, et al. Clinical outcomes and insulin secretion after islet transplantation with the Edmonton protocol. Diabetes 2001 Apr;50(4):710-9.

(12) Marcelli-Tourvieille S, Hubert T, Moerman E, Gmyr V, Kerr-Conte J, Nunes B, et al. In vivo and in vitro effect of sirolimus on insulin secretion. Transplantation 2007 Mar 15;83(5):532-8.

(13) Saitoh M, Pullen N, Brennan P, Cantrell D, Dennis PB, Thomas G. Regulation of an activated S6 kinase 1 variant reveals a novel mammalian target of rapamycin phosphorylation site. J Biol Chem 2002 May 31;277(22):20104-12.

(14) Moser BA, Dennis PB, Pullen N, Pearson RB, Williamson NA, Wettenhall RE, et al. Dual requirement for a newly identified phosphorylation site in p70s6k. Mol Cell Biol 1997 Sep;17(9):5648-55.

(15) Isotani S, Hara K, Tokunaga C, Inoue H, Avruch J, Yonezawa K. Immunopurified mammalian target of rapamycin phosphorylates and activates p70 S6 kinase alpha in vitro. J Biol Chem 1999 Nov 26;274(48):34493-8.

(16) Ferrari S, Bannwarth W, Morley SJ, Totty NF, Thomas G. Activation of p70s6k is associated with phosphorylation of four clustered sites displaying Ser/Thr-Pro motifs. Proc Natl Acad Sci U S A 1992 Aug 1;89(15):7282-6.

(17) Frodin M, Antal TL, Dummler BA, Jensen CJ, Deak M, Gammeltoft S, et al. A phosphoserine/threonine-binding pocket in AGC kinases and PDK1 mediates activation by hydrophobic motif phosphorylation. EMBO J 2002 Oct 15;21(20):5396-407.

(18) Biondi RM, Kieloch A, Currie RA, Deak M, Alessi DR. The PIF-binding pocket in PDK1 is essential for activation of S6K and SGK, but not PKB. EMBO J 2001 Aug 15;20(16):4380-90.

(19) Alessi DR, Kozlowski MT, Weng QP, Morrice N, Avruch J. 3-Phosphoinositide-dependent protein kinase 1 (PDK1) phosphorylates and activates the p70 S6 kinase in vivo and in vitro. Curr Biol 1998 Jan 15;8(2):69-81.

(20) Pullen N, Dennis PB, Andjelkovic M, Dufner A, Kozma SC, Hemmings BA, et al. Phosphorylation and activation of p70s6k by PDK1. Science 1998 Jan 30;279(5351):707-10.

(21) Sage J. Cyclin C makes an entry into the cell cycle. Dev Cell 2004 May;6(5):607-8.

(22) Ren S, Rollins BJ. Cyclin C/cdk3 promotes Rb-dependent G0 exit. Cell 2004 Apr 16;117(2):239-51.